Copper and Silver Metal Complexes Supported by Heteroscorpionate Ligands Based on Bis(Azolyl)Acetates: Chemistry and Spectroscopic Studies

Nello Mosca

Thesis to obtain the Master of Science Degree in
Chemistry

Supervisors

Prof[a]. Maria de Fátima Guedes da Silva

Prof. Carlo Santini

Prof[a]. Maura Pelli

Examination Committee

Chairperson:	Prof[a]. Maria Matilde Soares Duarte Marques
Supervisor:	Prof[a]. Maria de Fátima Guedes da Silva
Members of the Committee:	Doctor Luísa Martins
	Doctor Corrado Bacchiocchi

June 2016

Abstract

The poly(azolyl)acetates are a versatile class of potentially tridentate ligands, K^3N,N',O-donor, whose steric and electronic properties can be widely modulated by changing the type of substituent on the azole ring by, for example, the functionalization of the acetate group, with the formation of conjugate esters and amides with biomolecules. The coordination chemistry of these ligands is of particular interest for the potential applications of the related complexes both in catalysis and in the bioinorganic field as anticancer agents.
In this thesis I report the design, synthesis and characterization of a series of pyrazole-derived bis(azolyl)acetate binder ligands and the related Cu(II) complexes, characterized by the presence of counterions of different coordinating properties.
Moreover, I synthesized Cu(I) and Ag(I) complexes characterized by the presence of phosphinic coligands such as triphenylphosphine, tribenzylphosphine and 1,3,5-triaza-7-phosphaadamantane (PTA). The latter phosphine is of particular interest because it allows to obtain stable and hydrosoluble species in physiological conditions, which are of considerable interest for their catalytic applications and as potential antitumor agents. Biological studies were conducted in partnership with the Department of Pharmaceutical Sciences, University of Padova, on some of the most promising species, which have shown a considerable cytotoxic activity in *vitro* against a sizeable number of human tumor cell lines. Some complexes were also evaluated for anti-metastatic activity through tests of cellular invasion and inhibition of the PTP1B protein (protein tyrosine phosphatase-1B).

Key words: biofunctionalized ligands, copper(I/II) complexes, heteroscorpionate, silver(I) complexes, therapeutic agents, transition metal complexes.

Resumo

Os poli(azolil)acetatos são uma classe versátil de ligandos potencialmente tridentados, do tipo K^3N,N',O-doador, cujas propriedades estereoquímicas e electrónicas podem ser largamente moduladas por alteração do tipo de substituinte no anel de azole, por exemplo por funcionalização com o grupo acetato e formação de conjugados de tipo éster e amida com biomoléculas. A química de coordenação destes ligandos tem particular interesse devido a potenciais aplicações dos seus complexos, tanto em catálise como no campo bioinorgânico, como agentes antitumorais.
Nesta tese são descritos o desenvolvimento racional, síntese e caracterização de uma série de ligandos bis(azolil)acetato derivados do pirazole e seus complexos de Cu(II), caracterizados pela presença de contra-iões com diferentes propriedades de coordenação.
Foram ainda sintetizados complexos de Cu(I) e Ag(I) caracterizados pela presença de co-ligandos fosfínicos, como a trifenilfosfina, tribenzilfosfina e 1,3,5-triaza-7-fosfaadamantano (PTA). Esta última fosfina tem especial relevância porque permite obter espécies estáveis e hidro-solúveis em condições fisiológicas, de particular interesse para efeitos de aplicações catalíticas e como potenciais agentes antitumorais. Foram realizados estudos biológicos de alguns dos compostos mais promissores em colaboração com o Departamento de Ciências Farmacêuticas da Universidade de Pádua, tendo os compostos demonstrado actividade citotóxica considerável *in vitro* contra um número significativo de linhas de células tumorais humanas. Alguns complexos foram também avaliados em termos de actividade anti-metastática, mediante testes de invasão celular e inibição da proteína tirosina fosfatase 1B (PTP1B).

Palavras-chave: agentes terapêuticos, complexos de cobre(I/II), complexos de metais de transição, complexos de prata(I), heteroescorpionato, ligandos biofuncionalizados.

Index

Index of Figure

Index Of Scheme

Abbreviations

2008	Human ovarian carcinoma
A2780	Ovarian carcinoma cell
A2780cis	Cisplatin-resistant mutant cell
A375	Human malignant melanoma
A431	Epidermoid carcinoma
A-498	Human kidney adenocarcinoma
A549	Human lung cancer
Btza	bis(1,2,4-triazolyl) acetate
C13*	Human ovarian its cisplatin resistant
Cal-27	Squamous carcinoma tongue
Capan-1	Human pancreas adenocarcinoma
CEM	Human T-lymphocyte
CH1	Human ovarian carcinoma
DDP	Cis-Platinum
DPPE	1,2-bis(diphenylphosphino)ethane
DLD1	Human colon adenocarcinoma
DMSO	Dimethyl sulfoxide
H460	Lung cancer
HbzaH	Hydroxybenzoic acid
HCT-15	Human colon cancer
HeLa	Cervix adenocarcinoma
HepG2	Hepatocellular carcinoma
HL-60	Human promyelocytic leukemia
HOMO	Highest Occupied Molecular Orbital
HT1080	Human fibrosarcoma
IC_{50}	Inhibitory concentrations of the 50% of the cell cultures
HImSMe	1-methyl-2mercaptoimidazole
LMS	Leiomyosarcoma cell
LOVO	Human colon adenocarcinoma
LOX	Lipoxygenase
LUMO	Lowest Unoccupied Molecular Orbital
MB157	Cancerous breast cell

MCF-7	Human breast adenocarcinoma
MOF	Metal organic frameworks
MRC-5	Normal human fetal lung fibroblasts
MTT	Methyl thiazolyl tetrazolium
OE19	Human Caucasian oesophageal carcinoma
ORTEP	Oak Ridge Thermal-Ellipsoid Plot Program
OVCAR-3	Cancerous cell ovarian
PTA	1,3,5-triaza-7-phosphaadamantane
Pz	Pyrazole
SKOV-3	Intrinsically cisplatin resistant cell
THF	Tetrahydrofuran
Thp	Tris(hydroxymethyl)phosphine
Thpp	Tris(hydroxypropryl)phosphine
Tpp	Triphenylphosphine
PCN	Tris(cyanoethyl)phosphine
PySH	2-mercaptopyridine
$SalH_2$	Salicylic acid
TPPTS	Tris(3-sulfophenyl)phosphine trisodium salt
Tz	Triazole

1. Introduction

1.1. Novel scorpionate bis(azolyl)acetate ligands

Polydentate nitrogen-containing donor ligands derived from poly(pyrazol-1-yl)methanes with $[RR'C(az)_2]$ (az = azolyl groups; R = H or az) as general structure and bearing organic functional groups (R') on the bridging carbon have attracted considerable attention and their coordination chemistry towards main group and transition metals have been extensively studied.[1-3] If neither R nor R' is pz (pyrazole), the ligand is called heteroscorpionate, a description that also includes ligands where R' is a pyrazolyl group different from the other two bridging pyrazolyl units. These intriguing heteroscorpionate ligands[4-6] present different types of functional groups, which successfully broaden the scope of their applications.[7,8]

An azole is a class of five-membered nitrogen heterocyclic ring compounds containing at least one other non-carbon atom of either nitrogen, sulfur, or oxygen. (**Fig. 1.1**).

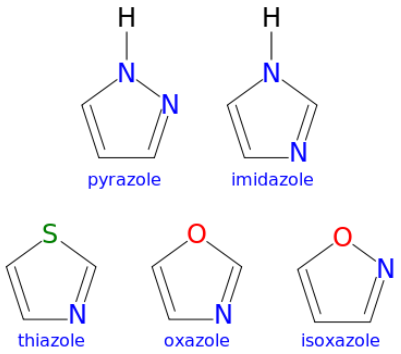

Figure 1.1. Azole structures.

Six-membered aromatic heterocyclic systems with two nitrogens include pyrimidine and purine, which are important biomolecules.

In recent years Burzlaff *et al.* found bis(3,5-dialkylpyrazol-1-yl)acetic acids[9,10] (which are accessible from dibromo- or dichloro-acetic acid in a one-step synthesis) to be a convenient starting material for linker modified ligands.[11] Complexes containing these ligands have been of considerable interest owing to their important use as metalloenzyme models relevant to biochemistry,[12-19] metalbased antitumor drugs[20,21] and development of homogeneous catalysts.[8,22-27]

During the last decade, the interest of the Inorganic Chemistry research group in which I worked for the thesis stage has focused in the synthesis of new heteroscorpionate ligands with pyrazole, triazole, 2-mercaptopyridine or 2-mercaptoimidazole rings.[20,28-41] Recent contributions are also related to the heteroscorpionate ligands derived from $[RR'C(az)_2]$ bearing a coordinating moiety

(R') such as acetate,[10,29,33,42-45] dithioacetate,[29,46] sulfonate,[28] ethoxide,[47,48] phenolate,[15,49-51] thiolate[52-54] or other classes of moieties.[55-58]

On this basis, the Inorganic Chemistry research group has focused on the study of the coordinative ability of the monoanionic heteroscorpionate acetate ligand, bis(3,5-dimethyl-pyrazol-1-yl)acetate ($[HC(CO_2)(pz^{Me2})_2]^-$) and some its derivates, toward copper(I/II) and silver(I) acceptors. Moreover, we have designed and synthesized the new triazole-based heteroscorpionate ligand, bis(triazol-1-yl)acetate ($[HC(CO_2)(tz)_2]^-$) and some its derivates; triazole-based ligands are electron-withdrawing relative to their pyrazole-based counterparts, and the *exo*-ring-nitrogen atoms may bridge between metal centers or may take part in hydrogen-bond interactions, assisting the formation of two-dimensional waterintercalate or water-layer clathrates,[59,60] thus leading to water soluble species.[61-63]

Besides, because it is of great importance to obtain complexes that are more or less soluble and stable under physiological conditions, an interesting solution is the use phosphine such as triphenylphosphine (PPh_3), tribenzyl phosphine (PBz_3), 1,3,5-Triaza-7-phosphaadamantane (PTA). About the azolyl derivates in literature the synthesis and the spectroscopic and analytic characterization of new azolyl-based scorpionate complexes containing the phosphine coligands are described to stabilize the Cu(I) and Ag(I) derivatives. In addition it's interesting to increase the solubility of this type of systems by the use of phosphines bringing highly polar functional groups such as $–SO_3^+$, -COOH, $-NR_3$, or –OH.[64]

Another class of this type of ligands is represented by poly(pyrazolyl)borates[65] and related scorpionates[66] that are potentially tridentate ligands extensively employed as anionic σ-donor chelates in a variety of metal complexes. The general structure of this type of system is $[RR'B(az)_2]^-$, where az can be the pz, and it is either an unsubstituted or C-substituted pyrazolyl group that can coordinate metals to give complexes of the type $[RR'B(\mu\text{-}pz)_2ML_n]$ (L_n = metal coligands). Modifications of poly(pyrazolyl)-borates can be made by replacement of the boron bridging atom by other elements such as carbon,[67] silicon,[68] or phosphorus.[69,70]

In **Figure 1.2** the structure of boron ligands used in the lecture[19,32,39,71] are reported.

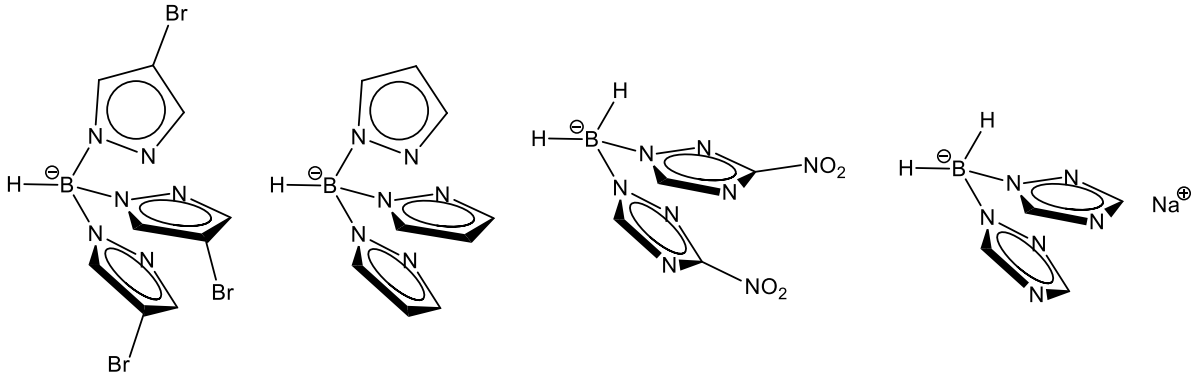

$[HB(4\text{-}Brpz)_3]^-$ $[HB(pz)_3]^-$ $[H_2B(tz^{NO2})_2]^-$ $Na[H_2B(pz)_2]$

Figure 1.2. Structure of some boron ligands.

It's interesting to know the difference between the borate ligands and the acetate ones. Although the anionic Tp^x (generic tris(pyrazolyl)borates) are often described as equivalent to C_5H_5 (Cp) or C_5Me_5 (Cp*), they also exhibit a number of significant differences arising from the lesser π-acceptor and greater σ-donor abilities of pyrazole.[66] It is now accepted that the electronic and steric properties of the Tp^x ligands can strongly influence both the structure and properties of their metal complexes. The poly(pyrazolyl)borate ligands are symmetrical with respect to the nitrogen donors, and are unable to mimic many metalloprotein active sites which lack similar monofunctional, highly organized donor spheres. Bis(pyrazolyl)acetates are ligands closely related to both neutral tris(pyrazolyl)methanes and anionic poly(pyrazolyl)borates in respect of their classical ''pinch and sting'' behaviour (**Fig. 1.3**), one of the pyrazolyl groups being replaced by a carboxylate moiety.[66] This change introduces a small degree of steric hindrance and considerable coordinative ligand flexibility. Bis(pyrazolyl)acetates can be easily deprotonated, behaving in the anionic form as N,N,O-tripodal donors, similar to tris(pyrazolyl)borates; alternatively they may react in the neutral form like the tris(pyrazolyl)alkanes.

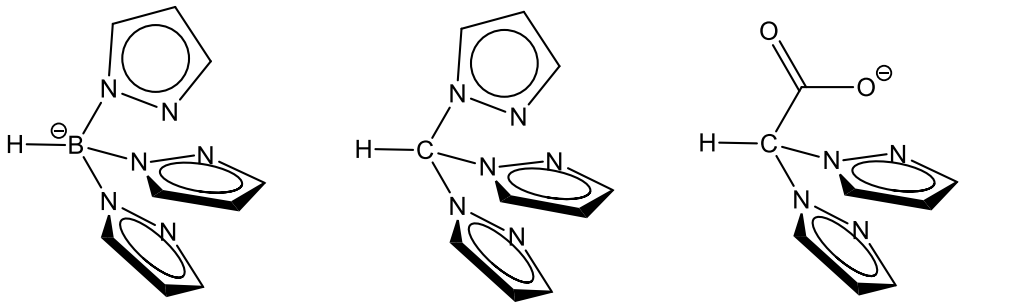

Figure 1.3. The three well-known classes of scorpionate ligands.

1.2. Novel scorpionate bis(mercapto)acetate ligands

In recent years there has been considerable interest in organotin derivatives. This is because in the past organotin compounds have been accumulated in nature due to their various industrial[72] and agricultural applications.[73] The discovery of their dangerous impacts on living organisms has led to a significant decrease of use from the late 1980s, however due to their high toxicity.[74] On the other hand, in recent years many organotin compounds have been tested for their *in vitro* activity against a large variety of tumor lines and have been found to be as effective or better than traditional heavy metal anticancer drugs, such as cis-platin.[75] In addition to the aforesaid applications organotin compounds are also of interest in view of the considerable structural diversity that they possess. This aspect has

been attracting the attention of a number of researchers and a multitude of structural types have been discovered.[76]

In recent years a number of authors[77] have synthesized S,N-ligands of the type $(CH_2)_n(SAz)_2$ based on a nitrogenated aromatic ring system, such as benzimidazole or pyridine (**Fig. 1.4)**. These ligands are able to coordination by both S and the neighbouring N atom, and hence to the formation of stable chelate rings of five or more atoms.[78-81]

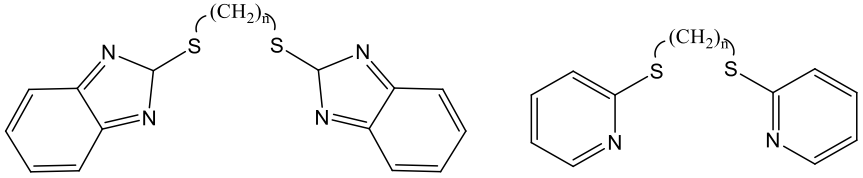

Figure 1.4. The $(CH_2)_n(SAz)_2$ based on a nitrogenated aromatic ring system.

In other works[38] a similar strategic way of synthesis has been carried out to obtain the ligand shown in **Figure 1.5**.

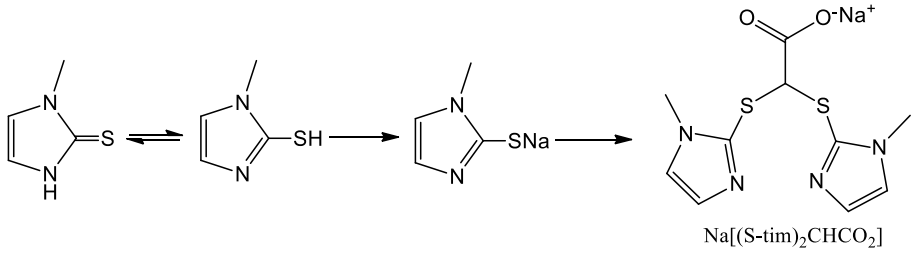

Figure 1.5. Synthesis of the sodium bis(1-methyl-1H-imidazol-2-ylthio)acetate ligand.

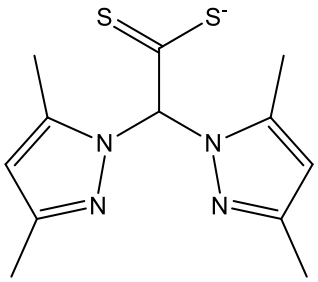

Figure 1.6. Schematic representation of the ligand $Li[LCS_2]$.

Some works with similar ligands, but in lithium salts (**Fig. 1.6**) as the bis(3,5-dimethylpyrazolyl)dithioacetate ligand ($Li[LCS_2]$) are reported in literature.[36]

In recent years many ligands of this type were studied for applications in medicinal and industrial chemistry in the formation of tin(IV) complexes. Many organotin compounds have been tested for their *in vitro* activity against a large variety of tumor lines.[75a,b,82] Recently organotin

compounds have been used as reagents in reduction, transmetallation and coupling reactions or as extremely versatile catalysts in organic reactions;[72b,d,c,83-88]. In the investigation of the possible utility of triorganotin trichloroacetates as CX_2 transfer agents it was found that they decompose with carbon dioxide evolution in the presence of an olefin.[89] In **Figure 1.7** a typology of this kind of complexes[31] is reported.

On the other hand the consequence is that considerable amounts of the organotins have entered various ecosystems.[90] Many studies[91,92] have reported the toxic effects of organotin compounds as contaminants of marine and freshwater ecosystems, and it has been demonstrated that, depending on the nature and the number of the organic groups bound to the tin cation, some organotins show specific toxic effects to different organisms even at very low concentrations.[93]

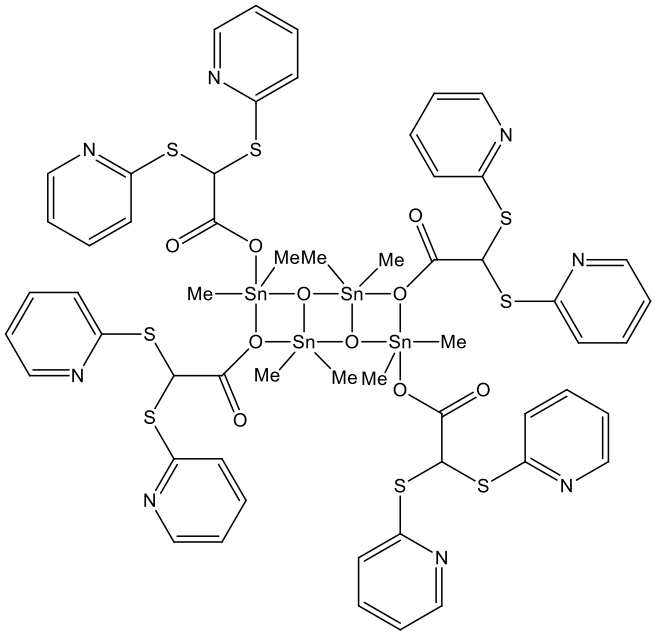

Figure 1.7. Structure of dimeric dicarboxylatotetramethyldistannoxane.

1.3. Conjugated heteroscorpionate ligands

In the last 10 years poly(pyrazol-1-yl)alkanes, especially bis(pyrazol-1-yl)methane, have been among the most widely used nitrogen-containing donor ligands. Modification of this system with organic functional groups on the bridging carbon atom to form novel heteroscorpionate ligands has also attracted considerable attention and their coordination chemistry towards main group and transition metals have been extensively studied.[1]

These intriguing heteroscorpionate ligands can contain different functional groups, such as carboxylate, dithiocarboxylate, alkoxide, thiolate, aryloxide, sulfonate, cyclopentadienyl, acetamidate,

thioacetamidate, amidate, amide and organometallic groups,[42,46,50] a situation that has broadened the scope of application of these novel ligands. Complexes containing these ligands have been of considerable interest owing to their important uses as biological enzyme models[13,20] and as olefin or cyclic ester polymerization catalysts.[8,22,27]

In this regard we have studied new functionalized ligands.

The first acetamidate and thioacetamidate heteroscorpionate ligands were prepared by Otero *et al*[94,95] by deprotonation at the methylene group of bis(3,5-dimethylpyrazol-1-yl)methane with *n*BuLi, followed by treatment with a series of isocyanates and isothiocyanates to yield the lithium compounds. Furthermore, enantiopure scorpionate ligands were obtained starting from chiral isocyanates or isothiocyanates.[96] These procedures can be applied to any type of substituted bis(pyrazol-1-yl)methanes and it is worth noting that it is possible to select the most appropriate pyrazole building block in the construction of the desired heteroscorpionate in order to tune both the electronic and steric effects in the subsequent coordination to a metal centre.[97]

Metronidazole (**Fig. 1.8**) are a class of hypoxia tracer that have been extensively investigated for hypoxia-selective cytotoxicity and hypoxic cell radiosensitisation *in vitro* and *in vivo*.[98] It has been shown that nitroimidazoles can be trapped in cells with low pO_2 values[99], and the 2-nitroimidazole compounds such as the [^{18}F]fluoromisonidazole (^{18}FMISO) have been used for PET imaging of stroke, myocardium ischemia and tumor hypoxia.[100-103] 2-Nitroimidazole cyclam derivatives radiolabelled with ^{99m}Tc, ^{64}Cu and ^{67}Cu have also been investigated as potential PET/SPECT agents for tumor hypoxia.[104] 4-Nitroimidazole-based thioflavin-T derivatives were synthesized, radiolabelled with iodine-131 and showed *in vitro* binding to viable hypoxic or aerobic tumor cells.[105]

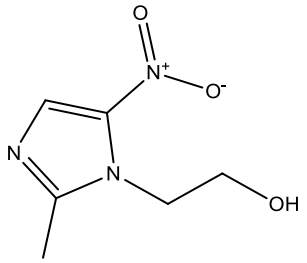

Figure 1.8. Structure of Metronidazole.

Recently, bis(thiosemicarbazonato)copper(II)–nitroimidazole conjugates were successfully synthesized in their cold and ^{64}Cu radiolabelled forms by Bayly *et al.*,[106] nitroimidazole conjugates of bis(thiosemicarbazonato)copper(II) showed additive or synergistic selectivity for tumor hypoxia compared to their individual components. In 2011 a new nitroimidazole(2-methyl-5-nitro-imidazole) conjugated heteroscorpionate ligand and its copper(II) derivative have been synthesized.[107]

1.4. Phosphanes

Phosphine (IUPAC name: Phosphane) is the compound with the chemical formula PH_3. It is a colorless, flammable, toxic gas. Pure phosphine is odorless, but technical grade samples have a highly unpleasant odor like garlic or rotting fish, due to the presence of substituted phosphine and diphosphane (P_2H_4). With traces of P_2H_4 present, PH_3 is spontaneously flammable in air, burning with a luminous flame. Phosphines are a group of organophosphorus compounds with the formula R_3P (R = organic derivative).

Phosphines and diphosphines are widely used in transition metal chemistry, bonding strongly to many different metals in a wide variety of oxidation states. A very large number of derivatives have been synthesized and structural studies undertaken. Steric and electronic properties of phosphines can be altered in a systematic and predictable way. Thus phosphines can stabilise, and facilitate the study of, many metal complexes. Additionally, the chemical reactivity of transition metal complexes can be modified by changing the coordinated phosphine, subtly altering the metal-ligand bonding interactions, and hence the reactivity. Phosphine ligands can also influence the rate of reaction at a metal centre, by stabilising the transition state or destabilising the ground state.

Many phosphines and their transition metal complexes are commercially available. Tertiary phosphines have become one of the most widely used class of reagents in organic synthesis due to their high nucleophilic reactivity and the strong bonds which P forms with C, N, O or S.

The nature of the transition metal-phosphine bond is an important feature of both transition metal and phosphorus chemistry. Electron density transfer occurs from the phosphine to the metal centre and from the metal to the phosphine ligand, therefore the phosphine significantly affects the electronic properties of the complex. The steric size of the phosphine will also affect the properties of the complex. Thus the influence of the metal-phosphine interaction has widespread implications on the reactivity of the complex. The nature of the metal-phosphorus bond has been well documented,[108-110] and is determined by both electronic and steric effects.[111]

In his landmark review, Tolman[111] showed that electronic and steric properties of phosphine ligands were important in understanding the chemistry of transition metal-phosphine complexes, and in determining the relative reactivity of each ligand. The electronic parameter (χ) consists of both σ-donor and π-acceptor bonding effects and can be measured quantitatively, based on the carbonyl stretching frequencies of the metal complex. Phosphine cone angles (θ) were used as a measure of the spatial volume required by the ligand in the complex. Steric effects can have important electronic consequences and vice versa, affecting the nature of the metal-phosphine interaction. Therefore the σ-donor, π-acceptor and steric components of the metal-phosphorus interaction cannot be easily separated and quantified, although theoretical QALE (Quantitative Analysis of Ligand Effects) calculations[110] provide convenient and accurate approximations.

Conventionally[109] the bonding between a metal and the phosphine ligand is thought to consist of synergic σ- and π-components (Dewar-Chatt model).[112-114] The σ-bond is formed by donation of electrons from the ligand lone-pair orbital to an empty orbital on the metal centre, the ligand behaving as a Lewis base (σ-base).

A d_{π}-d_{π} backbond is formed by electron donation from a full metal d-orbital to an empty 3d phosphorus orbital of similar symmetry, the ligand behaving as a Lewis acid (π-acid) (**Fig. 1.9**):

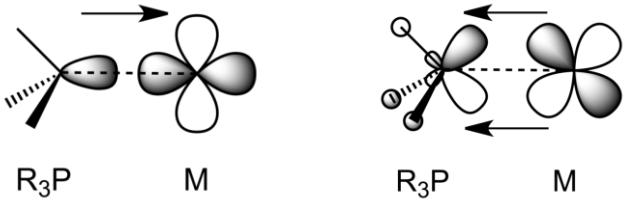

Figure 1.9. Bonding in metal-phosphine complexes.

Hybrid orbitals are involved in the non-bond, on coordination the sp^3 hybrid phosphorus orbitals are tetrahedral. Similarly, splitting of the crystal field generates d^2sp^3 hybrid metal acceptor orbitals, of σ-pseudo-symmetry. Crystal and ligand field theory[115,116] shows the effect on the energy of a metal atomic orbital (AO) in an electrostatic or ligand field. Field strength is dependent on the ligand basicity. Splitting of the d-orbital energy levels is caused by the spatial arrangement of the ligands about the metal, and affects the kinetic, thermodynamic and electronic properties of the metal.[117] Metal d-orbital degeneracy will be destroyed by the incoming ligands, because each orbital interacts with the ligands differently. In octahedral complexes, the $d_x2_{-y}2$ and d_z2 orbitals point directly at the incoming ligands, interacting with the ligand lone pair (bonding) electrons, d_{xy}, d_{xz} and d_{yz} orbitals point between the axes of ligand approach so their energy level is little affected by the incoming ligands. Thus the field is split into t_{2g} (d_{xy}, d_{xz} and d_{yz}) and e_g ($d_x2_{-y}2$ and d_z2) energy levels, with the metal electrons preferentially populating the lower (t_{2g}) energy level and leaving the e_g levels vacant. The difference between the two energy levels is the crystal field splitting energy (Δ_0). In octahedral transition metal complexes[118] the hybrid d-orbitals, of correct symmetry for non-bonding with the ligand, are the vacant e_g atomic orbitals (also forming the LUMOs). The populated t_{2g} atomic orbitals are not significantiy affected by the ligand's approach, becoming non-bonding molecular orbitals (HOMOs), and available for π-bonding.[119] The difference between HOMO and LUMO energies is a measure of the "hardness" of the system. Hardness[120] is a unifying concept for identifying shells and subshells in atoms and molecules. It is a measure of the resistance of the metal centre to the change in electron density distribution. For CO, alkenes and phosphines π-bonding occurs when the ligand possesses low-lying vacant atomic orbitals of the correct π-symmetry. Non-bonding electrons from the t_{2g} level (produced during a-bond formation) are stabilised by donation to a vacant orbital on the

phosphorus ligand. A schematic molecular orbital diagram for σ- and π-bond formation is shown below (**Fig. 1.10**):

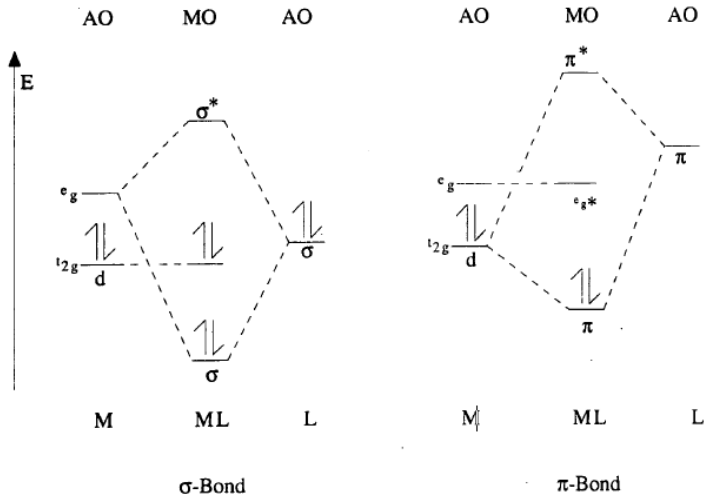

Figure 1.10. Molecular orbital-energy diagram for metal-phosphine bonding.

Low oxidation state metals are stabilised by π-bonding, the phosphine accepting the metal atom's excess electron density and thus lowering its reactivity. However the σ-donor and complimentary π-acceptor properties determine the overall electronic effect of the ligand.

Generally the attractive term in metal-phosphorus bonding is related to electronic factors and the repulsive component to steric factors. An electronic effect arises if changes to part of molecule result in a different electronic distribution within the molecule. This effect usually occurs via transmission along chemical bonds. A steric effect results when the size or shape of the molecule changes. For example, on going from $P(p\text{-}C_6H_4Cl)_3$ to $P(p\text{-}C_6H_4CH_3)_3$ a change in electronic effect would be expected, whilst for $P(p\text{-}C_6H_4CH_3)_3$ and $P(o\text{-}C_6H_4CH_3)_3$ the major change should be steric.[121] However, changing the steric effects can have significant electronic influence and vice versa. For example, greater angles between substituents because of increased bulk will reduce the amount of s-character in the phosphorus lone pair, so changing the electronic properties of the ligand. Changing the electronegativity of the attached atoms or groups may also affect the bond distances and angles at phosphorus. Consequently, electronic and steric effects (**Figure 1.11**) are inter-related and difficult to separate.

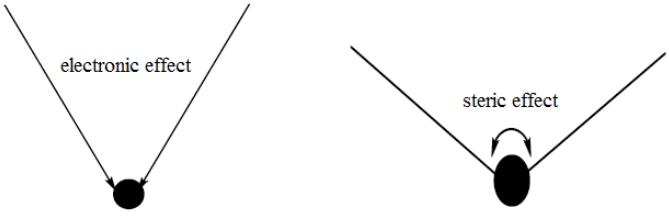

Figure 1.11. A schematic definition of electronic and steric effects.

Bearing in mind above the type of phosphines is essential to change the steric hindrance, the lipophilicity and then the solubility of the system.

In lecture[19,71] some works where a different type of phosphines was used are reported (**Fig. 1.12**).

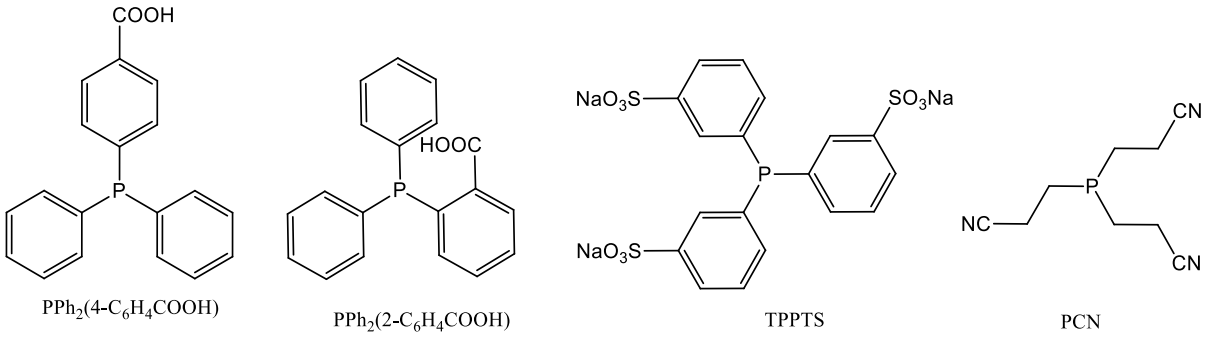

Figure 1.12. Structure of P-donor ligand.

1.5. Transition metal complexes as therapeutic agents

1.5.1. Platinum based anticancer drugs

Metals have an esteemed place in medicinal chemistry. Transition metals represent the d block element which includes groups 3-12 on the periodic table. Their d-shells are in process of filling. This property of transition metals resulted in the foundation of coordination complexes.

Metal complex or coordination compound is a structure consisting of a central metal atom, bonded to a surrounding array of molecules or anions. Sophus Jorgensen in Denmark synthesized metal conjugates for the first time in the mid 1870's. In 1893 the major breakthrough in this field was occurred when Alfred Werner investigated a series of compounds, which contained cobalt, chlorine and ammonia. He was awarded the Noble Prize in 1913 for his work.

The earliest reports on the therapeutic use of transition metal complexes in cancer and leukemia date from the sixteenth century. In 1960 the anti-tumor activity of an inorganic complex cis-diammine-dichloroplatinum(II) (cisplatin) was discovered. Cisplatin (**Fig. 1.13**) has developed into one of the most frequently used and most effective cytostatic drug for treatment of solid carcinomas. Other metal like gallium, germanium, tin, bismuth, titanium, ruthenium, rhodium, iridium, molybdenum, copper, gold were shown effective against tumors in man and animals.

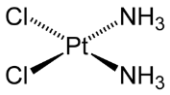

Figure 1.13. Structure of *cis*-diamminedichloroplatinum(II).

Platinum(II) complexes have been used as anti cancer drugs since long, among them cisplatin has proven to be a highly effective chemotherapeutic agent for treating various types of cancers.[122] Cisplatin moves into the cell through diffusion and active transport. Inside the cell it causes platination of DNA, which involves interstrand and intrastrand cross-linking as well as formation of adducts, usually through guanine, as it is the most electron rich site and hence, easily oxidized. Formation of cisplatin DNA adducts causes distortion and results in inhibition of DNA replication.[123] Cisplatin DNA adducts also serve as binding site for cellular proteins such as repair enzymes, histones, transcription factors and HMG-domain proteins.[124-126] The binding of HMGprotein to cisplatin-DNA adduct has been suggested to enhance anticancer effect of the drug.[127,128] Beside the effectiveness of cisplatin against cancer, it has encountered many side effects.

Drugs like cisplatin does not specifically affect cancer cells but they also effect the rapidly dividing cells of certain normal tissues, such as those found in hair follicles, bone marrow, and the lining of the gastrointestinal tract. Inside the cell it interacts with a number of other negatively charged bio-molecules besides DNA such as proteins, sulphur-containing compounds like metallothioneins and glutathiones that sequester heavy metals like Pt and remove it from the cell.

The clinical use of cisplatin is limited because of the toxicity to the normal cells and drug resistance, therefore, new platinum based anticancer drugs have also been synthesized such as carboplatin, oxaplatin, nedaplatin etc (**Fig. 1.14** and **1.15**). Other drugs are being developed that have slower hydrolysis rate than cisplatin, are longer acting and require more infrequent doses. One such drug is 2-pincoline Pt complex, which is active by injection and oral administration.

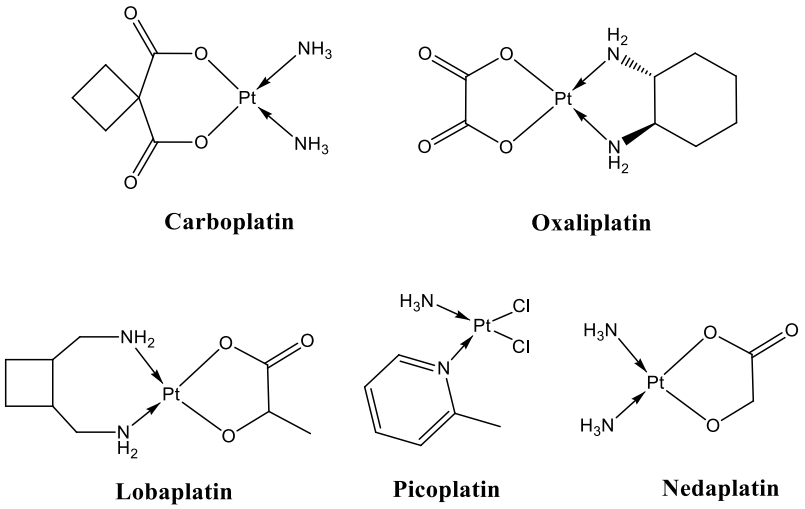

Figure 1.14. Structure of Pt(II)-based drugs.

Platinum complexes with distinctively different DNA binding modes from cisplatin may provide higher antitumor activity against cisplatin resistant cells. The trans isomer of diamminedichloro Pt(II) has also been studied; trans DDP offers a different attachment mode with DNA and is used as anticancer drug for cisplatin resistant cancer cells.

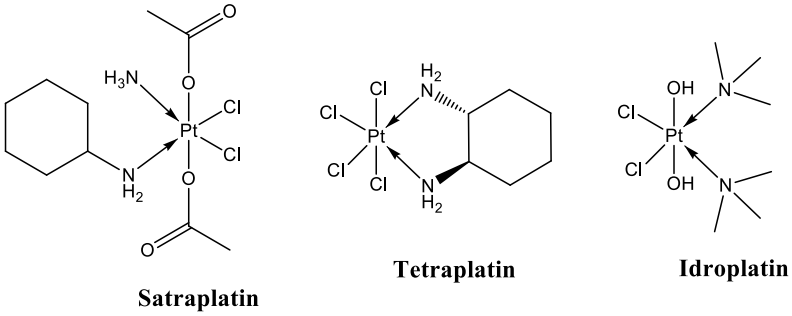

Figure 1.15. Structure of Pt(IV)-based drugs.

Platinum(IV) complexes are known to be less reactive and less toxic than Pt(II) complexes, so Sadler and coworkers based their design on Pt(IV) prodrugs (**Fig. 1.16**). To enable light activation,[130] Sadler *et al.*[129,131] incorporated azido ligands so as to introduce intense ligand-to-metal charge-transfer absorption bands.

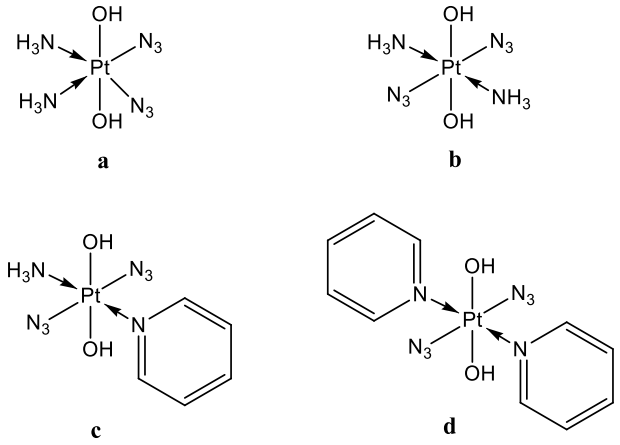

Figure 1.16. Structure of Pt(IV)-diazido system.

The cis-diazido Pt(IV) complex "a" is dark-stable and forms Pt(II)–GG cross-links similar to cisplatin on DNA, but only when irradiated with light by a mechanism involving electron transfer from azido (N_3^-) to Pt(IV) and the formation of N_2. Interestingly, when irradiated with UVA light, "b" is as active as cisplatin under conditions which might be used for photochemotherapy (short treatment and irradiation times of less than "a"). Moreover, when the geometry is changed from cis to trans, the ligand-to-metal charge-transfer (LMCT) band is shifted to a longer wavelength.[132] Short wavelength UVA light (365 nm) penetrates tissues to a depth of approximately 1 mm and could be

useful for surface cancers, such as bladder and esophageal cancer, but visible light penetrates more deeply (e.g. green to 3 mm and red to 5 mm). The potency of "b" as a photoactivated agent can be greatly increased by replacing one of the NH_3 ligands with pyridine, so that trans-$[Pt(N_3)_2(OH)_2(py)(NH_3)]$, "c" has little or no dark toxicity and when photoactivated it is considerably more potent towards human ovarian cancer cells (A2780) than cisplatin under similar conditions.[133] The introduction of a second pyridine ligand gives the all-trans complex "d" that can be activated in cells by UVA, blue, and green light, and is potently phototoxic at low light doses towards a number of human cancer cell lines, including parental (A2780) and cisplatin resistant (A2780CIS) ovarian carcinoma, esophageal adenocarcinoma (OE19), and hepatoma (HepG2) cells.[129]

However, cisplatin displays several limitations that restrict its utility to a great extent. For example, cisplatin is effective only for a narrow spectrum of tumor cells and additionally, because of its poor aqueous solubility (1 mg/mL), is administered intravenously. Moreover, the various toxicity in not target tissues like nephrotoxicity, neurotoxicity, hematogenesis, etc., associated with cisplatin, further complicates its usage. Therefore discovering new complexes selectively active on cancerous cells life cycle, in an anti-proliferative and/or pro-apoptotic manner, remains a challenge.

Several NHC (N-Heterocyclic Carbene) complexes of group 11 metals have been studied as an alternative to cisplatin. For example a series of innovative cytotoxic drugs, based on NHCs and amine ligands (NHC)(amine)PtI_2, was prepared by Marinetti *et al.*[134] and their efficacy against both cisplatin-sensitive (CEM and H460) and -resistant (A2780/DDP, CH1/DDP, and SKOV-3) cell lines was demonstrated by *in vitro* experiments. All novel complexes exhibited cytotoxic activities with IC_{50} at a micromolar range. In particular, complexes "f" and "g" (**Fig. 1.17**) were also significantly more potent than cisplatin against SKOV-3 cells, with IC_{50} of 2.8 and 2.6 μM, vs. 6.1 μM for cisplatin. These results demonstrated the potential anticancer activity of (NHC)PtI_2(amine) complexes and, therefore, offered a range of ligand pairs affording platinum complexes whose antitumor properties are associated with a trans geometry.

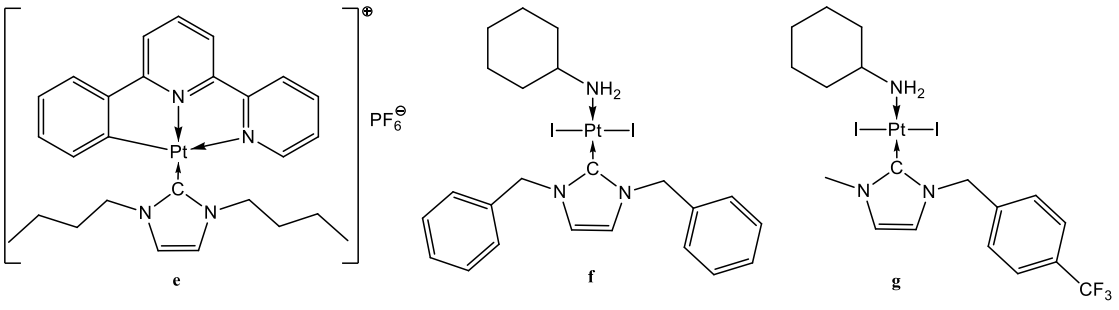

e f g

Figure 1.17. Structure of Pt(II) NHC systems.

1.5.2. Non-platinum anticancer agents

Platinum is not the only transition metal used in the treatment of cancer, various other transition metals being used as anticancer drugs.[135] Titanium complexes such as Titanocene dichloride had been recognized as active anticancer drug against breast and gastrointestinal carcinomas. Gold complexes also show anticancer activity, these complexes acting through a different mechanism as compared to cisplatin.[136] The target site of Au complexes is mitochondria and not DNA. Certain gold complexes with aromatic bipyridyl ligands have shown cytotoxicity against cancer cells.[137]

The 2-[(dimethylamino)methyl]phenyl gold(III) complex has also proven to be an antitumor agent against human cancers.[138] Gold nanoparticles when used in combination with radiotherapy or chemotherapy enhance DNA damage and make the treatment target specific.[139] Lanthanum has also been used to treat various forms of cancer.[140]

Ansari[141] studied some complexes of Mn(III) inducing tumor selective apoptosis of human cells.

Many ruthenium complexes were studied which showed anti-proliferative effects in human ovarian cancers. Ruthenium complexes with oxidation state +2 or +3 show antitumor activity against metastasis cancers. Ruthenocene derivatives act as anti estrogen.

The relative binding of ruthenocene derivatives were very high and even better than hydroxyl tamoxifen (**Fig. 1.18**) which is a novel antagonist for estrogen.[142]

Ruthenocene complexes with aromatic ligands represent a relatively new group of compounds with antitumor activity. Ru(III)imidazole and Ru(III)indazole exhibit anti cancer properties.

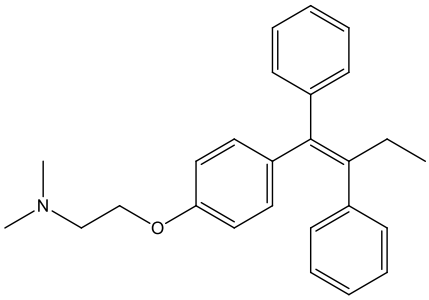

Figure 1.18. Tamoxifen.

Galanski[143] and his co-workers studied the anticancer properties of Ru(III) arene complexes. Ruthenocene-cymene complexes have shown to damage DNA by forming monofunctional adducts selectively with guanine bases.[144] Ruthenocene complexes show antiproliferative effect on the MCF-7 breast cancer cell lines. Many of Ru complexes exhibit anti-estrogen properties similar to that observed for novel anti-estrogen Tamoxifen.[145]

Complexes of transition metal like Iron have shown remarkable anti-proliferative properties.[146-148] Ferrocifenes exhibit anticancer activity against hormone dependent and hormone independent breast cancers. The ferrocene derivatives having hydroxyl groups in phenyl ring show high affinity for estrogen receptor.

1.5.3. Copper(I/II) complexes as new drugs

It is known that copper is an essential trace metal for living organisms.[149] This metal plays a crucial role in different enzymes (i.e., cytochrome-c oxidase, superoxide dismutase, ceruloplasmin, etc.) that catalyze oxidation/reduction reactions correlated with the antioxidant system of the organism.[150] It has been reported that certain copper complexes catalyze radical formation, while others seem to have efficacy as antioxidants.[151] The different behaviours depend upon the chemical environment and nature of the chelating agent. In this field, the study has been focused on copper(I/II) complexes containing "scorpionate" ligands.[152-154]

Copper is an endogenous element, so it could overcome some drawbacks presented by Pt(II) derivatives, especially their high toxicity and intrinsic or acquired resistance.[155] Moreover copper (or copper-containing fragments) has its own physiological transporters (Ctr) to enter the cell[156,157] and therefore, differently from other metal derivatives proposed as chemiotherapic agents, there is no need of coordination to the 'so called' cell penetrating peptides (CPP) in order to facilitate their internalization into the cell.[158]

Quantitative Structure-Activity relationship (QSAR) studies on these ternary complexes[159] indicated that:

• the presence of the central fused aromatic ring in the phen-containing complexes was necessary to preserve the antiproliferative activity;

• there was a strong relationship between IC_{50} and $E_{1/2}$, the most active species being the weaker oxidants;

• the nature of the O,O- or O,N-ligand had little influence on biological activity.

Copper is the centre of active sites of many metalloenzymes and metalloproteins and takes part to a large variety of biological processes. On the contrary, copper is reported to be also involved in a variety of processes related to cancer proliferation. In particular, an excess of copper appears to be an essential co-factor for angiogenesis,[160] and elevated levels of copper have been found in several types of human cancers.[161] These experimental evidences stimulated extensive investigations aimed at sequestrating the excess of copper by means of appropriate chelating agents.[162] Apparently in contrast with such an approach, several families of copper complexes comprising different ligands (e.g. thiosemicarbazones, Schiff bases, imidazoles derivatives, phosphines or carbenes) demonstrated notable anticancer activity.[163] The antiproliferative action of these copper complexes likely exploits the

altered homeostasis typical of cancer cells leading to copper unbalance (overloading) which, in turn, promotes cancer cell death by copper poisoning.

It has been reported that several copper complexes are able to overcome inherited or acquired cisplatin resistance exploiting alternative mechanisms of action that, even if not completely clarified yet, seem different from the covalent binding to DNA proper of Pt(II) drugs. For example, recent studies have evidenced the ability of some copper derivatives to induce oxidative stress[164] and/or inhibit proteasome activity.[165]

In the copper(II) complex $[Cu(nip)(acac)]NO_3$ (nip = 2-(naphthalen-1-yl)-1Himidazo[4,5-f][1,10]phenanthroline), "h" (**Fig. 1.19**), an intercalating mode of DNA binding has been proposed. Compound "h" oxidatively cleaved DNA without any exogenous additive.

The anticancer activity against human MCF-7, HeLa, HL-60 and MCF-12A (normal cell line) cells has been examined in comparison with the currently used drug paclitaxel under identical conditions by using MTT assay. It was found that the compounds exhibited significant cytotoxic activities in a time-dependent manner with IC_{50} values in the micro- and submicro-molar range and selectivity toward cancerous cells compared with normal cells. The ability of the drugs to induce either apoptosis or necrosis seems to be a primary factor in determining their efficacy.[166]

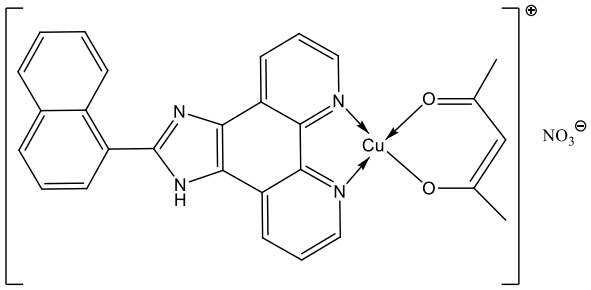

h

Figure 1.19. Structure of complex "h".

In the design of a new potentially active metallo-drug, beyond the nature of the metal, it is of paramount importance the choice of appropriate ligands, which affect the thermodynamic and kinetic stability as well as solubility and lipophilicity of the complexes.

In addition, bearing in mind that copper is usually bound to proteic domains rich in cysteine, methionine and histidine and considering the "soft" nature of Cu(I), the choice of ligands having soft donor atoms such as phosphorous in tertiary phosphines or aromatic sp^2 hybridized nitrogen of pyrazolyl derivatives, appear to be a promising strategy to obtain suitable derivatives for biological testing.

Many study have been focused to the copper and phosphine complexes: $[Cu_2(dppe)_3(CH_3CN)_2][ClO_4]_2$ exhibited a potent *in vitro* cytotoxicity against H460 human lung carcinoma cells (**Fig. 1.20**), with IC_{50} values comparable to those displayed by adriamycin.[167]

Mechanistic studies revealed that $[Cu_2(dppe)_3(CH_3CN)_2][ClO_4]_2$ damaged DNA *in vitro* and activated the p53 pathway eventually inhibiting the growth of cancer cells by inducing cell cycle arrest and apoptosis.[7] The authors also showed that simultaneous addition of $[Cu_2(dppe)_3(CH_3CN)_2][ClO_4]_2$ and of the DNA intercalating agent adriamycin increased the cytotoxicity of either compounds, suggesting the potential use of adriamycin with $[Cu_2(dppe)_3(CH_3CN)_2][ClO_4]_2$ in combination therapy.[167]

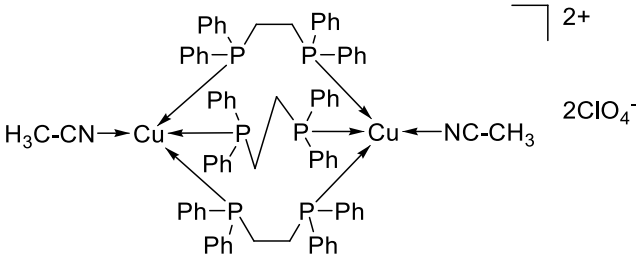

Figure 1.20. Structure of the $[Cu_2(dppe)_3(CH_3CN)_2][ClO_4]_2$ complex.

Following a similar mixed-ligand approach, several scorpionate ligands have been attached to a 'CuP_2' moiety. The use of dihydrobis(3-nitro-1,2,4-triazolyl)borate scorpionate ligands, $[H_2B(tz^{NO2})_2]^-$, had the double aim at increasing the water solubility and the kinetic inertness of the resulting mixed-complex.[168] Analogously, the choice for the hydrophilic tris(hydroxymethyl)phosphine (thp) allowed the preparation of perfectly aqueous soluble species with noteworthy cytotoxic properties.[20]

In particular, $\{[HC(CO_2)(pz^{Me2})_2]Cu(thp)_2\}$ was found to possess markedly higher antiproliferative activity against different human tumor cell lines (HL60, A549, MCF-7, A375 and LoVo) than that shown by cisplatin (**Fig. 1.21**).[20] Chemosensitivity tests performed on cisplatin sensitive and resistant human cancer cell lines established that (scorpionate)$Cu(thp)_2$ type compounds were able to overcome cisplatin resistance, supporting the hypothesis of a different mechanism of action compared to that exhibited by the reference drug.[20]

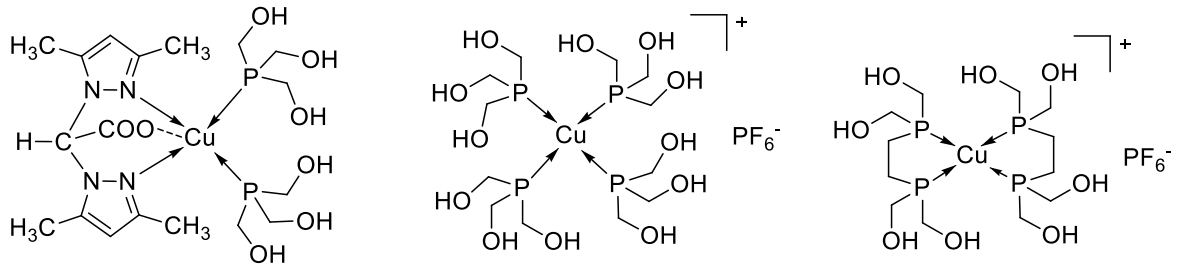

$\{[HC(CO_2)(pz^{Me2})_2]Cu(thp)_2\}$ $[Cu(thp)_4][PF_6]$ $[Cu(bhpe)_2][PF_6]$

Figure 1.21. Structure of phosphine copper(I) complexes.

Further information was provided by the design of two additional water soluble complexes featuring the 'CuP_4' coordination sphere, namely $[Cu(thp)_4][PF_6]$ and $[Cu(bhpe)_2][PF_6]$ (bhpe = bis[bis(hydroxymethyl)phosphino]ethane), (**Fig. 1.21**).[169] ESI-MS data supported the view of an

extremely stable substitution-inert entity in the case of $[Cu(bhpe)_2][PF_6]$ showing the molecular ion peak without detectable fragmentation, whereas $[Cu(thp)_4][PF_6]$ exhibited some lability showing the 'CuP_4' molecular ion along with the 'CuP_3' and 'CuP_2' molecular fragments at higher concentrations.[169] This remarkable different behaviour in the ion trap had a major impact on the cytotoxic profile of these two species. Complex $[Cu(bhpe)_2][PF_6]$ showed negligible *in vitro* antitumor activity suggesting that a marked kinetic inertness of the copper species is not a primary requirement.[169] On the contrary, it appeared that, as already shown by other cytotoxic copper complexes, labile sites at copper are necessary for the pro-drug to display its antiproliferative action.[20,168,169] Hence, $[Cu(thp)_4][PF_6]$ showed a potent cytotoxic activity on the same panel of tumor cells with IC_{50} values even over 30 times lower that those obtained with cisplatin; moreover, it overcame cisplatin resistance.[20,169] Different short-term proliferation assays measuring the damage to various subcellular organelles suggested that lysosomal damage represents the early cellular event associated with $[Cu(thp)_4][PF_6]$ cytotoxicity, probably mediated by an increased production of ROS.[169]

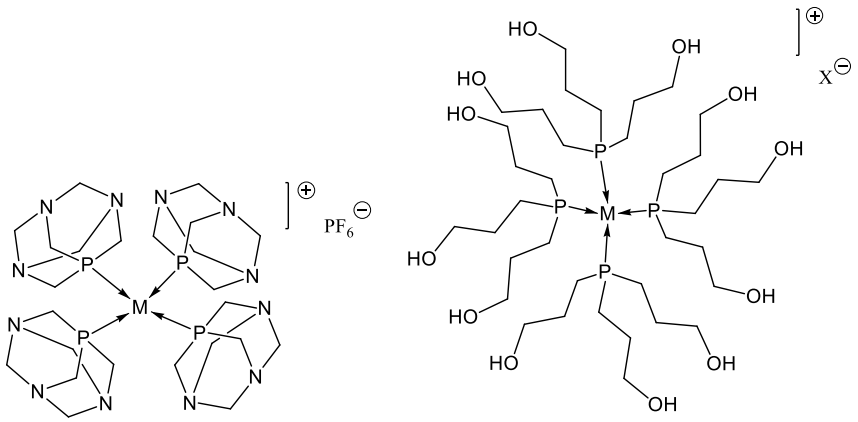

$[M(PTA)_4]PF_6$

i. M = Cu

j. M = Ag

k. M = Au

$[M(thpp)_4]X$

l. M = Cu X = PF_6

m. M = Ag X = PF_6

n. M = Au X = PF_6 , Cl

Figure 1.22. Structure of hydrophilic phosphine complexes of group 11 metals.

Considering the attractive cytotoxic properties shown by $[Cu(thp)_4]^+$ and $[Cu(PTA)_4]^+$, two series of water-soluble complexes were recently prepared ($[M(PTA)_4]^+$, "i-m" and $[M(thpp)_4]^+$, "l-n" where thpp is tris(hydroxypropyl)phosphine), whose steric electronic as well as hydrophilic-lipophilic properties could be tuned by modifications of the ligands (**Fig. 1.22**).

These phosphine complexes were evaluated for their cytotoxic activity toward a panel of seven human tumor cell lines, containing examples of ovarian (2008 and C13*), cervical (HeLa), lung (A549), colon (HCT-15), and breast (MCF-7) cancers and melanoma (A375). In general among the tested compounds, metal-thp species (**Fig. 1.21**) showed better cytotoxic activity compared to metal-

PTA and metal-thpp ones, and copper derivatives were always found to be the most efficacious.[170] In general, A549 and HCT-15 tumor cell lines were more sensitive toward all tested compounds with more than half metal(I) complexes having better cytotoxic activity compared to that shown by cisplatin. All investigated $[M(P)_4]^+$-type species were able to overcome cisplatin resistance.

Cytological stains and flow cytometric analyses indicated that $[Cu(thp)_4][PF_6]$ is able to inhibit the growth of tumor cells via G2/M cell cycle arrest and paraptosis accompanied with loss of mitochondrial transmembrane potential.[169] It is interesting to note that a similar cytotoxic profile was observed in HT1080 human fibrosarcoma cells treated with a Cu(II) thioxotriazolecomplex (**Fig. 1.23**).[171-173]

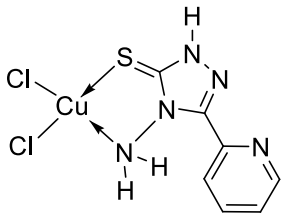

Figure 1.23. Structure of the 4-amino-5-(pyridin-2-yl)-2H-1,2,4-triazole-3(4H)-thione copper(II)complex.

Copper complexes bearing a thioxo group, such as disulfiram, showed strong toxicity against cancer cell lines or cancer xenografts.[174] Dallavalle *et al*.[171] demonstrated that the 4-amino-5-(pyridin-2-yl)-2H-1,2,4-triazole-3(4H)-thione copper(II) complex exhibited in HT1080 human fibrosarcoma cells a cytotoxic activity comparable to that exhibited by cisplatin. These effects were further investigated, leading to the conclusion that this triazole derivative complex caused a variant of programmed cell death (PCD) clearly distinct from apoptosis.[172] Indeed, the morphological hallmark of the death process induced by this complex was found to consist of a massive cytoplasmic vacuolization. No evidence of nuclear fragmentation neither of caspase-3 activation, biochemical features of apoptosis were observed.[172] These results suggested that the 4-amino-5-(pyridin-2-yl)-2H-1,2,4-triazole-3(4H)-thione copper(II) drove sensitive cells toward a non apoptotic PCD because it blocked caspase-3-dependent apoptotic pathways.

However other metal complexes with acetate ligands such as Nb, Re, Mn and Cr complexes have been reported in lecture.[9,42,43,175-177]

The antitumor properties of some acetate ligands (**Fig. 1.24**) and relative complexes (**Fig. 1.25**) were studied[20] and compared with the cisplatin (**Tab. 1**).[20]

Table 1. Cytotoxic Activity*

Compound	IC_{50} (μM) ± S.D.				
	HL60	A549	MCF-7	A375	LoVo
$[HC(CO_2)(tz)_2]Cu[P(CH_2OH)_3]_2$, **p**	34.31 ± 3.9	25.13 ± 1.1	11.29 ± 1.7	26.66 ± 2.0	32.28 ± 3.6
$[HC(CO_2)(pz^{Me2})_2]Cu[P(CH_2OH)_3]_2$, **q**	10.60 ± 2.5	2.10 ± 1.3	1.55 ± 0.19	2.55 ± 0.9	7.83 ± 1.3
$[(CH_3CN)_2Cu(P(CH_2OH)_3]_2]PF_6$, **r**	21.15 ± 2.8	14.81 ± 0.9	16.7 ± 2.7	21.52 ± 1.7	47.17 ± 2.9
$Na[HC(CO_2)(tz)_2]$, **o**	ND	ND	ND	ND	ND
$P(CH_2OH)_3$	58.67 ± 2.3	72.97 ± 2.4	64.21 ± 4.2	88.71 ± 3.8	65.21 ± 3.2
$Na[HC(CO_2)(pz^{Me2})_2]$, **o'**	ND	ND	88.81 ± 3.9	ND	ND
cisplatin	19.9 ±2.5	39.27 ± 1.9	30.18 ± 1.5	20.28 ± 1.3	24.97 ± 1.5

*ND = not detectable. S.D. = standard deviation. IC_{50} values were calculated by probit analysis ($P < 0.05$, χ^2 test). Cells (5-8 x 10^4•mL^{-1}) were treated for 48 h with increasing concentrations of tested compounds. Cytotoxicity was assessed by MTT test.

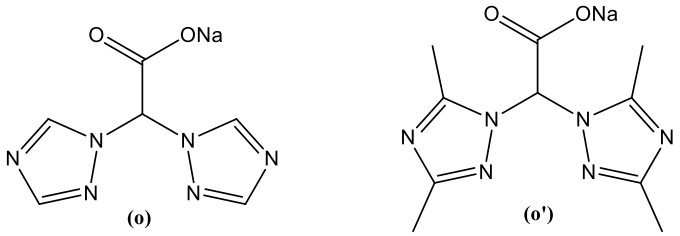

Figure 1.24. Structure of the ligands: (o) sodium bis(1,2,4-triazol-1-yl)acetate, $Na[HC(CO_2)(tz)_2]$; (o') sodium bis(3,5-dimethylpyrazol-1-yl)acetate, $Na[HC(CO_2)(pz^{Me2})_2]$.

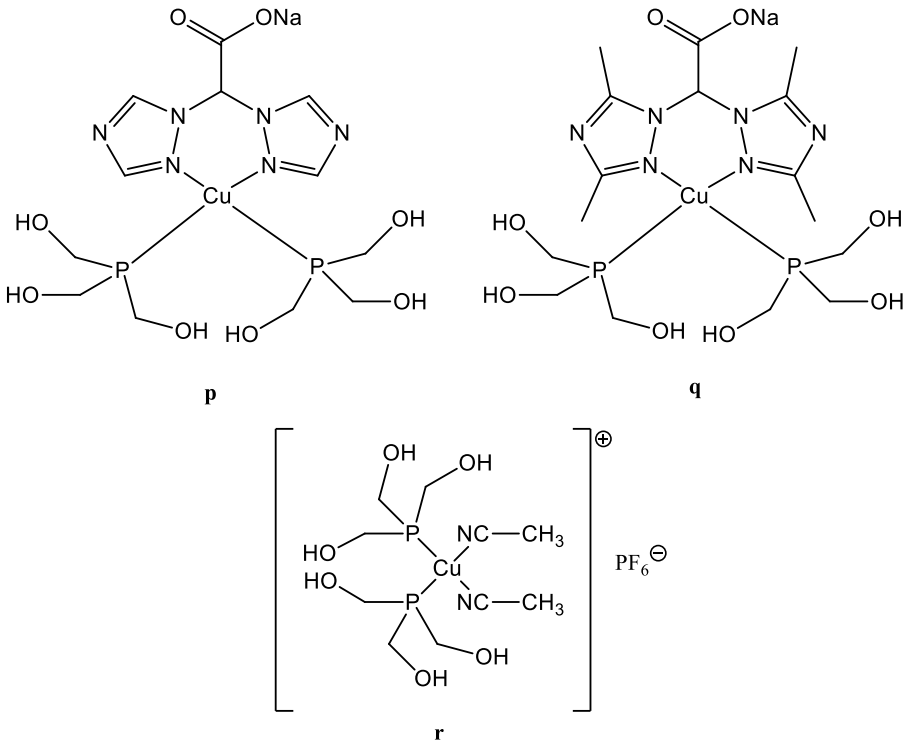

Figure 1.25. Structure of selected Cu(I) complexes.

The half maximal inhibitory concentration (IC_{50}) is a measure of the effectiveness of a substance in inhibiting a specific biological or biochemical function. This quantitative measure indicates how much of a particular drug or other substance (inhibitor) is needed to inhibit a given biological process (or component of a process, i.e. an enzyme, cell, cell receptor or microorganism) by half. It is commonly used as a measure of antagonist drug potency in pharmacological research. IC_{50} represents the concentration of a drug that is required for 50% inhibition *in vitro*. In **Table 1**. It is interesting to note that the IC_{50} values of some complexes (i.e., compound "q") are lower than those of cisplatin reference drugs, indicating a significantly greater activity than that of the chemotherapeutic reference.

1.5.4. Silver(I) complexes as new drugs

The history of silver goes back to the period that people started using this metal for coins and jewellery. Nowadays silver is still used for same purposes, as well as in conductors and in dentistry.

Silver is proving to have a number of medicinal applications; as antiseptic,[178] antibacterial,[179] anti-inflammatory[180] and chemotherapeutic agents.[181-187]

The antimicrobial activity of silver ions is closely related to their interaction with nucleic acids, preferentially with the bases in DNA rather than with the phosphate groups, although the significance of this in terms of their lethal action is unclear.[179] The antimicrobial activity of silver ions is also due to their interaction with thiol (sulfhydryl) groups of proteins by binding to key functional groups of enzymes.[179]

The potent anti-inflammatory properties of silver ions on wounds have been recognized for centuries and have been demonstrated histologically.[180] Nowadays, silver sulphadiazine is a topical anti-infective, used worldwide for dermal injuries, approved by the US Food and Drug Administration.[188] It has a broad antibacterial spectrum including virtually all microbial species likely to infect a burn wound.[188]

Biersack *et al*. have reviewed the antitumor activity of coinage metal complexes against breast cancer, concluding that silver complexes of cyclooxygenase inhibitors such as acetylsalicylate are conspicuously efficacious against breast cancers[189-191a] while Tan *et al*. have also reviewed developments in the design of coinage metal complexes with antitumor activity and discussed the emerging importance of quantitative structure–activity relationship methods in the study of anticancer metal complexes.[191b] Early reviews recording advances in the screening for antitumor potential of N-heterocyclic carbenes including silver(I) compounds are available,[192] but there is no specific review on the antitumor activity of silver(I) complexes. Given the importance of silver(I) in medicine it is surprising that a number of reviews of the particular subject of silver(I) compounds with anti-tumor activity are not available.

In literature some papers about silver(I) complexes and their biological activity are reported. For example $[Ag_2(NH_3)_2(salH)_2]$ (s) (**Fig. 1.26**) ($salH_2$ = salicylic acid) was synthesized and characterized by X-ray crystallography.[193] Each metal is coordinated with an oxygen atom from the carboxylic group of salicylic acid and with an ammonia nitrogen atom in an almost linear fashion.[193]

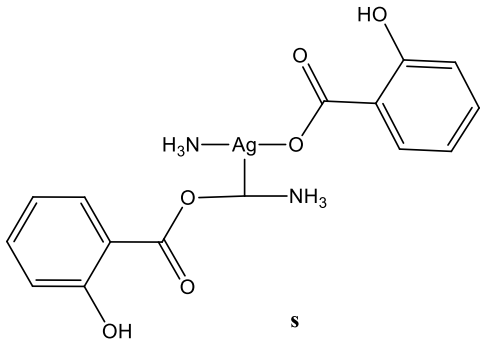

s

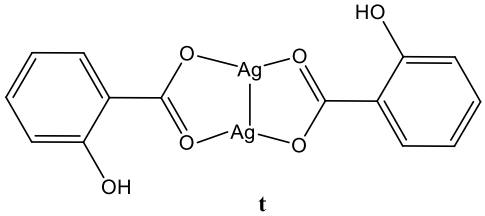

t

Figure 1.26. Structure of $[Ag_2(NH_3)_2(salH)_2]$, "s" and $[Ag_2(salH)_2]$, "t".

The two $[Ag(NH_3)(salH)]$ units of the complex are linked to each other by an Ag-Ag bond. $AgClO_4$, $salH_2$, "s" and $[Ag_2(salH)_2]$, "t" (**Fig. 1.26**) were tested against the three human cancer cell lines, squamous carcinoma tongue (Cal-27), HepG2 and human kidney adenocarcinoma (A-498) cells.[193] Silver salt and its complexes show stronger activity against all cell lines tested than the free ligand $salH_2$. Higher activity exhibited by "s" against Hep-G2 cells, which is higher than that of cisplatin but less than the corresponding one of $AgClO_4$. The stronger activity of "t" is observed towards A-498 cells, which is lower than the corresponding one of cisplatin.[193]

Mixed ligands silver(I) complexes of formulae $\{[Ag(tpp)_3\text{-}(asp)](dmf)\}$, "u" (aspH = o-acetylsalicylic acid and tpp = triphenylphosphine) and $[Ag(tpp)_2(o\text{-}Hbza)]$ "v" (o-HbzaH = o-hydroxy-benzoic acid) were synthesized and characterized by elemental analyses, spectroscopic techniques and X-ray crystallography (**Fig. 28**).[190] Complexes "u" and "v" and the $AgNO_3$ salt were tested for their *in vitro* cytotoxic activity against leiomyosarcoma cells (LMS), human breast adenocarcinoma (MCF-7) and normal human fetal lung fibroblasts (MRC-5) cells.[190] For both cancerous cell lines LMS and MCF-7 compounds "u" and "v" were found to be more active than cisplatin. Additionally, "u" and "v" exhibited lower activity on cell growth proliferation of MRC-5 cells than against sarcoma or carcinoma cells. Silver nitrate is less active than "u" and "v" against LMS and MRC-5 cells. The apoptotic type of LMS cell death caused by "u" and "v" was also confirmed by

the means of flow cytometry assay. Since the inhibition of the lipoxygenase (LOX) induces apoptosis in cells, the influence of the complexes "u" and "v" upon the catalytic peroxidation of linoleic acid to hydroperoxylinoleic acid by LOX was studied.[190] The results showed that "u" and "v" inhibit stronger LOX activity than cisplatin.

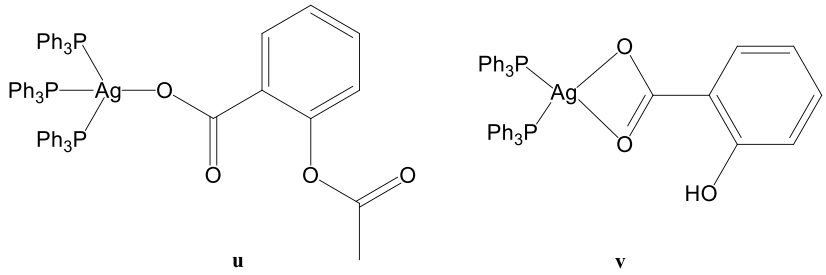

Figure 1.27. Structure of {[Ag(tpp)$_3$(asp)](dmf)} "u" and [Ag(tpp)$_2$(o-Hbza)] "v".

In literature several silver(I) complexes with amino acids ligands[194] (**Fig. 1.28)** and with nitrogen, nitrogen–oxygen, nitrogen–sulfur and sulfur donor ligands[195,196] are present (**Fig. 1.29)**.

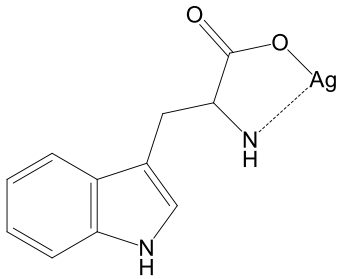

[Ag(TRP)]

TRPH = tryptophan

Figure 1.28. Structure of a silver(I) tryptophan complex.

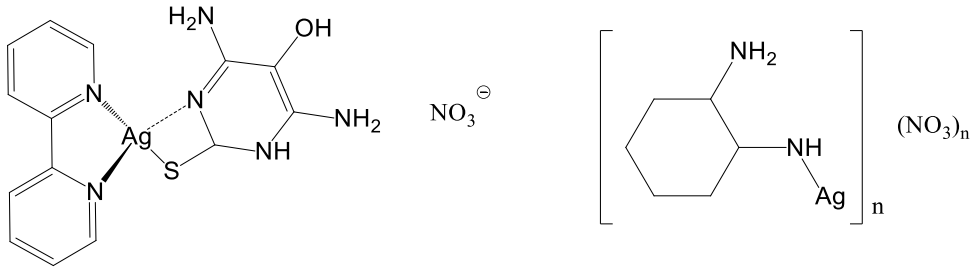

[Ag(bpy)(Hdahmp)]NO_3
Hdahmp = 4,6-diamino-5-hydroxy-2-mercaptopyrimidine

[Ag(dach)]$_n$(NO_3)$_n$
dach = 1,2-diaminocyclohexane

Figure 1.29. Structure of complexes with nitrogen, nitrogen–oxygen, nitrogen–sulfur and sulfur donor ligands.

Silver(I) *N*-Heterocyclic carbene complexes are another class of metallodrugs very much to the fore at present. Two comprehensive reviews on the anticancer properties of several metal NHC complexes, including silver ones, have been presented by Teyssot[197] and Gust.[198]

Youngs *et al.* described a series of Ag–NHC complexes derived from 4,5-dichloro-1H-imidazole[199], "w" (**Fig. 1.30**). All complexes exhibited cytotoxic activity against ovarian (OVCAR-3) and breast (MB157) cancer cells *in vitro*. However, they had little effect on cervical (HeLa) cancer cells. Further *in vivo* studies showed that [4,5-dichloro-1,3-dimethylimidazol-2-ylidene]-silver(I) acetate was active against ovarian cancer in mice, where the mode of delivery is through intraperitoneal injection. Panda *et al.* reported an analogous Ag–NHC complex, "y" and "y'" (**Fig. 1.30**) with low cytotoxic effects on HeLa cells.[147]

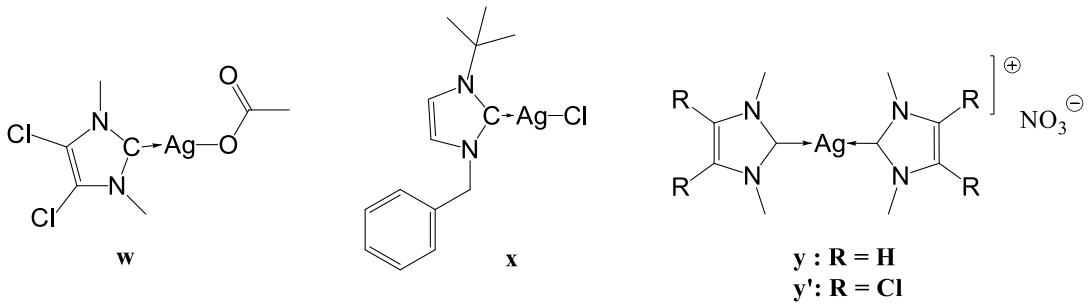

Figure 1.30. Structure of NHC-silver complexes.

Two Ag–bis(NHC) complexes, bis[1,3-dimethylimidazol-2-ylidene]silver(I) nitrate, "y" and bis[4,5-dichloro-1,3- dimethylimidazol-2-ylidene]silver(I) nitrate, "y", were prepared by the same group. They displayed similar antitumor efficacy against H460 lung cancer cells; however, they were less cytotoxic than cisplatin.[200]

A series of monodentate, bidentate and macrocyclic cationic Ag–bis(NHC) complexes was prepared by Willans *et al.* exhibiting cytotoxicity comparable to cisplatin (**Fig. 1.31**).[201] The complexes bearing bidentate ligands showed higher activity in human breast (MCF-7) and human colon (DLD-1) adenocarcinoma cell lines in comparison with the complexes with monodentate and macrocyclic ligands.

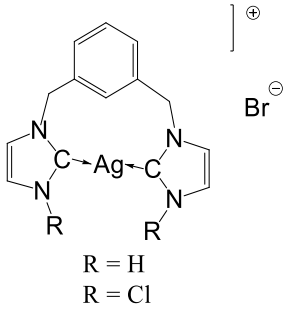

Figure 1.31. Structure of bidentate NHC-silver complexes.

1.6. Alternative structures: Metal-Organic Fraimeworks (MOFs)

Metal–organic frameworks (MOFs), also known as coordination polymers,[202] represent a new class of metal–ligand coordination compounds, in which the metal centers are interconnected by organic linkers to display a variety of infinite supramolecular networks, and such useful properties as magnetic ordering, microporosity and nonlinear optical activity.[203] Synthetic strategies for the predicted assembly of MOFs are of great importance for the desired new materials, and a modular construction or building-block methodology is proven to be efficient in the generation of premeditated frameworks, in which the connectivity information is encoded within the metal and ligand precursors.[204]

Network topology is an important and essential aspect of the design and analysis of MOFs and also of an inherent interest in understanding the supramolecular assembly. In this approach, complicated frameworks are simplified to simple node-and-connection reference nets.[205] New insights into the development of approaches for the engineering of MOFs are then possible on the basis of topological considerations.[202,204,205] Therefore, new or unusual network topologies are of considerable focus,[206] particularly those deliberately constructed from the nodes with connectivity commonly displayed by typical metal ions and organic ligands used in MOFs synthesis. Generally, they contain the required geometrical information and the directional binding modes that will facilitate the crystallization of MOFs with predesigned topologies.

Bearing in mind above it is important to know that some MOFs containing bis(1,2,4-triazol-1-yl)acetate (btza) derivates[207] namely [{[Mn(btza)$_2$(H$_2$O)$_2$]•2H$_2$O}$_n$], [{[Zn(btza)$_2$(H$_2$O)$_2$]•2H$_2$O}$_n$], [{[Cu(btza)$_2$]•H$_2$O}$_n$], and [{[Cd(btza)$_2$]•3H$_2$O}$_n$] were recently synthesized. These MOFs are simply generated from the solution-assembly of a new potential triconnected ligand (Hbtza), with familiar octahedral metal nodes such as Mn^{II}, Zn^{II}, Cu^{II}, and Cd^{II}. Metal-directed production of two isostructural 4-connected frameworks with a SrAl$_2$ (sra) topology, namely [{[Ag(btza)]glycol}$_n$] and [{[Ag(btza)]•CH$_3$OH}$_n$], is also described by use of an univalent silver ion as the tetrahedral metal node (**Fig. 1.32**).

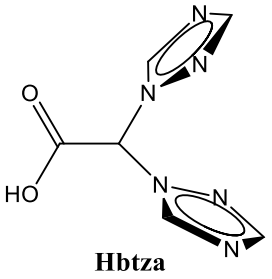

Hbtza

- [{[Mn(btza)$_2$(H$_2$O)$_2$]·2H$_2$O}$_n$]
- [{[Zn(btza)$_2$(H$_2$O)$_2$]·2H$_2$O}$_n$]
- [{[Cu(btza)$_2$]·H$_2$O}$_n$]
- [{[Cd(btza)$_2$]·3H$_2$O}$_n$]
- [{[Ag(btza)]·glycol}$_n$]
- [{[Ag(btza)]·CH$_3$OH}$_n$]

Figure 1.32. Structure of Hbtz and related complexes.

The design principles of this type of MOFs topologies are: a) the new ligand btza has three metal binding moieties and the tripodal backbone, which will be potentially able to behave as a triconnected node; b) the carboxylate group generally makes the ligand anionic and thus eliminates the requirement for charge balance of MOFs by inorganic counter anions, which may significantly influence the assembly and thus make it untraceable for structural prediction; c) the small steric size of the triazole ring and the coordinative flexibility of the overall backbone of the ligand due to the central sp^3 carbon atom jointly help to avoid crowding at the metal sphere and thus encourage the formation of highconnectivity networks. Presumably, when btza is properly coordinated to the first-row divalent metal cations, it is able to satisfactorily complete the coordination spheres and, as a consequence, lead to the generation of the (3,6)-connected frameworks with a general formula of $M(btza)_2$.

In **Figure 1.33** the local coordination geometry for the metal species are reported. The asymmetric unit contains one-half occupied Mn^{II} (isostructural to Zn^{II}) atom, one unique btza anionic ligand, one coordinated and one intercalated water molecule. The Mn^{II} center shows an octahedral coordination, coordinating to four different btza ligands through triazole nitrogen atoms in an equatorial fashion, and two trans axial water ligands. The ligands in turn coordinate to two metal atoms, through each of its triazole pendants, and are hydrogen bonded to a water ligand on a third metal through a carboxylate group. For the third compound, the asymmetric unit contains a half-occupied Cu^{II} atom, one btza ligand, and half a water molecule. Each octahedral Cu^{II} ion is bound to six separated btza ligands, coordinating to four through triazole nitrogen atoms , and to two through carboxylate oxygen atoms. Each ligand in turn coordinates to three Cu^{II} centers. Thus, the ligands and metals are combined to generate a 3D connected network. The intercalated water moiety is hydrogen bonded to the uncoordinated carboxylate oxygen atoms on two adjacent ligands, thus creating a hydrogen-bonded bridge. For the fourth compound, the asymmetric unit contains a half-occupied Cd^{II} ion, one ligand, and two unique water molecules. As in the previous structure, each octahedral Cd^{II} coordinates to six separate btza ligands, four through triazole nitrogen atoms, and two through carboxylate oxygen atoms. In turn, each ligand coordinates to three Cd^{II} centers. One of the intercalated water molecules is hydrogen bonded to both the coordinated carboxylate oxygen atom and the other intercalated water moiety. An overall 3D connected network is again formed. The structure of the last two compounds is isomorphous. However, because the methanol guests occupy the similar positions in the lattice to the glycol molecules, they each are hydrogen bonded to only one carboxylate oxygen atom. In turn, each uncoordinated carboxylate oxygen atom forms hydrogen bonds with only one methanol molecule, and thus there are no hydrogen-bonded bridges across the network in this case.

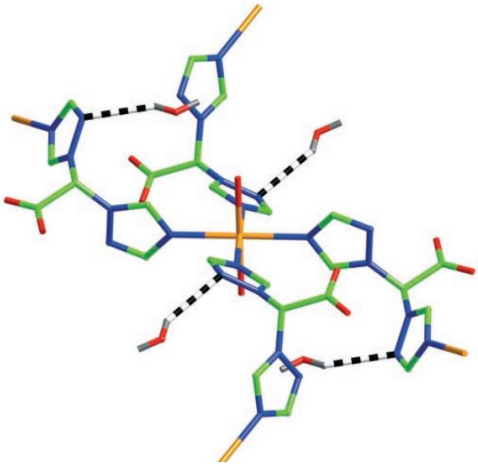

$[\{[M(btza)_2(H_2O)_2]\bullet 2H_2O\}_n]$ M = (Mn, Zn)

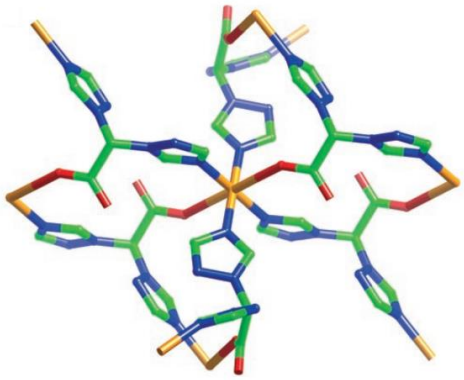

$[\{[Cu(btza)_2]\bullet H_2O\}$

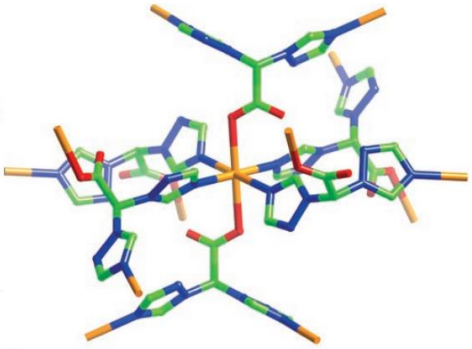

$[\{[Cd(btza)_2]\bullet 3H_2O\}_n]$

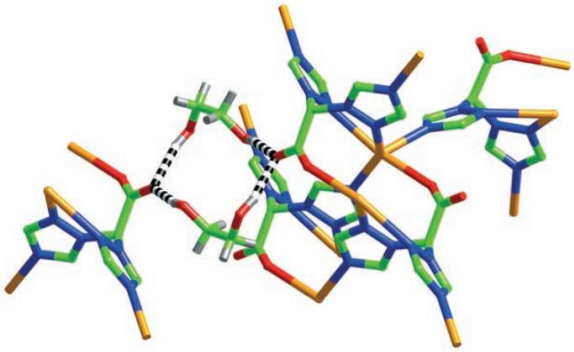

$[\{[Ag(btza)]\bullet glycol\}_n]$ isomorphous to $[\{[Ag(btza)]\bullet CH_3OH\}_n]$

Figure 1.33. Local coordination geometry of the metal species.

2. Experimental Section

2.1. Methods and materials

All reagents were purchased from Aldrich and used without further purification. All solvents were dried, degassed and distilled prior to use. Elemental analyses (C,H,N,S) were performed in house with a Thermo Fischer Flash 2000. Melting points were taken on an SMP3 Stuart Scientific Instrument. IR spectra were recorded as neat from 4000 to 600 cm^{-1} with a Perkin-Elmer Spectrum One System. IR annotations used: br = broad, m = medium, mbr = medium broad, s = strong, sbr = strong broad, sh = shoulder, w = weak.^{1}H-, ^{13}C- and ^{31}P-NMR spectra were recorded on a Oxford-400 Varian spectrometer (400.4 MHz for ^{1}H, 100.1 MHz for ^{13}C and 162.1 MHz for ^{31}P). Chemical shifts (δ) are quoted relative to internal $SiMe_4$. NMR annotations used: br = broad, m = multiplet, d= doublet, t = triplet, q = quartet. Electrospray mass spectra (ESI-MS) were obtained in positive- or negative-ion mode on a Series 1100 MSD detector HP spectrometer, using an acetone mobile phase. The compounds were added to reagent grade methanol, water or acetonitrile to give solutions of approximate concentration 0.1 mM. These solutions were injected (1 μL) into the spectrometer via a HPLC HP 1090 Series II fitted with an auto sampler. The pump delivered the solutions to the mass spectrometer source at a flow rate of 300 μL min^{-1}, and nitrogen was employed both as a drying and nebulizing gas. Capillary voltages were typically 4000 V and 3500 V for the positive- and negative-ion mode, respectively. Confirmation of all major species in this ESI-MS study was aided by comparison of the observed and predicted isotope distribution patterns, the latter calculated using the IsoPro 3.0 computer program.

2.1.1. Synthesis and characterization of the ligands

{[HC(CO_2H)($tz)_2$]} (1)

A THF solution (50 mL) of 1,2,4-triazole (1.910 g, 27.6 mmol) was added to a solution of NaOH (2.200 g, 55.0 mmol) and K_2CO_3 (7.600 g, 55.0 mmol) in 50 mL of THF. After 1 day of stirring, a methanol solution (10 mL) of dibromoacetic acid (3.010 g, 13.8 mmol) was added at room temperature dropwise to the salt; the mixture was gradually heated up to 150°C and was stirred for 2 days. The solution changed color to pale yellow after only 4 h. The solution was cooled to room temperature and dried under reduced pressure. Upon addition of a few millimeters of water, it was acidified with a HCl solution (2 M) until pH ≈ 2 and washed with $CHCl_3$ to obtain the ligand **1** in the aqueous phase, as a white solid in 61% yield. Compound **1** showed a good solubility in alcohols and water. M.p. 254°C. IR (cm^{-1}): 3388br (OH), 3102w, 3096w (CH), 2722w, 2481w, 1747s (ν_{asym} CO_2H), 1562m, 1520m (C=C + C=N), 1406s (ν_{sym} CO_2H). ^{1}H-NMR (D_2O, 293K): δ 7.58 (s, 1H, C*H*COO), 8.22 (s, 2H, 5-C*H*), 9.10 (s, 2H, 3-C*H*). ESIMS (major negative-ions, H_2O), *m/z* (%): 149 (55) [HC($tz)_2$]$^-$, 193 (100) [HC(CO_2)($tz)_2$]$^-$, 409 (60) [2HC(CO_2)($tz)_2$ + Na]$^-$. Calcd. for $C_6H_6N_6O_2$: C, 18.85; H, 1.78; N, 16.03%. Found: C, 18.64; H, 1.81; N, 17.85%.

{Na[HC(CO_2)($tz)_2$]} (2)

NaOH (0.400 g, 10.0 mmol) in a methanol solution (10 mL) was added to [HC(CO_2H)($tz)_2$], **1** (1.950 g, 10.0 mmol) to obtain the corrisponding sodium salt. The solution was stirred for 2 h and dried at reduced pressure to give derivative **2** as a white solid in 40% yield. Compound **2** showed a good solubility in methanol and water, but a lower solubility in DMSO and ethanol. The solubility was poor in chlorinated solvents too. M.p. 219-220°C. IR (cm^{-1}): 3139w, 3108w (CH), 1660s (ν_{asym} CO_2), 1500m, 1519m (C=C + C=N), 1377s (ν_{sym} CO_2). ^{1}H-NMR (DMSO, 293K): δ 6.93 (s, 1H, C*H*COO), 7.89 (s, 2H, 5-C*H*), 8.74 (s, 2H, 3-C*H*). ^{13}C-NMR (D_2O, 293K): δ 75.69 (*C*HCOO), 145.86 (2-*C*H), 152,69 (4-*C*H), 166.96 (*C*OO). ESIMS (major positive-ions, H_2O), *m/z* (%): 239 (100) [Na[HC(CO_2)($tz)_2$] + Na]$^+$, 455 (55) [2HC(CO_2)($tz)_2$ + 3Na]$^+$, 671 (90) [3HC(CO_2)($tz)_2$ + 4Na]$^+$. ESIMS (major negative-ions, H_2O), *m/z* (%): 149 (100) [HC($tz)_2$]$^-$, 193 (60) [HC(CO_2)($tz)_2$]$^-$, 409 (10) [2[HC(CO_2)($tz)_2$] + Na]$^-$. Calcd. for $C_6H_6N_6NaO_2$: C, 12.76; H, 0.91; N, 13.18%. Found: C, 12.93; H, 0.96; N, 15.01%.

{[HC(CO_2H)($pz^{Me2})_2$]} (3)

A THF solution (50 mL) of 3,5-dimethylpyrazole (2.647 g, 27.5 mmol) was added to a solution of NaOH (2.200 g, 55.0 mmol) and K_2CO_3 (7.600 g, 55.0 mmol) in THF (50 mL). After 1 day of stirring, a solution of dibromoacetic acid (3.010 g, 13.8 mmol) in methanol (10 mL) was added at room temperature dropwise to the salt and the mixture was stirred for 24 h. The solution was dried under reduced pressure. Upon addition of a few millimeters of water, it was acidified with a HCl solution (2

M) until pH ≈ 2 and whashed with $CHCl_3$ to obtain the ligand **3** as a white solid in 87% yield. Compound **3** showed a good solubility in alcohols, chlorinated solvents, DMSO but a lower solubility in water. M.p. 167-169°C. IR (cm^{-1}): 3451w (OH) 3126w, 3093w (CH), 2965w, 2926w, 1890mbr, 1741s (ν_{asym} CO_2H), 1560s, 1413s (ν_{sym} CO_2H), 1215sbr. ^{1}H-NMR ($CDCl_3$, 293K): δ 2.15 (s, 3H, C*H*$_3$), 2.21 (s, 3H, C*H*$_3$), 5.87 (s, C*H*), 6.82 (s, C*H*COO). ESIMS (major positive-ions, CH_3OH), *m/z* (%): 293 (100) $[Na[HC(CO_2)(pz^{Me2})_2] + Na]^+$. ESIMS (major negative-ions, CH_3OH), *m/z* (%): 247 (100) $[HC(CO_2)(pz^{Me2})_2]^-$. Calcd. for $C_{12}H_{16}N_4O_2$: C, 58.05; H, 6.50; N, 22.57%. Found: C, 57.83; H, 6.61; N, 21.93%.

{[HC(CO$_2$H)(pz)$_2$]} (4)

A THF solution (50 mL) of pyrazole (1.870 g, 27.5 mmol) was added to a solution of NaOH (2.200 g, 55.0 mmol) and K_2CO_3 (7.600 g, 55.0 mmol) in THF (50 mL). After 1 day of stirring, a solution of dibromoacetic acid (3.000 g, 13.8 mmol) in methanol (10 mL) was added at room temperature dropwise to the salt and the mixture was stirred for 24 h. The solution was dried under reduced pressure. Upon the addition of a few millimiters of water, it was acidified with a HCl solution (2 M) until pH ≈ 2 and whashed with $CHCl_3$ to obtain the ligand **4** as a white solid in 68% yield. Compound **4** showed a good solubility in alcohols, DMSO, and but a lower solubility in water by warming. M.p. 145-147°C. IR (cm^{-1}): 3429br (OH) 3177m, 3149m, 3130m, 3107m (CH), 2450mbr, 1720s (ν_{asym} CO_2H), 1517s, (ν_{sym} CO_2H), 1391s, 1351s, 1290s, 1257s, 1221s, 1169s, 1091s. ^{1}H-NMR (CD_3OD, 293K): δ 6.35 (t, 2H, C*H*), 7.34 (s, C*H*COO), 7.57 (d, C*H*$_2$), 7.90 (d, C*H*$_2$). ESIMS (major positive-ions, MetOH), *m/z* (%): 215 (100) $[HC(CO_2H)(pz)_2 + Na]^+$, 253 (50) $[Na[HC(CO_2)(pz)_2] + K]^+$, 269 (45) $[K[HC(CO_2)(pz)_2] + K]^+$, 193 (30) $[HC(CO_2H)(pz)_2 + H]^+$. ESIMS (major negative-ions, MetOH), *m/z* (%): 191 (100) $[HC(CO_2)(pz)_2]^-$, 405 (20) $[2HC(CO_2)(pz)_2 + Na]^-$. Calcd. for $C_8H_8N_4O_2$: C, 50.00; H, 4.20; N, 29.15%. Found: C, 48.97; H, 4.11; N, 28.93%.

{Na[(PyS)$_2$CHCO$_2$]} (5)

A methanol solution (100 mL) of 2-mercaptopyridine (PySH, 5.560 g, 50.0 mmol) was added to a solution of NaOH (3.600 g, 90.0 mmol) in absolute ethanol (40 mL) and the mixture was stirred for 24 h. A solution of dibromoacetic acid (5.450 g, 25.0 mmol) in absolute ethanol (40 mL) was added dropwise to the sodium obtained salt, and the mixture was stirred for 2 days, heating under reflux for 6 h to afford a pale yellow solid. The crude product was allowed to cool to r.t., concentrated under reduced pressure, and then filtered. A microcrystalline pale yellow precipitate was obtained that was recrystallized from methanol/acetone (1:2) to give ligand **5** in 86% yield. Compound **5** showed a good solubility in alcohols, water, DMSO, but it was insoluble in chlorinated solvents. M.p. 212-215°C. IR (cm^{-1}): 3053w (CH), 2905w, 1618s (ν_{asym} C=O), 1580m, 1555m (C=C + C=N), 1411m (ν_{sym} C=O), 1375m, 1133m. ^{1}H-NMR (D_2O, 293K): δ 5.78 (s, 1H, C*H*CO_2), 7.20 (m, 2H, 5-C*H*), 7.44 (m, 2H, 3-C*H*), 7.67 (m, 2H, 4-C*H*), 8.30 (m, 2H, 6-C*H*). ^{1}H-NMR (CD_3OD, 293K): δ 6.08 (s, 1H, C*H*CO_2), 7.08 (m, 2H, 5-C*H*),

7.45 (m, 2H, 3-C*H*), 7.62 (m, 2H, 4-C*H*), 8.33 (m, 2H, 6-C*H*). ^{1}H-NMR (DMSO, 293K): δ 5.68 (s, 1H, C*H*CO_2), 7.03 (m, 2H, 5-C*H*), 7.46 (m, 2H, 3-C*H*), 7.59 (m, 2H, 4-C*H*), 8.31 (m, 2H, 6-C*H*). ^{13}C-NMR (CD_3OD, 293K): δ 54.44 (*C*HCOO), 121.49 (5-*C*H), 123.93 (3-*C*H), 138.19 (4-*C*H), 150.28 (6-*C*H), 160.40 (2-*C*H), 200.93 (*C*OO). ESIMS (major positive-ions, CH_3OH), *m/z* (%): 301 (100) $[(PyS)_2CHCO_2H + Na]^+$, 579 (80) $[2(PyS)_2CHCO_2H + Na]^+$. ESIMS (major negative-ions, CH_3OH), *m/z* (%): 110 (100) $[PyS]^-$, 233 (30) $[(PyS)_2CHCO_2 - CO_2]^-$, 577 (30) $[(PyS)_2CHCO_2 + Na]^-$. Calcd. for $C_{12}H_9N_2NaO_2S_2$: C, 26.04; H, 1.69; N, 4.82; S, 11.40%. Found: C, 27.48; H, 1.79; N, 5.53; S, 12.67%.

{Na[(ImSMe)$_2$CHCO$_2$]} (6)

A methanol solution (100 mL) of 1-methyl-2(3H)mercaptoimidazole (HImSMe, 5.000 g, 43.8 mmol) was added to an absolute ethanol solution (40 mL) of NaOH (3.500 g, 87.6 mmol) and the mixture was stirred for 24 h. A solution of dibromoacetic acid (5.450 g, 25.0 mmol) in of absolute ethanol (40 mL) was added dropwise to the obtained sodium salt, and the mixture was stirred for 2 days, heating under reflux for 6 h to afford pale yellow solid. The crude product was allowed to cool to r.t., concentrated under reduced pressure, and then filtered. The solvent was removed under reduced pressure and the residue was treated with $CHCl_3$. The crude product was re-crystallized from chloroform/petroleum ether (1:4), to obtain the ligand **6** as a yellow solid in 74% yield. Compound **6** showed a good solubility in methanol, water, acetonitrile and chlorinated solvents. M.p. 112-118°C. IR (cm^{-1}): 3091w (CH), 2980w 1628s (ν_{asym} C=O), 1598m, 1574m (C=C + C=N), 1411m (ν_{sym} C=O), 1333m, 1276m. ^{1}H NMR ($CDCl_3$, 293K): δ 3.52 (s, 6H, CH_3), 5.05 (s, 1H, C*H*COO), 6.90 (s, 2H, C*H*), 6.97 (s, 2H, C*H*). ^{1}H-NMR (CD_3OD, 293K): δ 3.73 (s, 6H, CH_3), 5.01 (s, 1H, C*H*COO), 6.95 (d, 2H, C*H*), 7.14 (d, 2H, C*H*). ^{1}H-NMR (D_2O, 293K): δ 3.51 (s, 6H, CH_3), 4.77 (s, 1H, C*H*), 6.90 (d, 2H, C*H*), 7.00 (d, 2H, C*H*). ^{13}C NMR ($CDCl_3$, 293K): δ 34.13 (*C*H$_3$), 62.27 (*C*HCOO), 123.50 (*C*H), 129.94 (*C*H), 139.81 (*C*S), 173.16 (CH*C*OO). ^{13}C NMR (D_2O, 293K): δ 33.70 (*C*H$_3$), 60.79 (*C*HCOO), 125.10 (*C*H), 128.98 (*C*H), 137.81 (*C*S), 173.33 (CH*C*OO). ESIMS (major positive-ions, CH_3OH), *m/z* (%): 307 (100) $[Na[(ImSMe)_2CHCO_2] + H]^+$, 329 (85) $[Na[(ImSMe)_2CHCO_2] + Na]^+$. ESIMS (major negative-ions, CH_3OH), *m/z* (%): 285 (25) $[(ImSMe)_2CHCO_2]^-$, 239 (100) $[(ImSMe)_2CH]^-$. Calcd. for $C_{10}H_{12}N_4NaO_2S_2$: C, 42.24; H, 4.25; N, 19.7%. Found: C, 41.88; H, 4.36; N, 18.8%.

2,2-bis(3,5-dimethyl-1H-pyrazol-1-yl)-N-(2-(2-methyl-5-nitro-1H-imidazol-1-yl)ethyl)acetamide, {L^{MN}} (7)

A dichloromethane/dimethylformamide solution (5:1, 9 mL) of $[HC(CO_2H)(pz^{Me2})_2]$ (**3**) (0.124 g, 0.5 mmol) was added to a solution of triethylamine (0.303 g, 3.0 mmol), 1-(2-aminoethyl)-2-methyl-5-nitroimidazole dihydrochloride monohydrate (0.261 g, 1.0 mmol), 1-hydroxybenzotriazole hydrate (0.153 g, 1.0 mmol) and *N*-(3-dimethylaminopropyl)-*N'*-ethylcarbodiimide hydrochloride (0.192 g, 1.0 mmol) at 0°C. The mixture was allowed to warm to room temperature and it was stirred for 48 h. A chloroform solution (30 mL) was added and the mixture was washed with distilled water, and then

dried at reduced pressure. The residue was recrystallized from dichloromethane/diethyl ether (1:2), to obtain the ligand L^{MN} **7** as a white solid in 79% yield. Compound **7** showed a good solubility in alcohols, acetone, acetonitril, and chlorinated solvents, but it was insoluble in water. M.p. 155°C. IR (cm^{-1}): 3339m (NH), 2948mbr, 1670s (ν_{asym} C=O), 1562m, 1524s (C=C + C=N), 1478m, 1421s (ν_{sym} C=O), 1353m, 1257s, 1180s, 1147s, 1097s, 1028m, 877m. ^{1}H-NMR ($CDCl_3$, 293K): δ 2.18 (s, 6H, CH_3), 2.29 (s, 6H, CH_3), 2.46 (s, 3H, CH_3), 3.75 (t, 2H, CH_2NH), 4.49 (t, 2H, CH_2N), 5.85 (s, 2H, CH_{pz}), 6.54 (s, 1H, C*H*CO), 7.92 (s, 1H, CH_{MN}), 8.27 (mbr, 1H, N*H*). ^{13}C-NMR ($CDCl_3$, 293K): δ 11.42 (*C*H_3), 13.96 (*C*H_3), 14.39 (*C*H_3), 39.58 (*C*H_2NH), 45.04 (*C*H_2N), 69.97 (*C*HCO), 107.48 (*C*H), 133.44 (*C*H), 138.20 (*C*NO_2), 140.83 (*C*CH_3), 150.27 (*C*CH_3), 151.32 (*C*CH_3), 165.94 (*C*ONH). ESIMS (major positive-ions, CH_3OH), *m/z* (%): 401 (50) [L^{MN} + H]+, 423 (100) [L^{MN} + Na]$^+$, 824 (60) [$2L^{MN}$ + Na]$^+$. ESIMS (major negative-ions, CH_3OH), *m/z* (%): 399 (80) [L^{MN} - H]$^-$, 436 (100) [L^{MN} + Cl]$^-$. Calcd. for $C_{18}H_{24}N_8O_3$: C, 53.99; H, 6.04; N, 27.98%. Found: C, 54.07; H, 6.02; N, 27.78%.

N-(2-(2-methyl-5-nitro-1H-imidazol-1-yl)ethyl)-2,2-di(1H-pyrazol-1-yl)acetamide, {L^{MN1}} (8)

A dichloromethane/dimethylformamide solution (5:1, 9 mL) of [HC(CO_2H)($pz)_2$] (**4**) (0.096 g, 0.5 mmol) was added to a solution of triethylamine (0.303 g, 3.0 mmol), 1-(2-aminoethyl)-2-methyl-5-nitroimidazole dihydrochloride monohydrate (0.261 g, 1.0 mmol), 1-hydroxybenzotriazole hydrate (0.153, 1.0 mmol) and *N*-(3-dimethylaminopropyl)-*N'*-ethylcarbodiimide hydrochloride (0.192 g, 1.0 mmol) at 0 °C. The mixture was allowed to warm to room temperature and it was stirred for 48 h. A solution of chloroform (30 mL) was added and the mixture was washed with distilled water, and then dried at reduced pressure. The residue was recrystallized from dichloromethane/diethyl ether (1:2), to obtain the ligand L^{MN1}, **8** as a white solid in 80% yield. Compound **8** showed a good solubility in alcohols, acetone, acetonitrile, and chlorinated solvents, but it was insoluble in water. M.p. 140°C. IR (cm^{-1}): 3264m (NH), 3128m, 3084m, 2965m, 1686s (ν_{asym} C=O), 1548m, 1522s (C=C + C=N), 1457m, 1431s (ν_{sym} C=O), 1368s, 1260s, 1184s, 1152s, 1090s, 1050m, 964s. ^{1}H-NMR ($CDCl_3$, 293K): δ 2.48 (s, 3H, CH_3), 3.68 (t, 2H, CH_2NH), 4.48 (t, 2H, CH_2N), 6.33 (t, 2H, CH_{pz}), 6.91 (s, 1H, C*H*CO), 7.60 (d, 2H, CH_{pz}), 7.69 (mbr, 2H, CH_{pz}), 7.92 (s, 1H, CH_{MN}). ^{13}C-NMR ($CDCl_3$, 293K): δ 14.24 (*C*H_3), 39.70 (*C*H_2NH), 44.85 (*C*H_2N), 77.18 (*C*HCO), 107.56 (*C*H), 130.47 (*C*H), 133.50 (*C*NO_2), 141.81 (*C*CH_3), 165.04 (*C*ONH). ESIMS (major positive-ions, CH_3OH), *m/z* (%): 345 (100) [L^{MN1} + H]$^+$, 367 (90) [L^{MN1} + Na]$^+$, 711 (30) [$2L^{MN1}$ + Na]$^+$. ESIMS (major negative-ions, CH_3OH), *m/z* (%): 343 (100) [L^{MN1} - H]$^-$. Calcd. for $C_{14}H_{16}N_8O_3$: C, 48.26; H, 4.74; N, 31.27%. Found: C, 48.83; H, 4.68; N, 32.54%.

2.1.2. Synthesis and characterization of the $Cu^{(II)}$ complexes

{[HC(pz^{Me2})CO_2H]Cu[HC(pz^{Me2})CO_2]•ClO_4} (9)

An ethanol solution (25 mL) of $Cu(ClO_4)_2$•$6H_2O$ (0.137 g, 0.4 mmol) was added to an ethanol solution (25 mL) of [HC(CO_2H)(pz^{Me2})$_2$] (**3**) (0.184 g, 0.8 mmol). After the addition, the reaction mixture was stirred at room temperature for 24 h to obtain a blue precipitate which was filtered off and dried to constant weight to give complex **9** in 52% yield. Complex **9** showed a good solubility in methanol and DMSO, but but a lower solubility in water. M.p. 238°C dec. IR (cm^{-1}): 3138m, 2972mbr, 1705m (ν_{asym} C=O), 1560s, 1464m (ν_{sym} C=O), 1389m, 1311s, 1222mbr, 1077s. ESIMS (major positive-ions, CH_3OH), *m/z* (%): 581 (100) [{HC(pz^{Me2})CO_2}$_2$Cu + Na]$^+$, 558 (85) [{HC(pz^{Me2})CO_2}$_2$Cu + H]$^+$. ESIMS (major negative-ions, CH_3OH), *m/z* (%): 247 (100) [HC(CO_2)(pz^{Me2})$_2$]$^-$. Calcd. for $C_{24}H_{32}ClCuN_8O_8$: C, 43.69; H, 4.76; N, 15.61%. Found: C, 43.70; H, 4.89; N, 17.00%.

{[HC(CO_2)(tz)$_2$]$_2$Cu} (10)

An ethanol solution (25 mL) of $CuCl_2$•$2H_2O$ (0.170 g, 1.0 mmol) was added to an ethanol solution (25 mL) of Na[HC(CO_2)(tz)$_2$] (**2**) (0.216 g, 1.0 mmol). After the addition, the reaction mixture was stirred at room temperature for 24 h to obtain a green precipitate which was filtered off and dried to constant weight to give complex **10** in 31% yield. Complex **10** showed a good solubility in water but it was insoluble in alcohols and DMSO. M.p. 218°C. IR (cm^{-1}): 3136m, 3107m, 1667s (ν_{asym} C=O), 1519m, 1500m, 1376s (ν_{sym} C=O), 1275s, 1229s. ESIMS (major positive-ions, H_2O), *m/z* (%): 239 (100) [Na[HC(CO_2)(tz)$_2$] + Na]$^+$, 217 (55) [HC(CO_2H)(tz)$_2$ + Na]$^+$, 195 (30) [HC(CO_2H)(tz)$_2$ + H]$^+$, 279 (15) [{[HC(CO_2)(tz)$_2$]$_2$Cu$_2$(EtOH)}]$^{2+}$, 433 (20) [2[HC(CO_2)(tz)$_2$] + 2Na + H]$^+$, 455 (100) [2[HC(CO_2)(tz)$_2$] + 3Na]$^+$. ESIMS (major negative-ions, H_2O), *m/z* (%): 409 (100) [2HC(CO_2)(tz)$_2$ + Na]$^-$, 149 (40) [HC(tz)$_2$]$^-$, 193 (30) [HC(CO_2)(tz)$_2$]$^-$. Calcd. for $C_{12}H_{10}CuN_{12}O_4$: C, 32.06; H, 2.31; N, 32.05%. Found: C, 32.04; H, 2.24; N, 37.37%.

{[(PyS)$_2$CHCO_2]CuCl} (11)

An aqueous solution (25 mL) of $CuCl_2$•$2H_2O$ (0.084 g, 0.5 mmol) was added to an aqueous solution (25 mL) of Na[(PyS)$_2$CHCO_2] (**5**) (0.300 g, 1.0 mmol). After the addition, the reaction mixture was stirred at room temperature for 3 h to obtain a red-brown precipitate which was filtered off and dried to constant weight to give complex **11** in 29% yield. Complex **11** showed a good solubility in DMSO but a lower solubility in alcohols and water. M.p. 115°C dec. IR (cm^{-1}): 3050m, 1721m (ν_{asym} C=O), 1634m, 1579s, 1450s (ν_{sym} C=O), 1414s, 1334m, 1125s. ESIMS (major positive-ions, CH_3OH), *m/z* (%): 377 (100) [{(PyS)$_2$CHCO_2}CuCl + H]$^+$, 323 (95) [(PyS)$_2$CHCO_2 + 2Na]$^+$, 301 (45) [(PyS)$_2$CHCO_2H + Na]$^+$. ESIMS (major negative-ions, CH_3OH), *m/z* (%): 277 (100) [(PyS)$_2$CHCO_2]$^-$, 577 (90) [2(PyS)$_2$CHCO_2 + Na]$^-$. Calcd. for $C_{12}H_9ClCuN_2O_2S_2$: C, 39.86; H, 2.58; N, 7.60; S, 19.63%. Found: C, 38.30; H, 2.41; N, 7.44; S, 17.04%.

{[HC(CO$_2$H)(pz)$_2$]$_3$Cu(ClO$_4$)$_2$} (12)

An ethanol solution (25 mL) of Cu(ClO$_4$)$_2$•6H$_2$O (0.185 g, 0.5 mmol) was added to an ethanol solution (25 mL) of [HC(CO$_2$H)(pz)$_2$] (**4**) (0.192 g, 1.0 mmol). After the addition, the reaction mixture was stirred at room temperature for 24 h to obtain a blue precipitate which was filtered off and dried to constant weight to give complex **12** in 44% yield. Complex **12** show a good solubility in DMSO and methanol but a lower solubility in water. M.p. 234°C. IR (cm^{-1}): 3133m, 3012m, 1745mbr (ν_{asym} C=O), 1517m, 1450m, 1409s (ν_{sym} C=O), 1284s, 1105s, 1070s. ESIMS (major positive-ions, CH$_3$OH), *m/z* (%): 468 (100) [{HC(CO$_2$)(pz)$_2$}$_2$Cu + Na]$^+$. ESIMS (major negative-ions, CH$_3$OH), *m/z* (%): 191 (100) [HC(CO$_2$)(pz)$_2$]$^-$, 405 (75) [2HC(CO$_2$)(pz)$_2$ + Na]$^-$, 636 (40) [{HC(CO$_2$)(pz)$_2$}$_3$Cu]$^-$. Calcd. for C$_{24}$H$_{26}$Cl$_2$CuN$_{12}$O$_{15}$: C, 33.52; H, 2.61; N, 18.97%. Found: C, 33.64; H, 3.06; N, 19.61%.

{[HC(CO$_2$)(tz)$_2$]Cu(ClO$_4$)}•3H$_2$O (13)

A methanol solution (25 mL) of Cu(ClO$_4$)$_2$•6H$_2$O (0.370 g, 1.0 mmol) was added to a methanol solution (25 mL) of [HC(CO$_2$H)(tz)$_2$] (**1**) (0.388 g, 2.0 mmol). After the addition, the reaction mixture was stirred at room temperature for 24 h to obtain a green precipitate which was filtered off and dried to constant weight to give complex **13** in 23% yield. Complex **13** showed a good solubility in water but a lower solubility in alcohols and DMSO. M.p. 176°C dec. IR (cm^{-1}): 3447br (OH), 3127m, 1762m (ν_{asym} C=O), 1665mbr, 1526s, 1453m (ν_{sym} C=O), 1280s, 1118s, 1080sh. ESIMS (major positive-ions, H$_2$O), *m/z* (%): 195 (100) [HC(CO$_2$H)(tz)$_2$ + H]$^+$, 472 (30) [{HC(CO$_2$H)(tz)$_2$}$_2$Cu + Na]$^+$. ESIMS (major negative-ions, H$_2$O), *m/z* (%): 193 (100) [HC(CO$_2$)(tz)$_2$]$^-$, 149 (95) [HC(tz)$_2$]$^-$, 409 (45) [2HC(CO$_2$)(tz)$_2$ + Na]$^-$. Calcd. for C$_6$H$_{11}$ClCuN$_6$O$_9$: C, 18.24; H, 2.07; N, 19.39%. Found: C, 17.57; H, 2.70; N, 20.49%.

{(L^{MN})$_2$CuCl$_2$} (14)

A methanol solution (25 mL) of CuCl$_2$•2H$_2$O (0.085 g, 0.5 mmol) was added to a methanol solution (25 mL) of L^{MN} (**7**) (0.400 g, 1.0 mmol). After the addition, the reaction mixture was stirred at room temperature for 12 h to obtain a green solution which was dried under reduced pressure to constant weight to give complex **14** as a yellow solid in 76% yield. The complex **14** showed a good solubility in methanol and DMSO (in this case if the solution was warmed, it changed its color from green to yellow), but a lower solubility in water. M.p. 193°C. IR (cm^{-1}): 3412br (NH), 2963mbr (CH), 2791m, 1665s (ν_{asym} C=O), 1560s, 1526s, 1460s (ν_{sym} C=O), 1423s, 1358s, 1257s, 1182s, 1147m, 1050m. ESIMS (major positive-ions, CH$_3$OH), *m/z* (%): 401 (70) [L^{MN} + H]$^+$, 432 (100) [(L^{MN})$_2$Cu]$^{2+}$, 863 (20) [(L^{MN})$_2$Cu - H]$^+$. ESIMS (major negative-ions, CH$_3$OH), *m/z* (%): 399 (40) [L^{MN} - H]$^-$, 436 (100) [L^{MN} + Cl]$^-$. Calcd. for C$_{14}$H$_{16}$N$_8$O$_3$: C, 44.44; H, 5.18; N, 22.58%. Found: C, 46.23; H, 5.17; N, 23.96%.

{(L^{MN1})$_2$CuCl$_2$} (15)

A methanol solution (25 mL) of CuCl$_2$•2H$_2$O (0.045 g, 0.27 mmol) was added to a methanol solution (25 mL) of L^{MN1} (**8**) (0.196 g, 0.59 mmol). After the addition, the reaction mixture was stirred

at room temperature for 12 h to obtain a blue precipitate which was filtered off and dried to constant weight to give complex **15** as a blu in 43% yield. The complex **15** showed a good solubility in water, methanol and DMSO. M.p. 141°C. IR (cm^{-1}): 3276m, 3115m, 2749mbr, 1668s (ν_{asym} C=O), 1564m, 1523s, 1457m (ν_{sym} C=O), 1405m, 1360m, 1258s, 1184s, 1066s. ESIMS (major positive-ions, CH_3OH), *m/z* (%): 367 (100) $[L^{MN1} + Na]^+$, 345 (70) $[L^{MN1} + H]^+$. ESIMS (major negative-ions, CH_3OH), *m/z* (%): 343 (100) $[L^{MN1} - H]^-$, 313 (80) $[L^{MN1} + Cl]^-$. Calcd. for $C_{28}H_{32}Cl_2CuN_{16}O_6$: C, 38.60; H, 3.83; N, 24.77%. Found: C, 40.86; H, 3.92; N, 27.23%.

2.1.3. Synthesis and characterization of the $Cu^{(I)}$ complexes

{[HC(CO₂)(tz)₂]Cu} (16)

An acetonitrile solution (25 mL) of CuCl (0.099 g, 1.0 mmol) was added to an acetonitrile solution (25 mL) of Na[HC(CO₂)(tz)₂] (**2**) (0.216 g, 1.0 mmol). After the addition, the reaction mixture was stirred at room temperature for 24 h to obtain a green precipitate which was filtered off and dried to constant weight to give complex **16** in 57% yield. Complex **16** showed a good solubility in DMSO, water, but a lower solubility in chlorinated solvent and alcohols. M.p. 223°C. IR (cm^{-1}): 3108m, 1661s (ν_{asym} C=O), 1500m, 1519m, 1377s (ν_{sym} C=O), 1275s, 1202m, 1129s, 1016m, 1006m. ^{1}H-NMR (DMSO, 293K): δ 9.97 (s, 1H, C*H*COO), 8.14 (s, 2H, 5-C*H*), 9.12 (s, 2H, 3-C*H*). ESIMS (major positive-ions, CH_3OH), *m/z* (%): 239 (100) $[Na[HC(CO_2)(tz)_2] + Na]^+$, 216 (80) $[HC(CO_2H)(tz)_2 + Na]^+$, 323 (20) $[[HC(CO_2H)(tz)_2]Cu]^+$. ESIMS (major negative-ions, H_2O), *m/z* (%): 193 (80) $[HC(CO_2)(tz)_2]^-$, 409 (90) $[2HC(CO_2)(tz)_2 + Na]^-$. Calcd. for $C_6H_5CuN_6O_2$: C, 18.33; H, 1.55; N, 20.00%. Found: C, 17.24; H, 1.21; N, 20.10%.

{[HC(CO₂H)(tz)₂]Cu(PF₆)}•H₂O (17)

An acetonitrile solution (25 mL) of $Cu(CH_3CN)_4PF_6$ (0.372 g, 1.0 mmol) was added to an acetonitrile solution (25 mL) of $HC(CO_2H)(tz)_2$ (**1**) (0.194 g, 1.0 mmol). After the addition, the reaction mixture was stirred at room temperature for 24 h to obtain a blue precipitate which was filtered off and dried to constant weight to give complex **17** in 14% yield. The complex **17** showed a good solubility in methanol by warming, but a lower solubility in DMSO, while it was insoluble in water. M.p. 210°C dec. IR (cm^{-1}): 3437mbr (OH), 3125m, 2942mbr 1759s (ν_{asym} C=O), 1671m, 1522s, 1447m (ν_{sym} C=O), 1279s, 1176m, 1121s, 1019m, 990m. ^{1}H-NMR (DMSO, 293K): δ 7.11 (s, 1H, C*H*COO), 7.39 (s, 2H, 5-C*H*), 7.68 (s, 2H, 3-C*H*). ESIMS (major positive-ions, CH_3OH), *m/z* (%): 217 (100) $[HC(CO_2H)(tz)_2 + Na]^+$, 411 (40) $[HC(CO_2)(tz)_2 + 2Na]^+$. ESIMS (major negative-ions, CH_3OH), *m/z* (%): 144 (100) $[PF_6]^-$, 193 (20) $[HC(CO_2)(tz)_2]^-$.Calcd. for $C_6H_8CuF_6N_6O_3P$: C, 17.36; H, 1.76; N, 16.93%. Found: C, 17.13; H, 1.92; N, 19.98%.

{[HC(CO$_2$)(tz)$_2$][Cu(PBz$_3$)]$_4$}•(PF$_6$)$_3$ (18)

An acetonitrile solution (25 mL) of Cu(CH$_3$CN)$_4$PF$_6$ (0.372 g, 1.0 mmol) was added to an acetonitrile solution (25 mL) of tribenzyl phosphine (PBz$_3$, 0.608 g, 2.0 mmol). After the addition, the reaction mixture was stirred at room temperature for 2 h. Na[HC(CO$_2$)(tz)$_2$] (**2**) (0.216 g, 1.0 mmol) was added and the solution was stirred at room temperature for 24 h to obtain a green solution which was filtered off and dried to constant weight to give complex **18** as a green solid in 38% yield. Complex **18** showed a good solubility in DMSO, but it was insoluble in water, alcohols acetone and chlorinated solvent. M.p. 218°C dec. IR (cm^{-1}): 3423br (OH), 3029m, 1667mbr (ν_{asym} C=O), 1600m, 1495s, 1452s (ν_{sym} C=O), 1417m, 1282m, 1224m, 1066m, 1029m. ^{1}H-NMR (DMSO, 293K): δ 6.87 (s, 1H, C*H*COO), 7.00 (d, 6H, C*H*$_2$), 7.10 (m, 15H, C*H*$_{PBz3}$), 7.87 (s, 2H, 5-C*H*), 8.79 (s, 2H, 3-C*H*). ^{1}H-NMR (CD$_3$CN, 293K): δ 6.98 (s, 1H, C*H*COO), 7.06 (d, 6H, C*H*$_2$), 7.16 (m, 15H, C*H*$_{PBz3}$), 7.81 (s, 2H, 5-C*H*), 8.62 (s, 2H, 3-C*H*). ESIMS (major positive-ions, CH$_3$CN), *m/z* (%): 318 (100) [HC(CO$_2$)(tz)$_2$ + 2Cu]$^+$, 367 (90) [PBz$_3$ + Cu]$^+$, 671 (70) [2PBz$_3$ + Cu]$^+$. Calcd. for C$_{90}$H$_{89}$Cu$_4$F$_{18}$N$_6$O$_2$P$_7$: C, 52.51; H, 4.59; N, 3.05%. Found: C, 51.48; H, 4.27; N, 4.00%.

{[(L^{MN})Cu(PTA)$_2$]}(PF$_6$) (19)

An acetonitrile solution (25 mL) of Cu(CH$_3$CN)$_4$PF$_6$ (0.241 g, 0.6 mmol) was added to an acetonitrile solution (25 mL) of 1,3,5-Triaza-7-phosphaadamantane (PTA, 0.203 g, 1.2 mmol). After the addition, the reaction mixture was stirred at room temperature for 2 h. L^{MN} (**7**) (0.259 g, 0.6 mmol) was added and the solution was stirred at room temperature for 12 h to obtain a yellow solution which was dried to constant weight to give complex **19** as a yellow solid in 70% yield. Complex **19** showed a good solubility in DMSO and by warming in acetonitrile, water, methanol. It showed a lower solubility in chlorinated solvent. M.p. 184°C. IR (cm^{-1}): 3398br (NH), 2924mbr (CH), 1672s (ν_{asym} C=O), 1561m, 1531m, 1417m (ν_{sym} C=O), 1363m, 1248s, 1187s, 1101s, 1014s, 970s. ^{1}H-NMR (D$_2$O, 293K): δ 2.06 (s, 6H, C*H*$_3$), 2.22 (s, 6H, C*H*$_3$), 3.56 (s, 3H, C*H*$_3$), 4.48 (t, 2H, C*H*$_2$NH), 4.64 (t, 2H, C*H*$_2$N), 6.02 (s, 2H, C*H*$_{pz}$), 6.49 (s, 1H, C*H*CO), 7.81 (s, 1H, C*H*$_{MN}$). ^{13}C-NMR (D$_2$O, 293K): δ 10.16 (*C*H$_3$), 12.58 (*C*H$_3$), 13.32 (*C*H$_3$), 38.73 (*C*H$_2$NH), 49.84 (*C*H$_2$N), 70.78 (*C*HCO), 107.46 (*C*H), 132.90 (*C*H), 133.40 (*C*NO$_2$), 138.78 (*C*CH$_3$), 142.75 (*C*CH$_3$), 151.32 (*C*CH$_3$), 152.33 (*C*ONH). ^{31}P-NMR (CD$_3$OD, 293K): δ -89.05 (s), -143.44 (septet, $J_{(F-P)}$) 701.2 Hz, PF$_6$. ^{31}P-NMR (CD$_3$OD, 218K): δ -88.20 (s), -143.24 (septet, $J_{(F-P)}$) 701.0 Hz. ^{31}P-NMR (D$_2$O, 293K): δ -81.37 (br), -143.90 (septet, $J_{(F-P)}$) 703.4 Hz, PF$_6$). ESIMS (major positive-ions, CH$_3$OH), *m/z* (%): 401 (100) [L^{MN} + H]$^+$, 423 (95) [L^{MN} + Na]$^+$, 620 (70) [(L^{MN})Cu(PTA)]$^+$, 158 (40) [PTA + H]$^+$, 463 (30) [(L^{MN})Cu]$^+$. ESIMS (major negative-ions, CH$_3$OH), *m/z* (%): 144 (100) [PF$_6$]$^-$, 313 (80) [2PTA – H]$^-$, 399 (55) [L^{MN} – H]$^-$. Calcd. for C$_{30}$H$_{48}$CuF$_6$N$_{14}$O$_3$P$_3$: C, 38.56; H, 5.74; N, 21.04%. Found: C, 38.57; H, 5.75; N, 21.05%.

{[(L^{MN1})Cu(PTA)$_2$]}(PF_6)•2H_2O (20)

An acetonitrile solution (25 mL) of $Cu(CH_3CN)_4PF_6$ (0.186 g, 0.5 mmol) was added to an acetonitrile solution (25 mL) of 1,3,5-Triaza-7-phosphaadamantane (PTA, 0.157 g, 1.0 mmol). After the addition, the reaction mixture was stirred at room temperature for 2 h. L^{MN1} (**8**) (0.172 g, 0.5 mmol) was added and the solution was stirred at room temperature for 12 h to obtain a yellow solution which was dried to constant weight to give complex **20** as a yellow solid in 79% yield. Complex **20** showed a good solubility in DMSO and by warming in acetonitrile, water, methanol. It showed a lower solubility in chlorinated solvent. M.p. 168°C. IR (cm^{-1}): 3453br (NH, OH), 2926mbr (CH), 1694s (ν_{asym} C=O), 1524mbr, 1531m, 1448m (ν_{sym} C=O), 1415m, 1364m, 1292s, 1241s, 1187s, 1101s, 1013s, 969s. ^{1}H-NMR (D_2O, 293K): δ 2.23 (s, 3H, CH_3), 4.41 (m, 2H, CH_2NH), 4.64 (t, 2H, CH_2N), 6.40 (t, 2H, CH_{pz}), 7.24 (s, 1H, C*H*CO), 7.61 (s, 2H, CH_{pz}), 7.81 (s, 2H, CH_{MN}). ^{31}P-NMR (CD_3OD, 293K): δ -90.58, -143.38 (septet, $J_{(F-P)}$) 701.6 Hz, PF_6). ^{31}P-NMR (CD_3OD, 218K): δ -92.90, 143.51 (septet, $J_{(F-P)}$) 703.1 Hz, PF_6). ^{31}P-NMR (D_2O, 293K): δ -87.29, -143.93 (septet, $J_{(F-P)}$) 703.5 Hz, PF_6). ESIMS (major positive-ions, CH_3OH), *m/z* (%): 367 (100) [L^{MN1} + Na]$^+$, 158 (55) [PTA + H]$^+$, 345 (30) [L^{MN1} + H]$^+$, 804 (30) [{(L^{MN1})$_2$Cu}$_2$($CuCH_3CN$) - H]$^{2+}$ ESIMS (major negative-ions, CH_3OH), *m/z* (%): 144 (100) [PF_6]$^-$, 313 (95) [2PTA – H]$^-$, 342 (40) [L^{MN1} – H]$^-$, 126 (30) [$Im^{(4Me)NO2}$]$^-$. Calcd. for $C_{26}H_{44}CuF_6N_{14}O_5P_3$: C, 34.69; H, 4.74; N, 21.10%. Found: C, 34.58; H, 4.91; N, 21.71%.

2.1.4. Synthesis and characterization of $Ag^{(I)}$ complexes

{[$HC(CO_2)(tz)_2$]Ag} (21)

An acetonitrile solution (25 mL) of $AgNO_3$ (0.167 g, 1.0 mmol) was added to an acetonitrile solution (25 mL) of Na[$HC(CO_2)(tz)_2$] (**2**) (0.216 g, 1.0 mmol). After the addition, the reaction mixture was stirred at room temperature for 24 h to obtain a grayish precipitate which was filtered off and dried to constant weight to give complex **21** as a grey solid in 63% yield. Complex **21** showed a good solubility in DMSO, but a lower solubility in chlorinated solvent, water and it was insoluble in alcohols, THF and acetonitrile. M.p. 179-180°C. IR (cm^{-1}): 3137w, 3108m, 1659s (ν_{asym} C=O), 1518m, 1500m, 1429sh (ν_{sym} C=O), 1352s, 1275s, 1221m, 1202m, 1137m, 1129s, 1015m. ^{1}H-NMR (DMSO, 293K): δ 6.88 (s, 1H, C*H*COO), 7.88 (s, 2H, 5-C*H*), 8.72 (s, 2H, 3-C*H*). ESIMS (major positive-ions, CH_3OH), *m/z* (%): 239 (100) [Na[$HC(CO_2)(tz)_2$] + Na]$^+$, 216 (80) [$HC(CO_2H)(tz)_2$ + Na]$^+$, 323 (20) [[$HC(CO_2)(tz)_2$]Ag + Na]$^+$. ESIMS (major negative-ions, H_2O), *m/z* (%): 193 (80) [$HC(CO_2)(tz)_2$]$^-$, 409 (90) [2$HC(CO_2)(tz)_2$ + Na]$^-$. Calcd. for $C_6H_5AgN_6O_2$: C, 14.74; H, 1.02; N, 17.60%. Found: C, 14.74; H, 1.03; N, 17.19%.

{[$HC(CO_2)(tz)_2$]Ag} (22)

An acetonitrile solution (25 mL) of $AgNO_3$ (0.169 g, 1.0 mmol) was added to an acetonitrile solution (25 mL) of triphenylphosphine (PPh_3, 0.262 g, 1.0 mmol). After the addition, the reaction

mixture was stirred at room temperature for 2 h. Na[HC(CO_2)(tz)$_2$] (**2**) (0.216 g, 1.0 mmol) was added and the solution was stirred at room temperature for 24 h to obtain a grayish precipitate which was filtered off and dried to constant weight to give complex **22** as a grey solid in 40% yield. Complex **22** showed a good solubility in DMSO, water and methanol but it was insoluble in chlorinated solvent. M.p. 188-190°C. IR (cm^{-1}): 1743w, 1660s (ν_{asym} C=O), 1518m, 1500m, 1427sh (ν_{sym} C=O), 1374s, 1274s, 1220m, 1202m, 1129s, 1015m, 1005m. ^{1}H-NMR (DMSO, 293K): δ 6.86 (s, 1H, C*H*COO), 7.87 (s, 2H, 5-C*H*), 8.72 (s, 2H, 3-C*H*). ^{1}H-NMR (D_2O, 293K): δ 7.33 (s, 1H, C*H*COO), 7.95 (s, 2H, 5-C*H*), 8.63 (s, 2H, 3-C*H*). ESIMS (major positive-ions, CH_3OH), *m/z* (%): 216 (100) [HC(CO_2H)(tz)$_2$ + Na]$^+$, 239 (80) [Na[HC(CO_2)(tz)$_2$] + Na]$^+$, 323 (20) [[HC(CO_2)(tz)$_2$]Ag + Na]$^+$. ESIMS (major negative-ions, H_2O), *m/z* (%): 193 (80) [HC(CO_2)(tz)$_2$]$^-$, 409 (90) [2HC(CO_2)(tz)$_2$ + Na]$^-$. Calcd. for $C_6H_5AgN_6O_2$: C, 13.51; H, 1.60; N, 15.65%. Found: C, 14.22; H, 0.99; N, 16.58%.

{[HC(CO_2)(tz)$_2$]Ag(PBz_3)} (23)

A methanol solution (25 mL) of $AgNO_3$ (0.084 g, 0.5 mmol) was added to a methanol solution (25 mL) of tribenzyl phosphine (PBz_3, 0.304 g, 1.0 mmol). After the addition, the reaction mixture was stirred at room temperature for 2 h. Na[HC(CO_2)(tz)$_2$] (**2**) (0.108 g, 0.5 mmol) was added and the solution was stirred at room temperature for 24 h to obtain a white solution which was filtered off and dried to constant weight to give complex **23** as a white solid in 56% yield. Complex **23** showed a good solubility in DMSO, but it was insoluble in alcohols and water. M.p. 232°C. IR (cm^{-1}): 3396br (OH), 3062w, 3029w, 2990w, 1951w, 1888w, 1810w, 1766w, 1661s (ν_{asym} C=O), 1602m, 1511m, 1495s, 1454m (ν_{sym} C=O), 1355s, 1277s, 1237m, 1186m, 1124m, 1067m, 1029m. ^{1}H-NMR (DMSO, 293K): δ 6.96 (s, 1H, C*H*COO), 7.07 (d, 6H, CH_2), 7.19 (m, 15H, CH_{PBz3}), 7.9 (s, 2H, 5-C*H*), 8.75 (s, 2H, 3-C*H*). ^{31}P-NMR (DMSO, 293K): δ 17.49 (br). ESIMS (major positive-ions, CH_3OH), *m/z* (%): 216 (100) [HC(CO_2H)(tz)$_2$ + Na]$^+$, 239 (80) [Na[HC(CO_2)(tz)$_2$] + Na]$^+$, 323 (20) [[HC(CO_2)(tz)$_2$]Ag + Na]$^+$. ESIMS (major negative-ions, H_2O), *m/z* (%): 193 (80) [HC(CO_2)(tz)$_2$]$^-$, 409 (90) [2HC(CO_2)(tz)$_2$ + Na]$^-$, 493 (20) [2HC(CO_2)(tz)$_2$ + Ag]$^-$. Calcd. for $C_{27}H_{26}AgN_6O_2P$: C, 38.91; H, 3.20; N, 8.79%. Found: C, 39.98; H, 3.23; N, 10.36%.

{[(PyS)$_2$CHCO$_2$]Ag[(PyS)$_2$CHCO$_2$H](PPh_3)} (24)

A methanol solution (25 mL) of $AgNO_3$ (0.169 g, 1.0 mmol) was added to a methanol solution (25 mL) of triphenylphosphine (PPh_3, 0.524 g, 2.0 mmol). After the addition, the reaction mixture was stirred at room temperature for 2 h. {Na[(PyS)$_2$CHCO$_2$]} (**5**) (0.300 g, 1.0 mmol) was added and the solution was stirred at room temperature for 12 h to obtain a yellow solution which was filtered off and dried to constant weight to give complex **24** as a brown solid in 43% yield. Complex **24** showed a good solubility in DMSO and acetonitrile, but it was insoluble in chlorinated solvent and water. M.p. 191-193°C. IR (cm^{-1}): 3382br (OH), 3049w (CH), 2906w, 1980w, 1901w, 1789w, 1615s (ν_{asym} C=O), 1579s, 1556s (C=C + C=N), 1452m, 1434m, 1411s (ν_{sym} C=O), 1343s, 1122s, 1090m. ^{1}H-NMR (DMSO, 293K): δ 6.08 (s, 1H, C*H*CO$_2$), 7.07 (m, 2H, 5-C*H*), 7.23 (m, 15H, CH_{PPh3}), 7.42 (m, 2H, 3-C*H*), 7.60 (m, 2H, 4-C*H*),

8.31 (m, 2H, 6-C*H*). ^{31}P-NMR (CD_3OD, 293K): δ 8.53 (s). ^{31}P-NMR (CD_3OD, 218K): δ 7.52 (s), 9.72 (s). ESIMS (major positive-ions, CH_3OH), *m/z* (%): 301 (100) $[(PyS)_2CHCO_2H + Na]^+$, 633 (100) $[Ag(PPh_3)_2]^+$, 579 (80) $[2(PyS)_2CHCO_2H + Na]^+$. ESIMS (major negative-ions, CH_3OH), *m/z* (%): 110 (100) $[PyS]^-$, 233 (30), 577 (30) $[2(PyS)_2CHCO_2 + Na]^-$. Calcd. for $C_{42}H_{34}AgN_4O_4PS_4$: C, 45.14; H, 2.96; N, 7.64; S, 10.42%. Found: C, 44.52; H, 3.03; N, 4.95; S, 11.33%.

{[(PyS)$_2$CHCO$_2$]Ag[(PyS)$_2$CHCO$_2$H](PBz$_3$)} (25)

A methanol solution (25 mL) of $AgNO_3$ (0.0849 g, 0.5 mmol) was added to a methanol solution (25 mL) of tribenzyl phosphine (PBz_3, 0.30438 g, 1.0 mmol). After the addition, the reaction mixture was stirred at room temperature for 2 h. {Na[$(PyS)_2CHCO_2$]} (**5**) (0.150 g, 0.5 mmol) was added and the solution was stirred at room temperature for 12 h to obtain a yellow solution which was filtered off and dried to constant weight to give complex **25** as a yellow solid in 37% yield. Complex **25** showed a good solubility in DMSO and acetonitrile, but it was insoluble in chlorinated solvents and water. M.p. 161°C. IR (cm^{-1}): 3387br (OH), 3029w (CH), 2906w, 1981w, 1900w, 1787w, 1615s (ν_{asym} C=O), 1580s, 1555s (C=C + C=N), 1494m, 1452m, 1411s (ν_{sym} C=O), 1375s, 1236m, 1186m, 1122m. ^{1}H-NMR (DMSO, 293K): δ 6.08 (s, 1H, C*H*CO_2), 7.08 (m, 2H, 5-C*H*), 7.24 (m, 15H, C*H*$_{PBz3}$), 7.46 (m, 2H, 3-C*H*), 7.61 (m, 2H, 4-C*H*), 8.32 (m, 2H, 6-C*H*). ^{31}P-NMR (CD_3OD, 218K): δ 18.34 (br). ESIMS (major positive-ions, CH_3OH), *m/z* (%): 301 (100) $[(PyS)_2CHCO_2H + Na]^+$, 717 (100) $[Ag(PBz_3)_2]^+$, 579 (80) $[2(PyS)_2CHCO_2H + Na]^+$. ESIMS (major negative-ions, CH_3OH), *m/z* (%): 110 (100) $[PyS]^-$, 233 (30), 577 (30) $[2(PyS)_2CHCO_2 + Na]^-$. Calcd. for $C_{45}H_{40}AgN_4O_4PS_4$: C, 44.98; H, 3.48; N, 5.07; S, 7.66%. Found: C, 46.05; H, 3.44; N, 4.77; S, 10.93%.

{[(ImSMe)$_2$CHCO$_2$]Ag(PPh$_3$)$_2$} (26)

A methanol solution (25 mL) of $Ag(PPh_3)_2NO_3$ (0.694 g, 1.0 mmol) was added to a methanol solution (25 mL) of {Na[$(ImSMe)_2CHCO_2$]} (**6**) (0.306 g, 1.0 mmol). After the addition, the reaction mixture was stirred at room temperature for 24 h to obtain a grayish precipitate which was filtered off and dried to constant weight to give complex **26** as a grey solid in 77% yield. The complex **26** showed a good solubility in DMSO and chlorinated solvent, but a lower solubility in water, while it was insoluble in alcohols. IR (cm^{-1}): 3051w (CH), 2944w, 1964w, 1891w, 1824w, 1767w, 1637s (ν_{asym} C=O), 1514w, 1478s, 1457s, 1433s (ν_{sym} C=O), 1322s, 1236m, 1181m, 1092s. ^{1}H NMR ($CDCl_3$, 293K): δ 3.79 (s, 6H, CH_3), 4.83 (s, 1H, C*H*COO), 6.75 (s, 2H, C*H*), 7.01 (s, 2H, C*H*), 7.30 (m, 15H, C*H*$_{PPh3}$). ^{31}P-NMR (CD_3OD, 293K): δ 6.24 (s). ^{31}P-NMR (CD_3OD, 218K): δ 5.47 (d, J(^{107,109}Ag-^{31}P)) 358.0 Hz. ESIMS (major positive-ions, CH_3OH), *m/z* (%): 633 (100) $[Ag(PPh_3)_2]^+$, 263 (40) $[PPh_3 + H]^+$, 414 (15) $[[(ImSMe)_2CHCO_2]Ag + Na]^+$. ESIMS (major negative-ions, CH_3OH), *m/z* (%): 223 (100) [(ImSMe)Ag – H]$^-$, 113 (50) $[ImSMe]^-$. Calcd. for $C_{46}H_{41}AgN_4O_2P_2S_2$: C, 59.66; H, 4.32; N, 5.67; S, 6.86%. Found: C, 60.33; H, 4.51; N, 6.12; S, 7.00%.

3. Results and Discussion

3.1. Preface

In recent years *Burzlaff et al*. found bis(3,5-dialkylpyrazol-1-yl)acetic acids[9,10] (which are accessible from dibromo- or dichloro-acetic acid in a one-step synthesis) to be a convenient starting material for linker modified ligands.[11] Complexes containing these ligands have been of considerable interest owing to their important use as metalloenzyme models relevant to biochemistry,[12-19] metal-based antitumor drugs[20,21] and development of homogeneous catalysts.[22] During the last decade, the interest of the Inorganic Chemistry research group in which I worked for the thesis stage has focused in the synthesis of new heteroscorpionate ligands with pyrazole, triazole, 2-mercaptopyridine or 2-mercaptoimidazole rings.[12,19,20] In addition, as part of ongoing research efforts in the design and development of radiometal-based anticancer agents, the ^{64}Cu-labeled complexes of $[HC(CO_2)(pz^{Me2})_2Cu(thp)_2]$ and $[HC(CO_2)(tz)_2Cu(thp)_2]$, (thp = tris(hydroxymethyl) phosphine) have been prepared to evaluate their usefulness as PET radiopharmaceuticals.[208] Recently, bis(thiosemicarbazonato)copper(II)–nitroimidazole conjugates were successfully synthesized[106] in their cold and ^{64}Cu radiolabelled forms by *Bayly et al*.: nitroimidazole conjugates of bis(thiosemicarbazonato)copper(II) showed additive or synergistic selectivity for tumor hypoxia compared to their individual components. In this work, Prof. Santini research group has investigated the design of new nitroimidazole(2-methyl-5-nitro-imidazole) conjugated heteroscorpionate ligands useful for the synthesis of novel copper derivatives to be evaluated for their cytotoxic activity. In this thesis I report the synthesis and characterization of two nitroimidazole conjugated heteroscorpionate ligands and the related copper(I/II) complexes as well as a brief investigation of their biological activity. It was also reported the synthesis and caracterization of ligands based on triazole, pyrazole and mercapto groups and the related copper(I/II) and silver(I) complexes.

3.1.1. Synthesis of triazole ligands and related complexes

Following a simple and efficient synthetic methodology,[20] a neutral ligand and the related salt, namely 2,2-di(1H-1,2,4-triazol-1-yl)acetic acid ({$[HC(CO_2H)(tz)_2]$}, (**1**) and sodium 2,2-di(1H-1,2,4-triazol-1-yl)acetate ({$Na[HC(CO_2)(tz)_2]$}, (**2**) respectively were prepared by a acid-base reaction, nucleophilic substitution and salification reaction, using 1,2,4-triazole (tz), dibromoacetic acid and sodium hydroxide at room temperature (**Fig. 3.1** and **Fig. 3.2**).

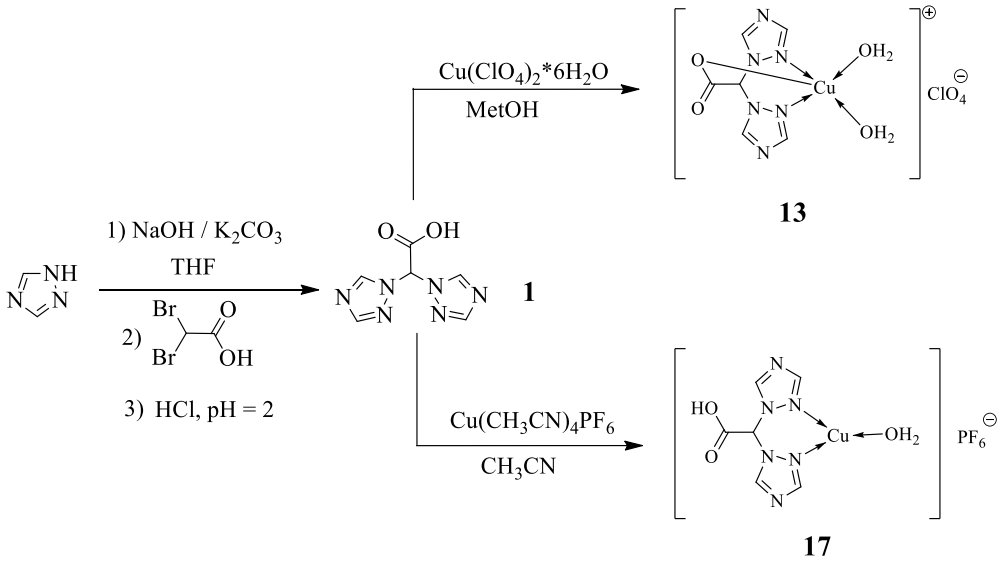

Figure 3.1. Reaction scheme of the synthesis of the ligand 1 and the related copper(I/II) complexes 13 and 17.

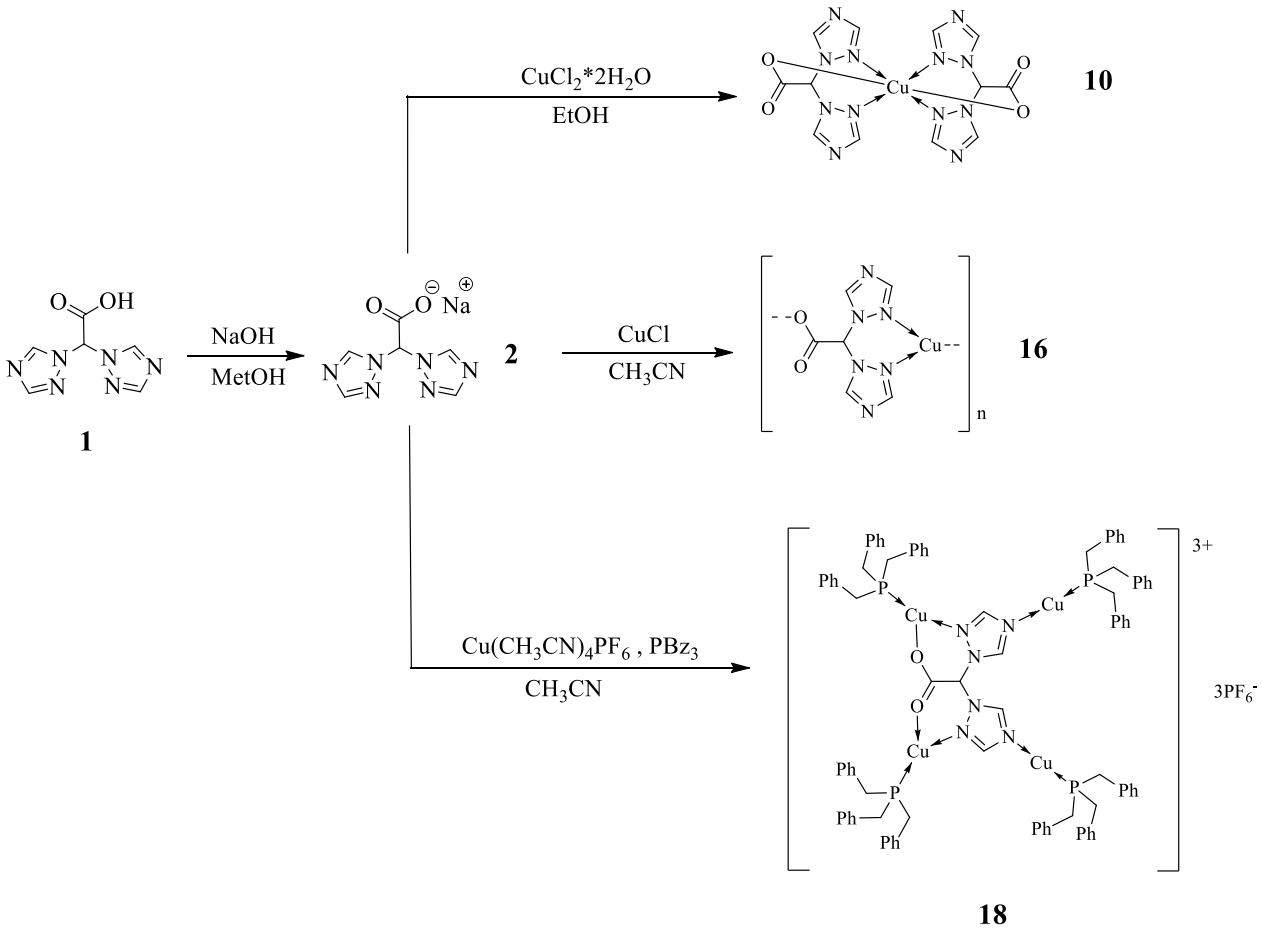

Figure 3.2. Reaction scheme of the synthesis of the ligand 2 and related copper(I/II) complexes 10, 16 and 18.

Compounds **1** and **2** show a good solubility in alcohols and water. The infrared spectra carried out on the solid samples showed all the expected bands for the ligands: weak absorptions in the range 3139-3102 cm^{-1} due to the triazole rings C–H stretching and medium absorptions in the range 1500-1562 cm^{-1} related to ring ''breathing'' vibrations; for the ligand **1** broad peaks at 3388 cm^{-1} attributable to the O–H stretching are visible too. The presence of the CO moiety is detected by intense absorptions at 1747 and 1660 cm^{-1}, respectively, due to the asymmetric CO stretching mode (**Fig. 3.3** and **Fig. 3.4**).

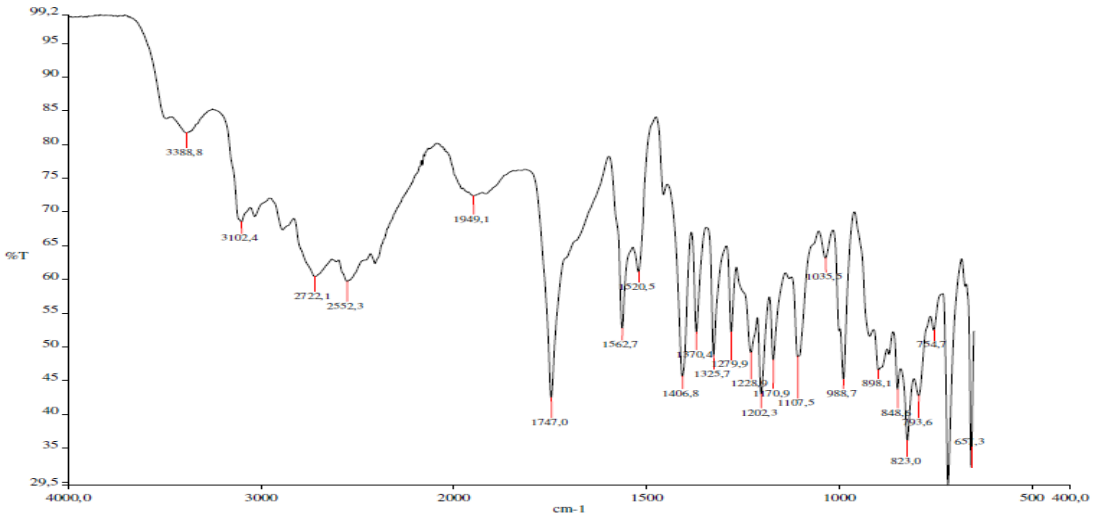

Figure 3.3. FT-IR spectrum of compound 1.

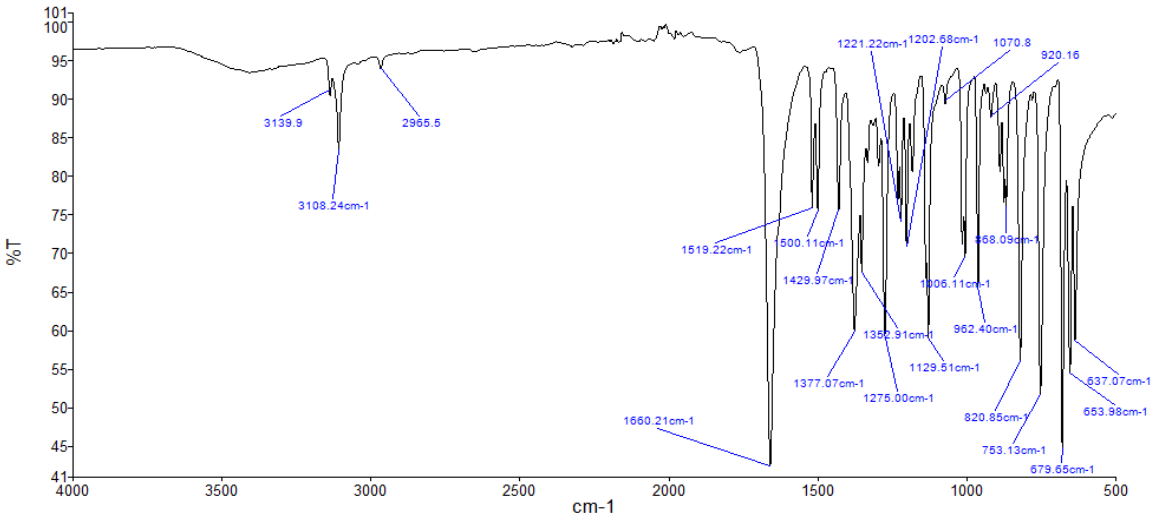

Figure 3.4. FT-IR spectrum of compound 2.

The ^{1}H- and ^{13}C-{H} NMR spectra of **1** and **2** show a single set of resonances for the rings, indicating that the triazoles are equivalent. The positive and negative-ion ESI-MS spectra of compound (**2**) (**Fig. 3.5** and **Fig. 3.6**) showed molecular peak and others relative fragments corresponding to the fragmentation of the ligand:

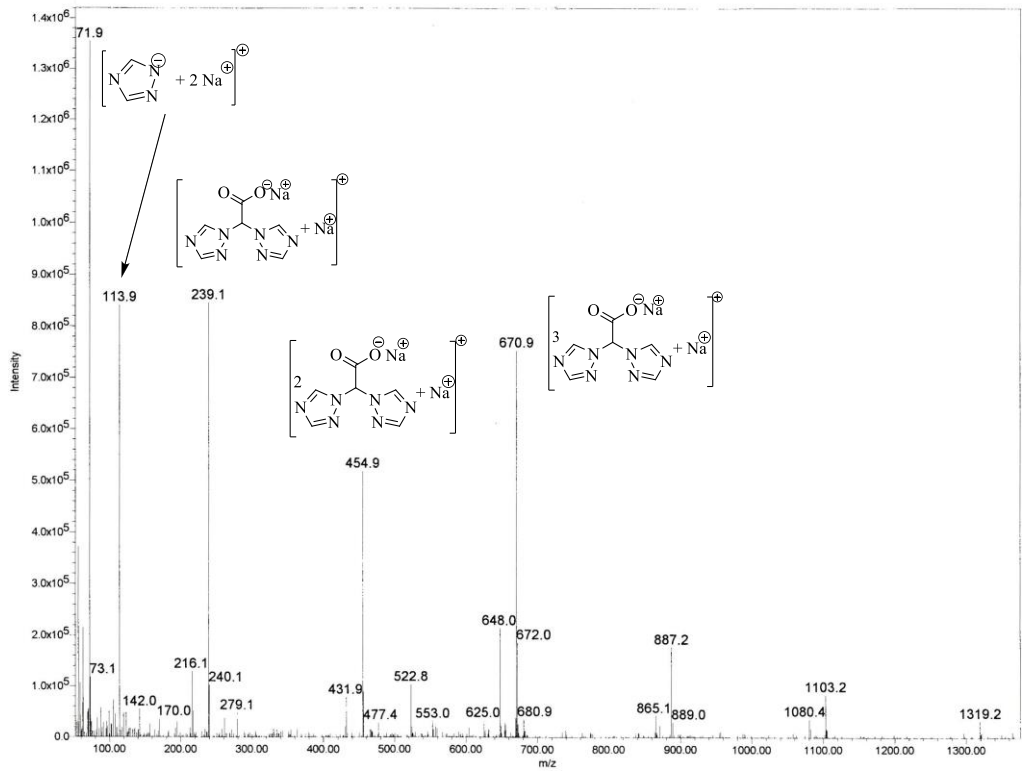

Figure 3.5. Positive-ion ESI-MS spectrum of compound 2.

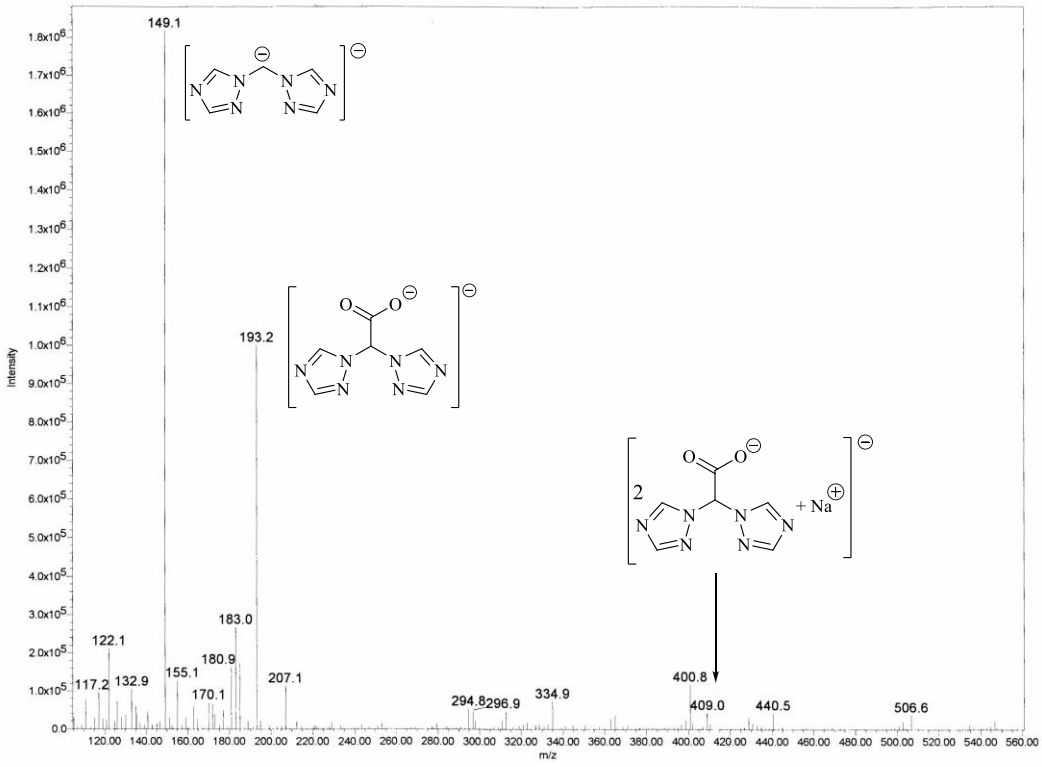

Figure 3.6. Negative-ion ESI-MS spectrum of compound 2.

The related copper(II) complexes {[HC(CO_2)(tz)$_2$]$_2$Cu} (**10**) and {[HC(CO_2)(tz)$_2$]Cu(ClO_4)}•3H_2O (**13**) have been prepared at room temperature from the reaction of $CuCl_2$•2H_2O with {Na[HC(CO_2)(tz)$_2$]} (**2**) in ethanol solution and from the reaction of Cu(ClO_4)$_2$•6H_2O with {[HC(CO_2H)(tz)$_2$]} (**1**) in methanol solution, respectively (**Fig. 3.1** and **Fig. 3.2**). The compounds **10** and **13** are soluble in water and air stable even as solutions. The authenticity of **10** and **13** was confirmed by elemental analysis, IR spectroscopy and Electrospray mass spectra. The infrared spectra show all the bands required by the presence of the scorpionate donors. Broad absorptions at 1667 and 1762 cm^{-1}, respectively, due to the carbonylic asymmetric stretching are slightly shifted with respect to the same absorptions observed for the free ligands

The related copper(I) complexes {[HC(CO_2)(tz)$_2$]Cu} (**16**), {[HC(CO_2H)(tz)$_2$]Cu(PF_6)}•H_2O (**17**), and {[HC(CO_2)(tz)$_2$][Cu(PBz_3)]$_4$}•(PF_6)$_3$ (**18**)
have been prepared from the reaction of CuCl and Cu(CH_3CN)$_4PF_6$ with ligand **1** and from the reaction Cu(CH_3CN)$_4PF_6$ and PBz_3 with ligand **2**, respectively, in acetonitrile solution at room temperature (**Fig. 3.1** and **Fig. 3.2**). Compound **16** is soluble in water and DMSO, **17** is soluble in DMSO and by warming in methanol and **18** is soluble in DMSO and acetonitrile; all complexes are air stable even as solutions. The authenticity of **16**, **17** and **18** was confirmed by elemental analysis, IR spectroscopy and Electrospray mass spectra. The infrared spectra show all the bands required by the presence of the scorpionate donors and in the case of compound **18** of the phosphine coligand. Sharp absorptions at 1661, 1759 and broad absorbtion at 1667 cm^{-1}, respectively, due to the carbonylic asymmetric stretching are slightly shifted with respect to the same absorptions observed for the free ligands

The complex {[HC(CO_2)(tz)$_2$]Ag} (**21**) has been prepared from the reaction of $AgNO_3$ with {Na[HC(CO_2)(tz)$_2$]} (**2**) in acetonitrile at room temperature; complexes {[HC(CO_2)(tz)$_2$]Ag} (**22**) and {[HC(CO_2)(tz)$_2$]Ag(PBz_3)} (**23**) have been prepared from the reaction of the ligand (**2**) with $AgNO_3$ and PPh_3 in acetonitrile solution and with $AgNO_3$ and PBz_3 in methanol solution, respectively at room temperature (**Fig. 3.7**). The compounds **21** and **23** are soluble in DMSO while **22** is soluble in DMSO, methanol and water and all are not air stable because the silver tends to reduce. The authenticity of **21**, **22** and **23** was confirmed by elemental analysis, IR spectroscopy and Electrospray mass spectra. The infrared spectra show all the bands required by the presence of the scorpionate donors: broad peaks at 3421, 3365, and 3396 cm^{-1}, respectively, attributable to the O–H stretching; sharp absorptions at 1659, 1660 and 1661 cm^{-1}, respectively, due to the carbonylic asymmetric stretching. All the characteristic signals are slightly shifted with respect to the same absorptions observed for the free ligands.

The related silver(I) complexes have also been studied (**Fig. 3.7)**.

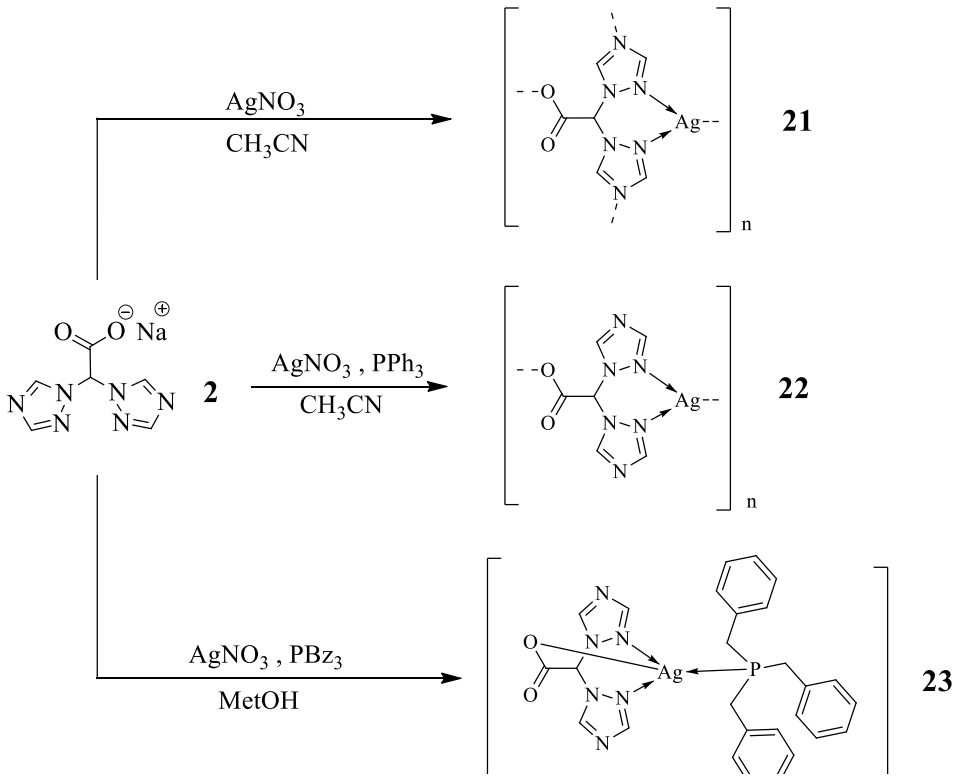

Figure 3.7. Reaction scheme of the synthesis of the silver(I) complexes 21, 22 and 23.

3.1.2. Synthesis of pyrazole ligands and related complexes

Following a simple and efficient synthetic methodology,[28] neutral ligands namely 2,2-bis(3,5-dimethyl-1H-pyrazol-1-yl)acetic acid ({[HC(CO_2H)(pz^{Me2})$_2$]}, (**3**) and 2,2-di(1H-pyrazol-1-yl)acetic acid ({[HC(CO_2H)(pz)$_2$]}, (**4**) respectively, were prepared by a acid-base reaction and a nucleophilic substitution, using 3,5-dimethylpyrazole (pz^{Me2}) or pyrazole (pz), dibromoacetic acid and sodium hydroxide at room temperature (**Fig. 3.8** and **Fig. 3.9**).

Compound **3** shows a good solubility in alcohols, DMSO and chlorinated solvents while **4** shows a good solubility in alcohols, DMSO and water by warming. The infrared spectra carried out on the solid samples showed all the expected bands for the ligands: broad peaks at 3451 and 3429 cm^{-1}, respectively, attributable to the O–H stretching, weak absorptions in the range 3093-3107 cm^{-1} due to the pirazole rings C–H stretching and medium absorptions in the range 1517-1560 cm^{-1} related to ring ''breathing'' vibrations. The presence of the CO moiety is detected by an intense absorption at 1741 and 1720 cm^{-1}, respectively, due to the asymmetric CO stretching mode.

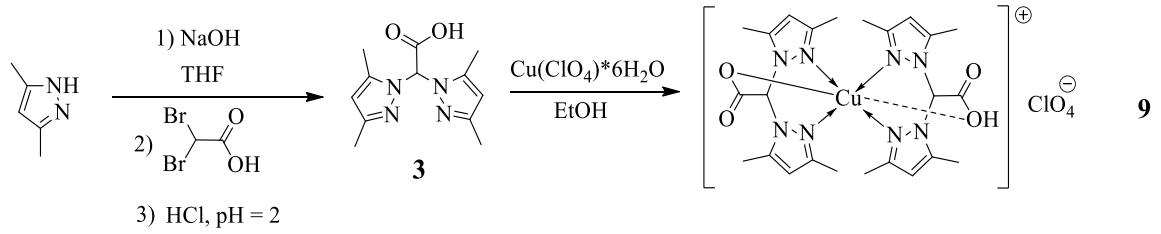

Figure 3.8. Reaction scheme of the synthesis of the ligand 3 and the related copper(II) complex 9.

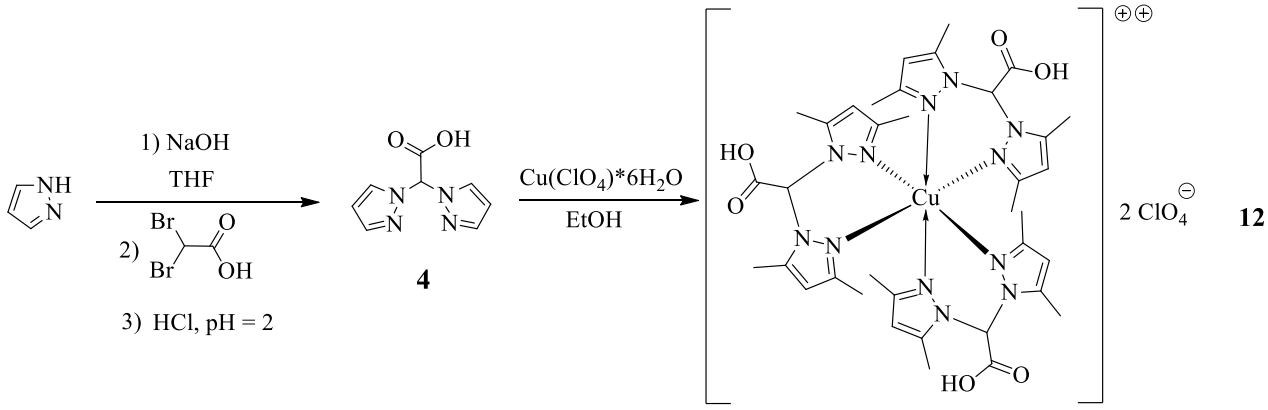

Figure 3.9. Reaction scheme of the synthesis of the ligand 4 and the related copper(II) complex 12.

The ^{1}H- and ^{13}C-{H} NMR spectra of **3** and **4** show a single set of resonances for the pyrazole rings, indicating that the pyrazoles are equivalent (**Fig. 3.10** and **Fig. 3.11**).

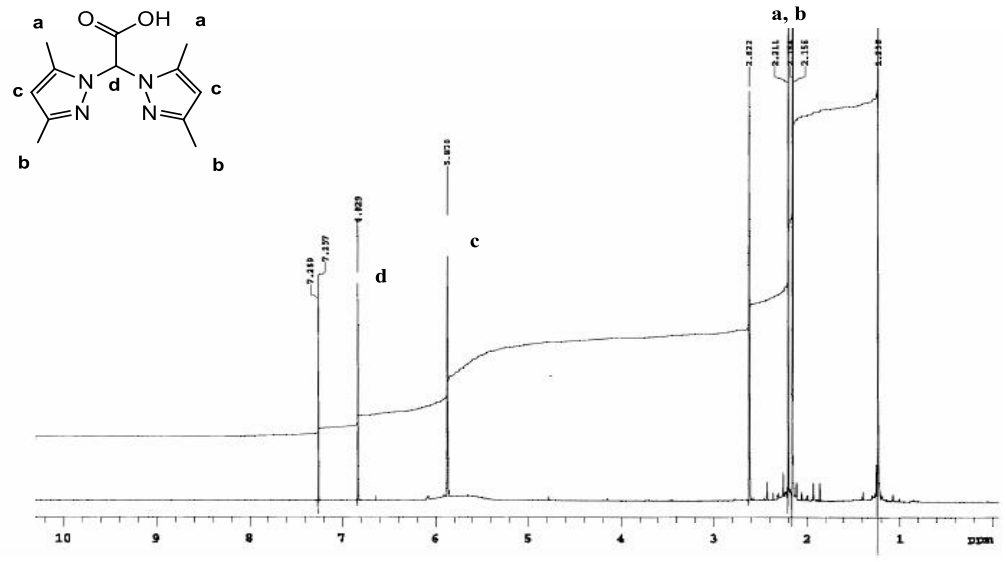

Figure 3.10. ^{1}H-NMR spectrum of compound 3.

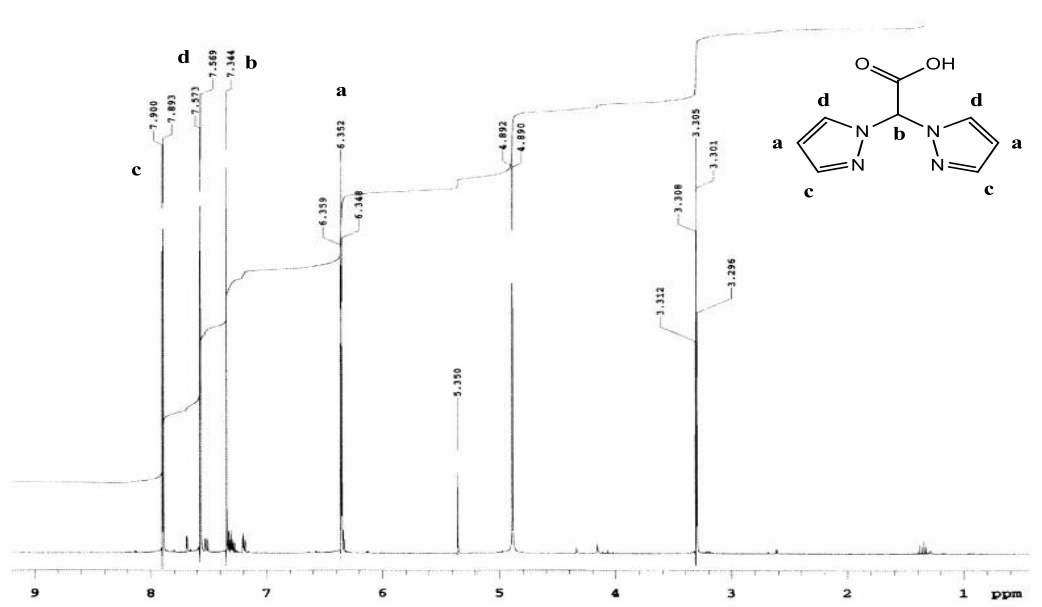

Figure 3.11. ^{1}H-NMR spectrum of compound 4.

The negative-ion ESI-MS spectrum of compound (**3**) (**Figure 3.12**) showed the molecular peak and the pyrazolate fragment.

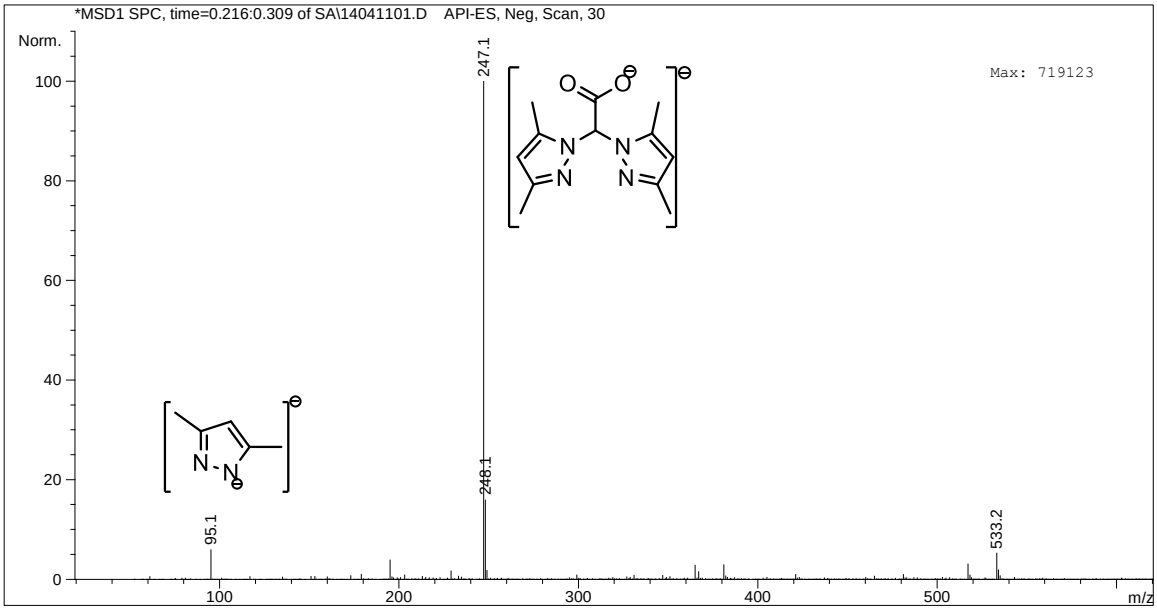

Figure 3.12. Negative-ion ESI-MS spectra of compound 3.

The related copper(II) complexes {CH[(pz^{Me2})COOH]Cu[CH(pz^{Me2})COO]•ClO_4} (**9**) and {[HC(CO_2H)$(pz)_2$]$_3$Cu$(ClO_4)_2$} (**12**) have been prepared from the reaction of $Cu(ClO_4)_2$•$6H_2O$ with {[HC(CO_2H)(pz^{Me2})$_2$]} (**3**) and {[HC(CO_2H)$(pz)_2$]} (**4**), respectively, in ethanol solution at room temperature (**Fig. 3.8** and **Fig. 3.9**). The compounds **9** and **12** are soluble in methanol and DMSO and air stable even as solutions. The authenticity of **9** and **12** was confirmed by elemental analysis, IR

spectroscopy and Electrospray mass spectra. The infrared spectra show all the bands required by the presence of the scorpionate donors. Medium absorptions at 1705 and 1745 cm^{-1}, respectively, due to the carbonylic asymmetric stretching are slightly shifted with respect to the same absorptions observed for the free ligands.

3.1.3. Synthesis of mercapto ligands and related complexes

Following a simple and efficient synthetic methodology,[38] ligands namely 2,2-bis(pyridin-2-ylthio)acetic acid ({Na[$(PyS)_2CHCO_2$]}, (**5**) and 2,2-bis((1-methyl-4,5-dihydro-1H-imidazol-2-yl)thio)acetic acid ({Na[$(ImSMe)_2CHCO_2$]}, (**6**), respectively, were prepared by a acid-base reaction and a nucleophilic substitution, using 2-mercaptopyridine (PySH) or 2-mercapto-1-methylimidazole (HImSMe), dibromoacetic acid and sodium hydroxide at room temperature (**Fig. 3.13** and **Fig. 3.14**).

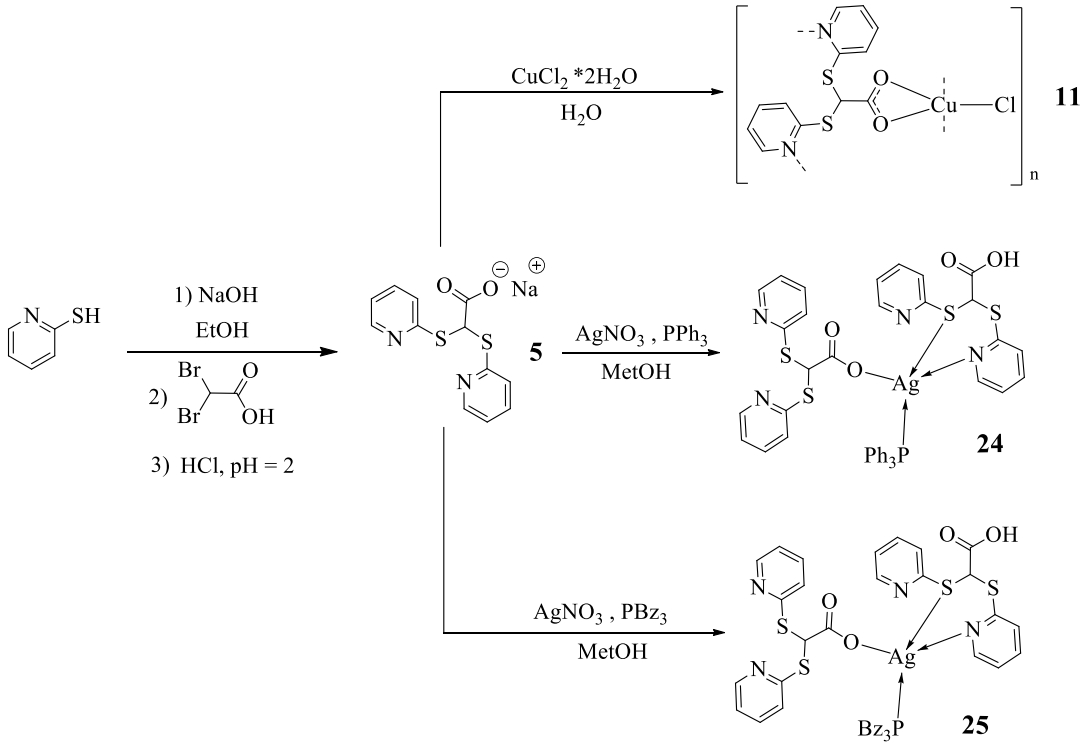

Figure 3.13. Reaction scheme of the synthesis of the ligand 5 and related copper(II) and silver(I) complexes 11, 24 and 25.

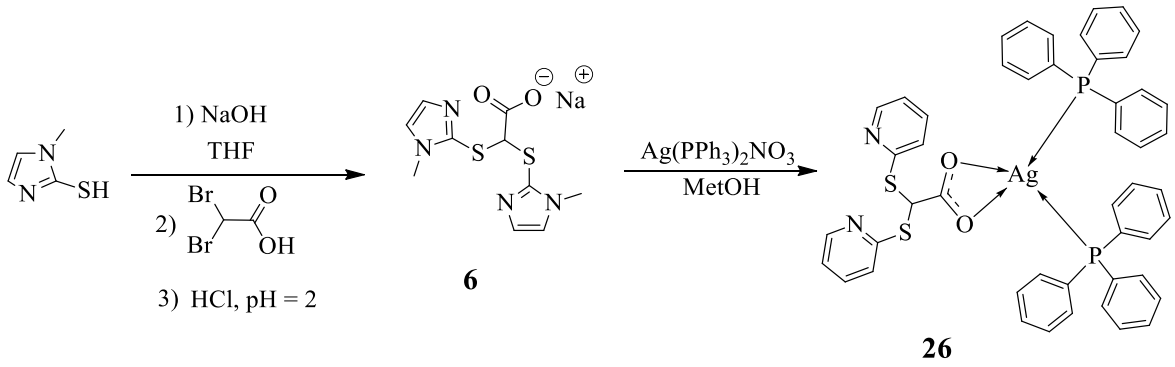

Figure 3.14. Reaction scheme of the synthesis of the ligand 6 and related silver(I) complex 26.

Compound **5** shows a good solubility in alcohols, DMSO and water while **6** shows a good solubility in methanol, water, acetonitrile, and chlorinated solvents. The infrared spectra carried out on the solid samples showed all the expected bands for the ligands: weak absorptions in the range 3053-2905 cm^{-1} and 3091-2980 cm^{-1} rispectively due to the pirazole and imidazole rings C–H stretching and medium absorptions in the range 1580-1598 cm^{-1} related to ring ''breathing'' vibrations. The presence of the CO moiety is detected by an intense absorption at 1618 and 1628 cm^{-1}, respectively, due to the asymmetric CO stretching mode. The ^{1}H- and ^{13}C-{H} NMR spectra of **5** and **6** show a single set of resonances for the pyrazole and imidazole rings, indicating that the pyrazoles and imidazoles are equivalent (**Fig. 3.15** and **Fig. 3.16**).

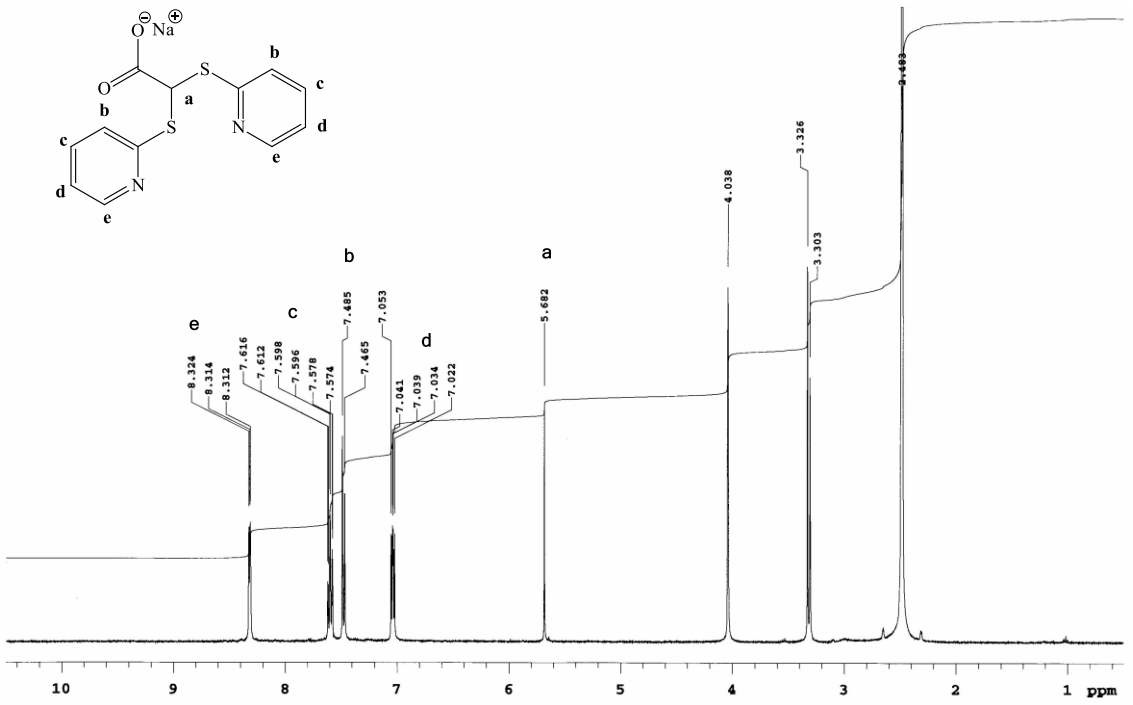

Figure 3.15. ^{1}H-NMR spectrum of compound 5.

The related copper(II) complex {[$(PyS)_2CHCO_2$]CuCl} (**11**) has been prepared from the reaction of $CuCl_2 \bullet 2H_2O$ with {Na[$(PyS)_2CHCO_2$]} (**5**), in acqeous solution at room temperature (**Fig. 3.13**). The compound **11** is soluble only in DMSO and air stable even as solutions. The infrared spectra show all the bands required by the presence of the scorpionate donors. Strong absorptions at 1721 cm^{-1}, due to the carbonylic asymmetric stretching are slightly shifted with respect to the same absorptions observed for the free ligands

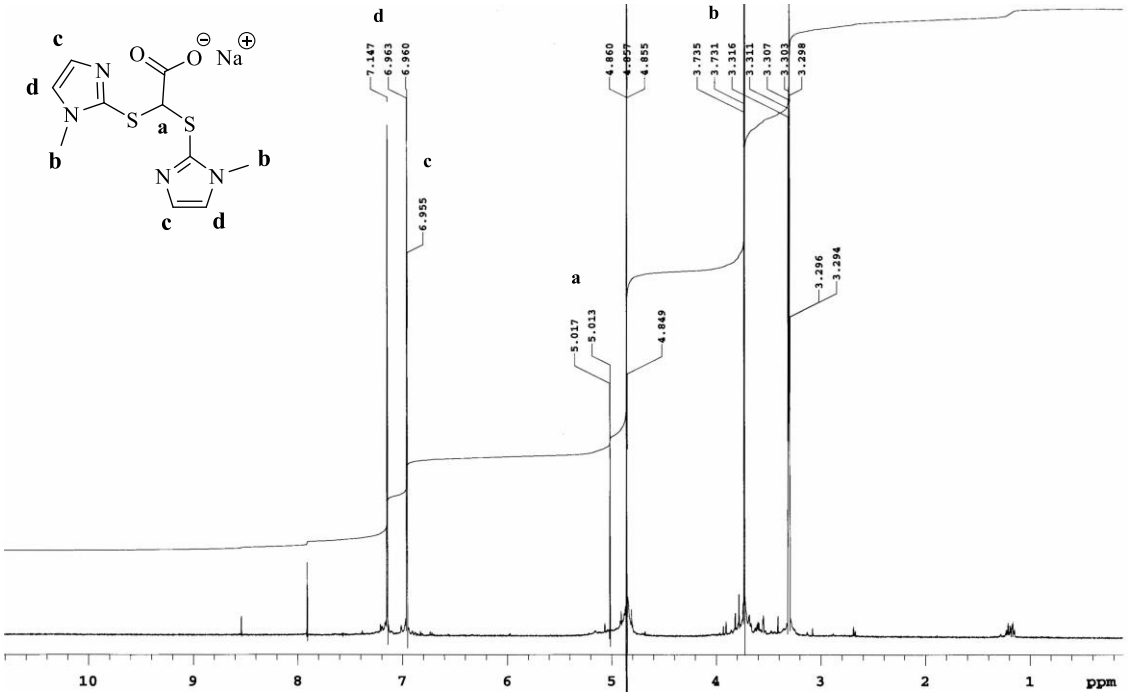

Figure 3.16. ^{1}H-NMR spectrum of compound 6.

The related silver(I) complexes {[$(PyS)_2CHCO_2$]Ag[$(PyS)_2CHCO_2H$](PPh_3)} (**24**) and {[$(PyS)_2CHCO_2$]Ag[$(PyS)_2CHCO_2H$](PBz_3)} (**25**) have been prepared at room temperature from the reaction of $AgNO_3$ and Na[$(PyS)_2CHCO_2$]} (**5**) in methanol solution with PPh_3 and PBz_3, respectively (**Fig. 3.13**). The compounds **24** and **25** are soluble in DMSO and acetonitrile and not air stable; {[$(ImSMe)_2CHCO_2$]Ag(PPh_3)$_2$} (**26**) has been prepared from the reaction of Ag(PPh_3)$_2NO_3$ with {Na[$(ImSMe)_2CHCO_2$]} (**6**) in methanol solution at room temperature (**Fig. 3.14**) The authenticity of **24**, **25** and **26** was confirmed by elemental analysis, IR spectroscopy and Electrospray mass spectra. The infrared spectra show all the bands required by the presence of the scorpionate donors and the phosphine coligands: broad peaks at 3382, 3387 and 3354 cm^{-1}, respectively, are attributable to the O–H stretchings. The presence of the CO moiety is detected by intense absorptions at 1618, 1628 and 1637 cm^{-1}, respectively, due to the carbonylic asymmetric stretching; they are slightly shifted with respect to the same absorptions observed for the free ligands

3.1.4 Synthesis of biofunctionalized ligands and related complexes

Following a simple and efficient synthetic methodology,[97] neutral acetamide compounds, namely 2,2-bis(3,5-dimethyl-1H-pyrazol-1-yl)-N-(2-(2-methyl-5-nitro-1H-imidazol-1-yl)ethyl)acetamide (L^{MN}, **7**) and N-(2-(2-methyl-5-nitro-1H-imidazol-1-yl)ethyl)-2,2-di(1H-pyrazol-1-yl)acetamide (L^{MN1}, **8**) were prepared by direct coupling of preformed side chain acid and amine components, using the ligands [$HC(CO_2H)(pz^{Me2})_2$] (**3**) and {[$HC(CO_2H)(pz)_2$]} (**4**), 1-(2-aminoethyl)-2-methyl-5-nitroimidazole dihydrochloride, triethylamine, 1-hydroxybenzotriazole hydrate and N-(3-dimethylaminopropyl)-N′-ethylcarbodiimide hydrochloride at 0°C (**Fig. 3.17** and **Fig. 3.18**).

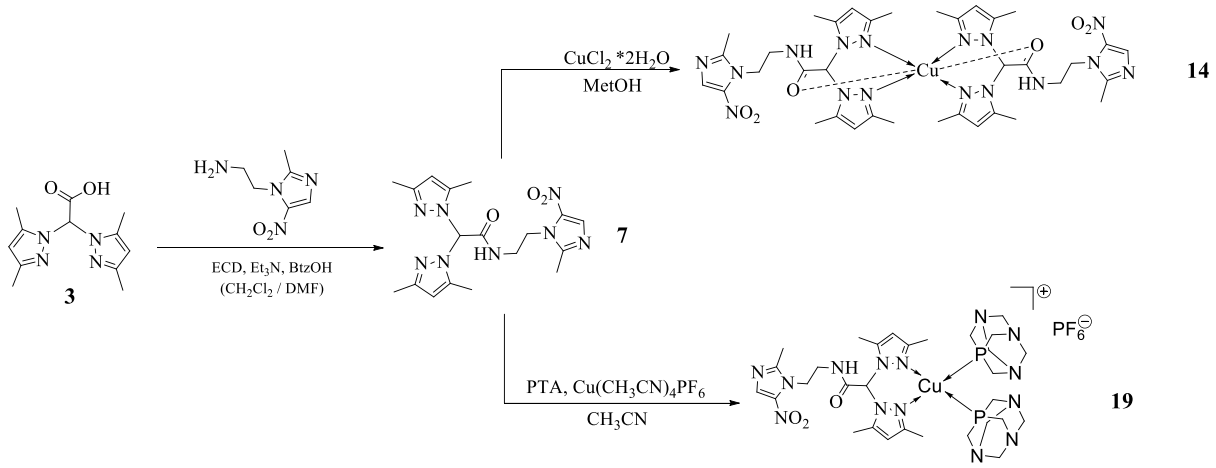

Figure 3.17. Reaction scheme of the synthesis of the new ligand L^{MN} (7) and related copper(I/II) complexes 14 and 19.

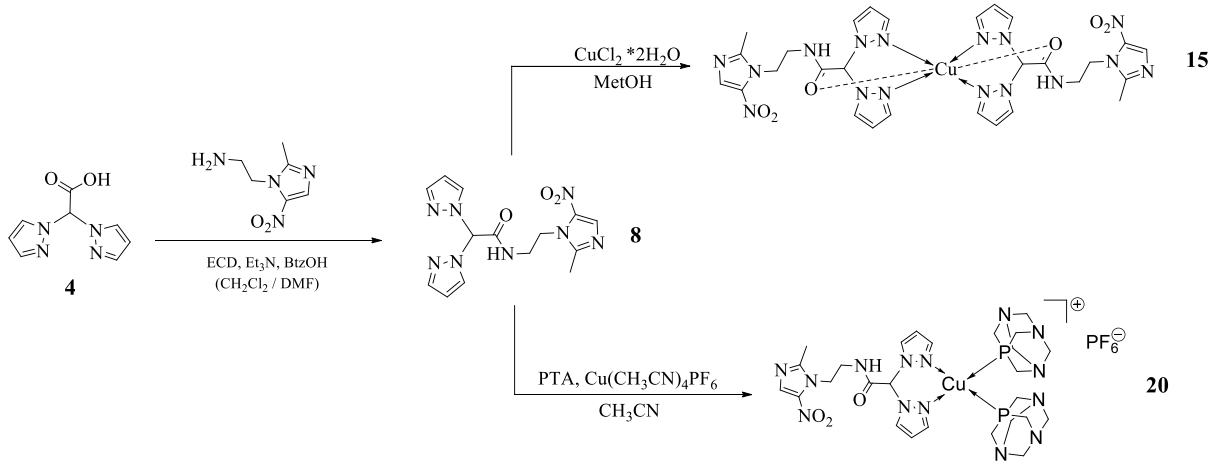

Figure 3.18. Reaction scheme of the synthesis of the new ligand L^{MN1} (8) and related copper(I/II) complexes 15 and 20.

From such reactions, three tautomers are possible[107] (**Fig. 3.19**); however, ^{1}H-NMR, ^{13}C-NMR and IR spectroscopic data indicate that only tautomer (a) is present.

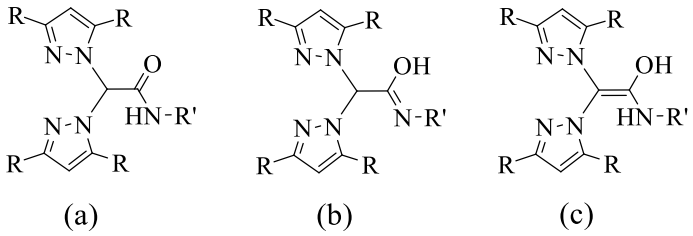

Figure 3.19. Possible tautomers for the ligands L^{MN} and L^{MN1}.

Compounds **7** and **8** show a good solubility in alcohols, acetone, acetonitrile and chlorinated solvents. The infrared spectra carried out on the solid samples showed all the expected bands for the tautomer (a) of the ligands: broad peaks at 3072 and 3084 cm^{-1}, respectively, attributable to the N–H stretching, weak absorptions in the range 2948-2965 cm^{-1} due to the pirazole and imidazole rings C–H stretching and medium absorptions in the range 1562-1548 cm^{-1} related to ring ''breathing'' vibrations. The presence of the CON moiety is detected by an intense absorption at 1670 and 1686 cm^{-1}, respectively, due to the asymmetric CO stretching mode (**Fig. 3.20** and **Fig. 3.21**).

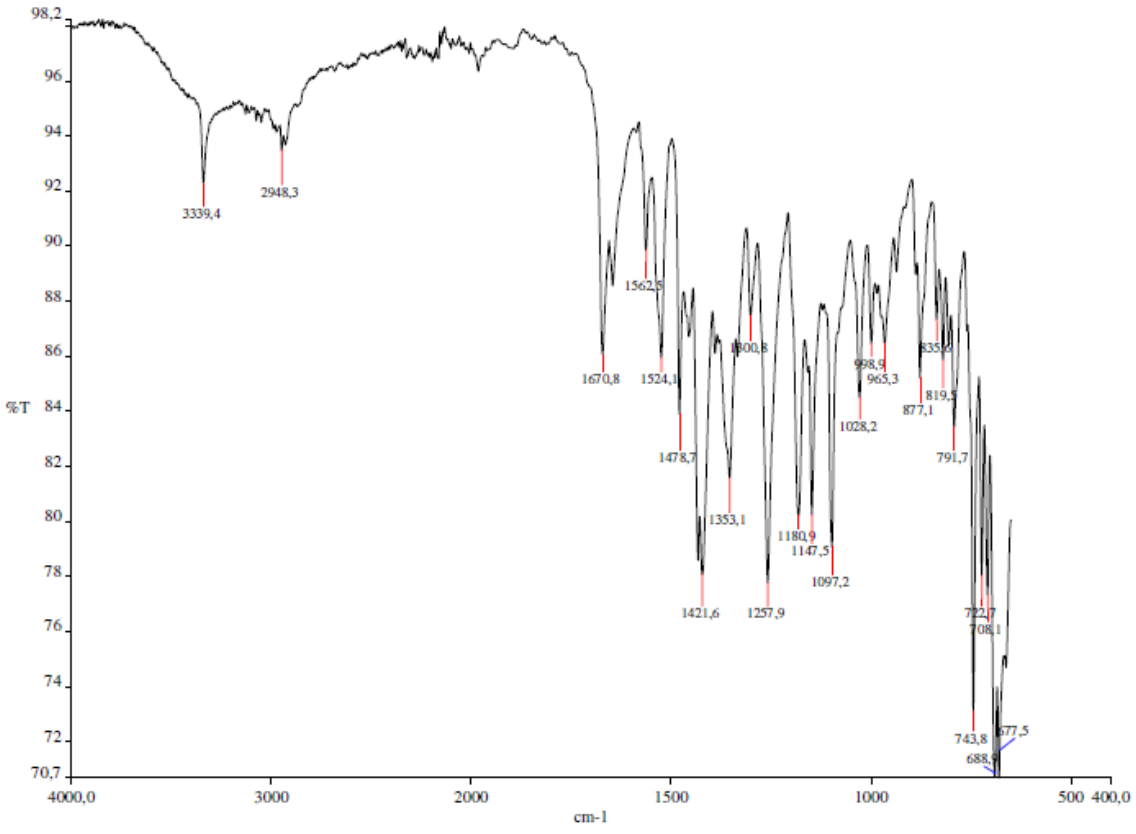

Figure 3.20. FT-IR spectrum of compound 7.

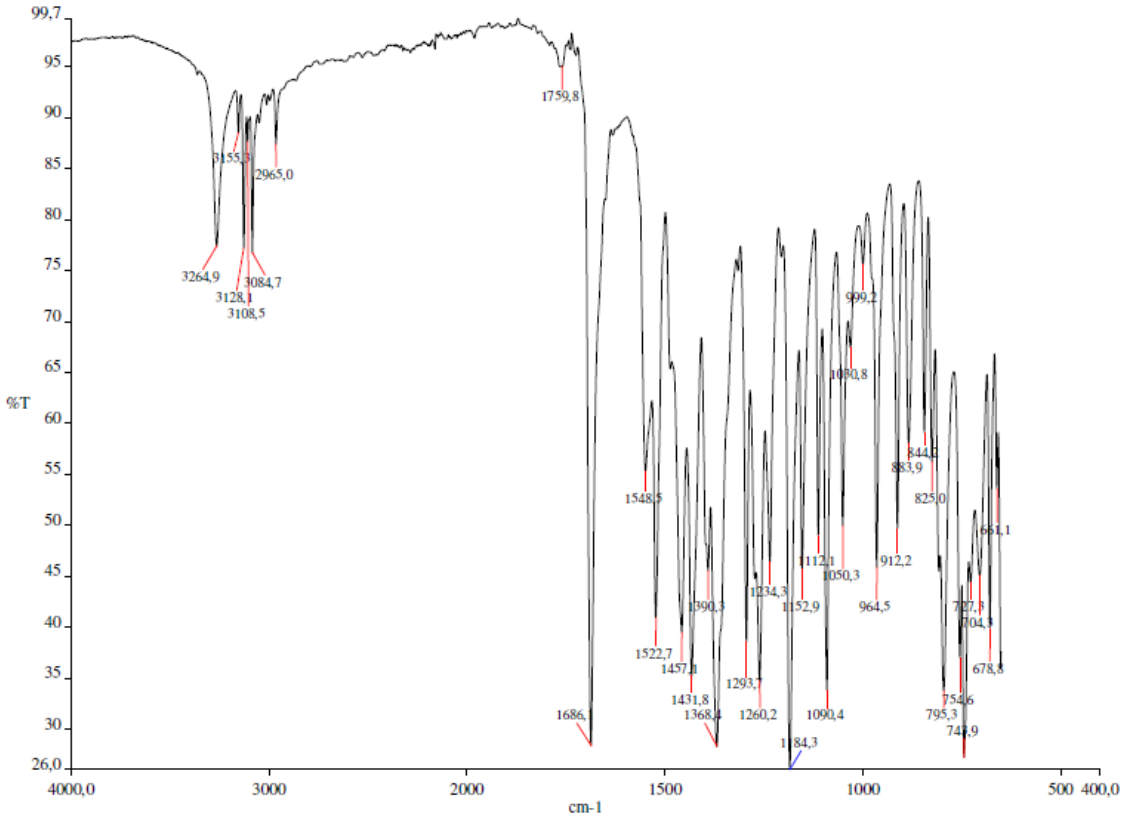

Figure 3.21. FT-IR spectrum of compound 8.

The ^{1}H- and ^{13}C-{H} NMR spectra of **7** and **8** show a single set of resonances for the pyrazole rings, indicating that the pyrazoles are equivalent.

The related copper(II) complexes $\{[(L^{MN})_2Cu]Cl_2\}$ (**14**) and $\{[(L^{MN1})_2Cu]Cl_2\}$ (**15**) have been prepared from the reaction of $CuCl_2 \bullet 2H_2O$ with L^{MN} and L^{MN1}, respectively, in methanol solution at room temperature (**Fig. 3.17** and **Fig. 3.18**). The compounds **14** and **15** are soluble in water, methanol and DMSO and air stable even as solutions. The authenticity of **14** and **15** was confirmed by elemental analysis, IR spectroscopy and Electrospray mass spectra. The infrared spectra show all the bands required by the presence of the scorpionate donors. Broad absorptions at 1665 and 1668 cm^{-1}, respectively, due to the carbonylic asymmetric stretching are slightly shifted with respect to the same absorptions observed for the free ligands

The related copper(I) complexes $\{[(L^{MN})Cu(PTA)_2]\} \bullet (PF_6)$ (**19**) and $\{[(L^{MN1})Cu(PTA)_2]\}(PF_6) \bullet 2H_2O$ (**20**) have been prepared from the reaction of PTA, $Cu(CH_3CN)_4PF_6$ with L^{MN} and L^{MN1}, respectively, in methanol solution at room temperature (**Fig. 3.17** and **Fig. 3.18**). The compounds **19** and **20** are soluble in DMSO and by warming in acetonitrile, water and methanol and air stable even as solutions. The authenticity of **19** and **20** was confirmed by elemental analysis, IR spectroscopy and Electrospray mass spectra (**Fig. 3.22-Fig. 3.25**).

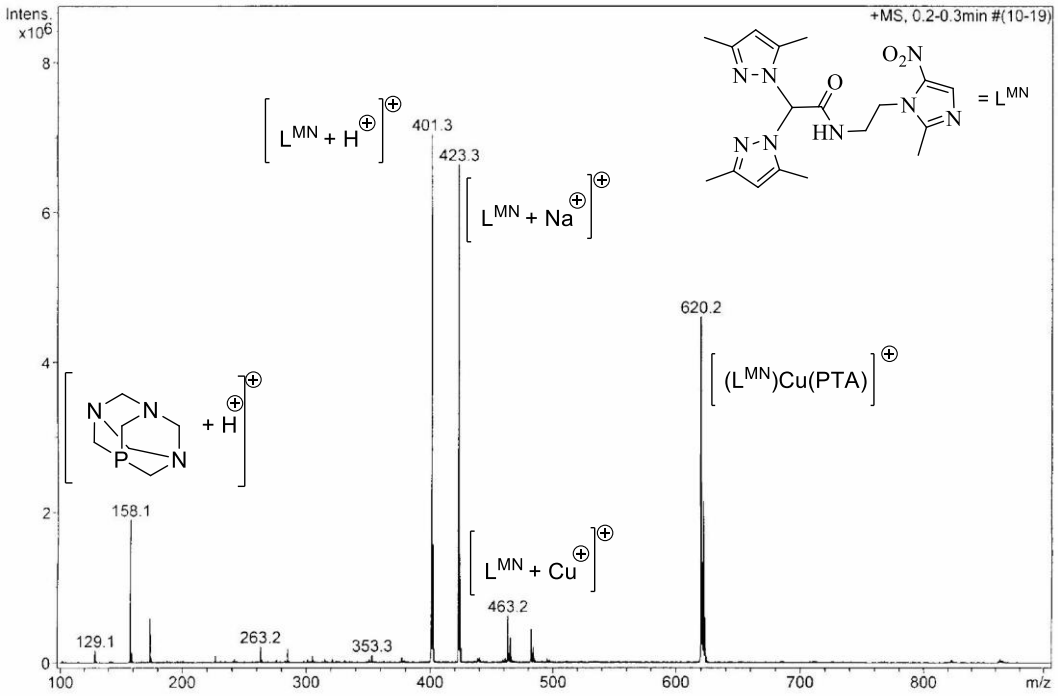

Figure 3.22. Positive-ion ESI-MS spectrum of compound 19.

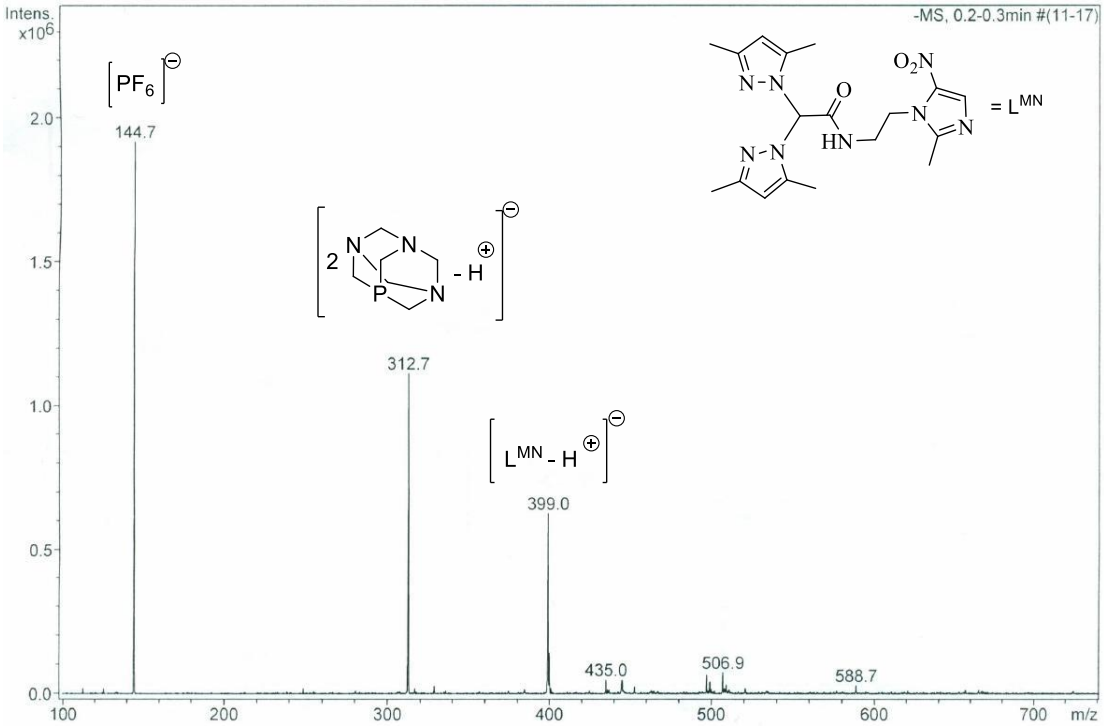

Figure 3.23. Negative-ion ESI-MS spectrum of compound 19.

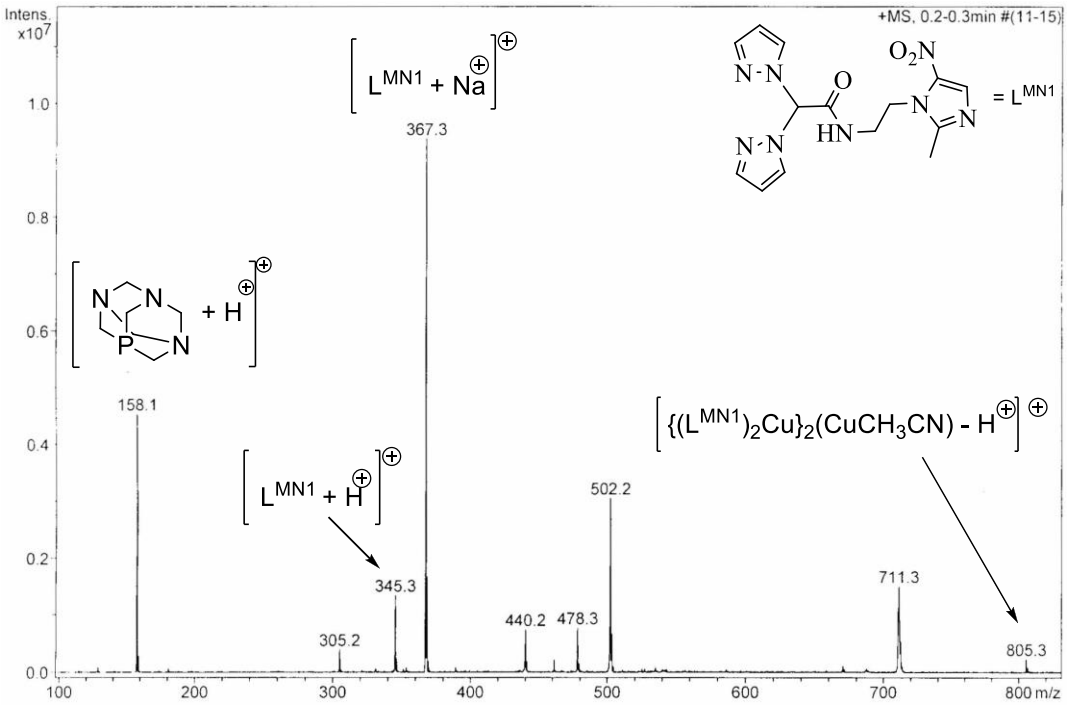

Figure 3.24. Positive-ion ESI-MS spectrum of compound 20.

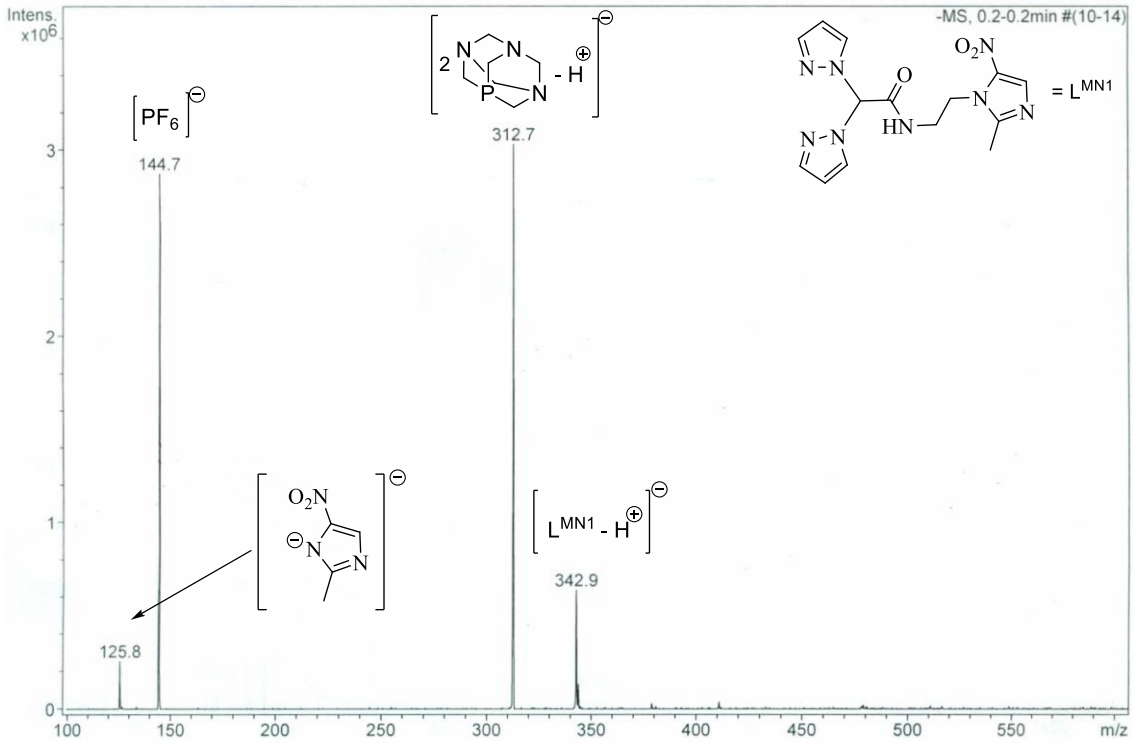

Figure 3.25. Negative-ion ESI-MS spectrum of compound 20.

The infrared spectra show all the bands required by the presence of the scorpionate and phosphine donors: broad peaks at 3398 and 3453 cm^{-1}, respectively, attributable to the OH/NH

stretching and broad absorptions at 1672 and 1694 cm^{-1}, respectively, due to the carbonylic asymmetric stretching are slightly shifted with respect to the same absorptions observed for the free ligands

Proposed structures for compounds **19** and **20** are reported in **Figure 3.26**.

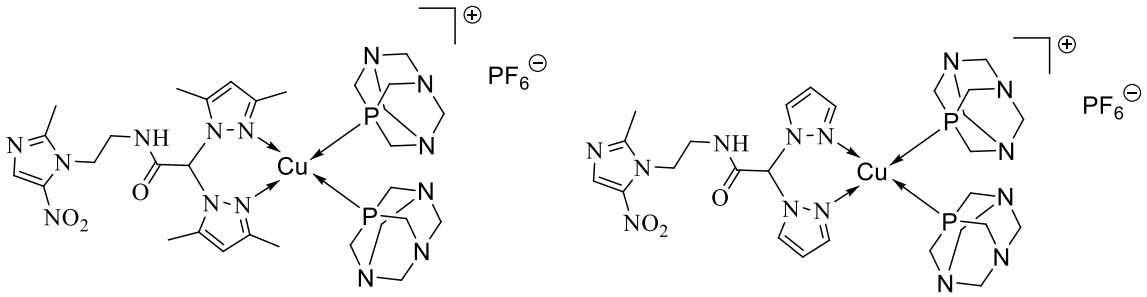

Figure 3.26. Proposed structures of compound 19 and 20, respectively.

3.1.4.1 X-ray analysis

The crystal structure 2,2-bis(3,5-dimethyl-1H-pyrazol-1-yl)-N-(2-(2-methyl-5-nitro-1H-imidazol-1-yl)ethyl)acetamide (**7**) was determined and compared to similar structures available from the *Cambridge Crystallographic Data Centre* (*CCDC*).[107] This comparison revealed that the bond lengths and angles in **7** do not show exceptional features and do not deserve any comment. The ORTEP[107] diagram of the molecule is reported in **Figure 3.27**.

Empirical formula	$C_{18}\ H_{24}\ N_8\ O_3$
Formula weight	400.45
Wavelength (Å) / Temperature (K)	1.54184 / 297
Crystal system	monoclinic
Crystal size	0.30 × 0.10 × 0.04
Space group	$P\ 2_1/c$
a (Å)	11.781(1)
b (Å)	16.308(1)
c (Å)	10.432(1)
β (deg)	90.82(1)
Volume ($Å^3$)	2004.0(4)
Z (molecules/unit cell)	4
Calculated density ($Mg\ m^{-3}$)	1.327
Absorption coefficient, μ (mm^{-1})	0.784
F(000)	848

Total reflections	8383
Independent (unique) reflections / R_{int}	3346/ 0.033
Observed reflections [I > 2σ(I)]	2565
Data / parameters / restraints	3346 / 267/ 0
Goodness–of–fit [a] ***on F^2***	1.061
Final R indices [I > 2σ(I)]	R_1[b] = 0.0587 wR_2[c] = 0.1731
Largest difference peak and hole ($eÅ^{-3}$)	0.210 and –0.233

Table. 2. Crystallographic Data for L^{MN} (7).

C(1)–O(1)	1.212	(3)	***C(1)–N(1)***	1.326	(3)
C(1)–C(8)	1.545	(3)			
N(5)–C(8)	1.440	(3)	***N(7)–C(8)***	1.446	(3)
N(5)–N(6)	1.372	(2)	***N(7)–N(8)***	1.374	(2)
N(5)–C(11)	1.358	(3)	***N(7)–C(16)***	1.360	(3)
N(6)–C(9)	1.316	(3)	***N(8)–C(14)***	1.326	(3)
C(10)–C(9)	1.400	(4)	***C(15)–C(14)***	1.394	(4)
C(11)–C(10)	1.358	(4)	***C(16)–C(15)***	1.361	(3)
O(1)–C(1)–N(1)	124.2	(2)	***O(1)–C(1)–C(8)***	118.9	(2)
N(5)–C(8)–C(1)	114.5	(2)	***N(7)–C(8)–C(1)***	112.1	(2)
N(6)–N(5)–C(8)	119.6	(2)	***N(8)–N(7)–C(8)***	116.0	(2)
C(9)–N(6)–N(5)	104.4	(2)	***C(14)–N(8)–N(7)***	104.4	(2)
C(11)–N(5)–N(6)	112.0	(2)	***C(16)–N(7)–N(8)***	112.2	(2)
C(10)–C(11)–N(5)	105.8	(2)	***C(15)–C(16)–N(7)***	105.4	(2)

Table 3. Selected Bond Lengths (Å) and Angles (deg) for L^{MN} (7).

The pyrazole and imidazole rings of **7** are planar within 0.01 Å, while the C8C1O1N1 ('amide' plane) atom set is also planar within 0.03 Å. The mean planes encompassing the five-membered rings and the amide plane define with each other dihedral angles ranging from 56.6° to 84.4°. In the absence of a coordinated metal core, the ligand assumes an overall arrangement that is determined by the number and efficiency of intra- and inter-molecular nonbonding contacts. The ligand has a folded shape, with the two pyrazole rings oriented in such a way to have N6 facing H18C and N8 facing H13C, at a mean distance of about 2.8 Å. In the same time, the imidazole ring is bent towards the O1 atom so that the centroid of the imidazole is about 4.0 Å far from O1.

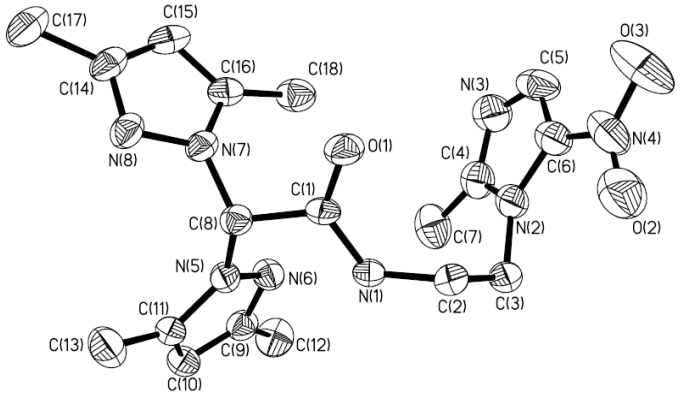

Fig 3.27. ORTEP view of L^{MN} (7).

An examination of crystal packing reveals two very loose hydrogen bonds, in which the donor atom is always the HN1 hydrogen and the acceptors are either the pyrazole N6 of the same molecule (intramolecular bonding) or the O1 atom of an adjacent molecule (at *x*, ½ - *y*, ½ + *z*). The donor-hydrogen-donor angles are far from the ideal 180° (117 and 138°, respectively) and so are the distances between the nucleophiles involved in the interactions (N1/N6 2.95 Å; N1/O1 3.01 Å); the intermolecular hydrogen bond involving O1 runs along the crystallographic *c* axis.

Due to the XAFS studies,[107] the coordination core of the copper(II) complexes can be modeled with two different ligands interacting with one copper atom as displayed in **Figure 3.28**, hence describing an octahedral environment for the copper site.

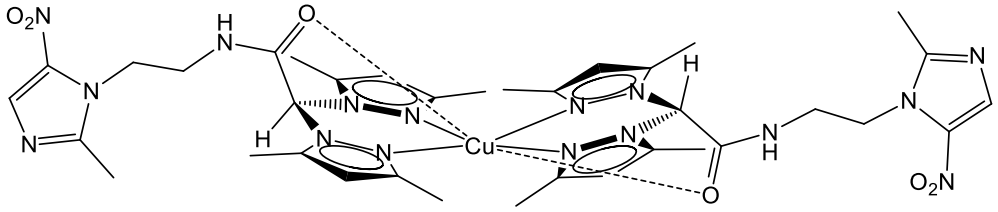

Figure 3.28. Model compound for complex 14.

Taking into account the characterization above, we could hypothesize that the model compound for the copper(II) complex of {[$(L^{MN1})_2$Cu]Cl_2} (**15**) could have a similar tridimentional structure (**Fig. 3.29**).

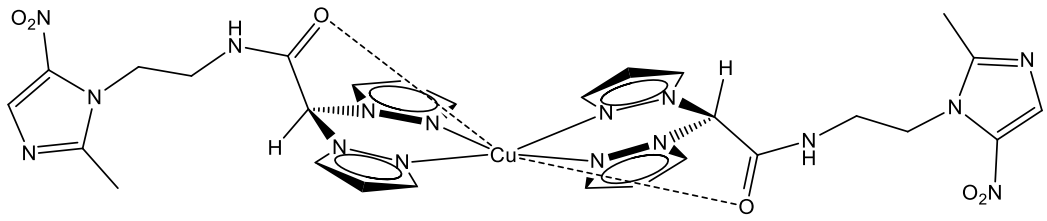

Figure 3.29. Assumed model compound for complex 15.

3.1.4.2 Cytotoxic activity

Cu(II) complex {[(L^{MN})$_2$Cu]Cl_2} (**14**) as well as the corresponding uncoordinated ligand L^{MN} was evaluated for its cytotoxic activity towards a panel of six human tumour cell lines including examples of cervical (A431), colon (HCT-15), lung (A549), pancreas (Capan-1) and breast (MCF-7) cancer along with melanoma (A375). Cytotoxicity was evaluated by means of MTT test after 72 hours of treatment with increasing concentrations of the tested compounds. For comparison purposes, the cytotoxicity of cisplatin, the most widely used anticancer metallodrug, was evaluated in the same experimental conditions. IC_{50} values, calculated from dose-survival curves, are shown in **Table. 4**.

Compound	*IC_{50} (μM) ± S.D.*					
	HCT-15	***A375***	***MCF-7***	***A549***	***A431***	***Capan-1***
{[(L^{MN})$_2$Cu]Cl_2} (14)	4.13±2.13	18.01±2.03	14.53±2.12	15.03±3.09	17.53±1.32	13.31±2.54
L^{MN} (7)	62.56±2.03	79.05±1.25	88.84±3.58	77.84±2.63	97.84±3.65	99.97±2.97
Cisplatin	12.34±2.37	3.11±0.98	8.78±1.32	12.51±2.35	2.15±0.87	7.65±1.05
S.D.=standard deviation Cells (3-8 ·10^4 ·mL^{-1}) were treated for 72 h with increasing Concentrations of tested compounds. Cytotoxicity was assessed by MTT test. IC_{50} values were calculated by four parameter logistic model ($P < 0.05$).						

Table 4. Cytotoxic activity of {[(L^{MN})$_2$Cu]Cl_2} (14) and the corresponding uncoordinated ligand L^{MN}.

Uncoordinated ligands prove to be ineffective over all cell lines. On the contrary, copper complexes display a similar growth inhibitory potency that is in the micromolar range towards the different types of tumor cells and slightly lower than that shown by cisplatin. Interestingly, in HCT-15 colon adenocarcinoma cells, the cytotoxicity of the copper(II) complex **14** exceeds that of the reference drug by a factor of about **14**. Actually, very recently a hydrophilic phosphine copper(I) complex has been found to kill human colon cancer cells more efficiently than cisplatin and oxaliplatin and to overcome platinum drug resistance.[209] In this view, the new copper(II) derivative has also been tested for its *in vitro* antitumor activity in a cell line pair which has been selected for its resistance to cisplatin: 2008/C13* human ovarian cancer cells. Although cisplatin resistance is multifactorial, the main molecular mechanisms involved in drug resistance in C13* cancer cells have almost been identified. Indeed, in this cell line resistance is correlated to high cellular glutathione and thioredoxin reductase levels,[210] a reduced cellular drug uptake, and enhanced repair of DNA damage.[211] Cytotoxicity in sensitive and resistant cells was assessed after a 48 h drug exposure by MTT test. Cross-resistance profiles were evaluated by means of the resistance factor (RF), which is defined as the ratio between

IC_{50} values calculated for the resistant cells and those arising from the sensitive ones (**Tab. 5**). Copper(II) complex **14** induces a similar pattern of response across the parental and the resistant subline with R.F. values roughly 7-fold lower than that of cisplatin, suggesting the absence of a cross-resistance with cisplatin.

Compound	***IC_{50} (μM) ± SD***		
	2008	***C13****	***R.F.***
{[$(L^{MN})_2$Cu]Cl_2} (14)	17.85±2.36	17.65±1.25	1
Cisplatin	13.47±2.08	89.97±2.25	6.7
S.D.= standard deviation Cells ($3\text{-}8 \cdot 10^4 \cdot mL^{-1}$) were treated for 48 h with increasing concentrations of tested compounds. Cytotoxicity was assessed by MTT test. IC_{50} values were calculated by four parameter logistic model ($P < 0.05$). R.F. = IC_{50} resistant/IC_{50} sensitive			

Table 5. Cisplatin cross-resistance profiles.

However, a complete overview about cytotoxic activity of some compounds was done (**Tab. 6-9**). Computational studies about the mode of action and about the cytotoxic activities of silver species are in progress.

Compound	IC_{50} (μM) ± D.S					
	A431	**BxPC3**	**HCT-15**	**MCF-7**	**A549**	**2008**
{[HC$(CO_2)(tz)_2$]Cu} (**16**)	12,08±3,46	7,45±2,08	17,52 ±2,46	16,09 ±2,52	8,56±1,23	18,16±3,12
{[HC$(CO_2H)(tz)_2$]Cu(PF_6)}•H_2O (**17**)	>50	>50	38,85 ±3,88	28,89±3,85	4,30±1,97	41,41±2,58
{[HC$(CO_2)(tz)_2$][Cu$(PBz_3)]_4$}•$(PF_6)_3$ (**18**)	1,30±0,38	1,75±0,96	2,87±1,15	3,26±1,08	0,26±0,01	2,87±1,15
Cisplatin	1,65±0,51	7,34±1,17	15,25±2,21	8,78±1,38	7,46±1,21	2,22±1,03
Cells (3-8 × 10^4 mL−1) were treated for 72 h with increasing concentrations of tested compounds, Cytotoxicity was assessed by MTT test, IC50 values were calculated by a four parameter logistic model (P < 0,05), S.D.= standard deviation.						

Table 6. Cytotoxic activity of Cu(I) based complexes.

Compound	IC_{50} (μM) ± D.S.					
	A431	**BxPC3**	**HCT-15**	**MCF-7**	**A549**	**2008**
{[HC$(CO_2H)(pz^{Me2})_2$]Cu[HC$(CO_2)(pz^{Me2})_2$]•ClO_4} (**9**)	3,76±1,08	1,94±0,56	16,50±0,58	10,50±2,14	3,56±0,52	10,75±1,25
{[HC$(CO_2)(tz)_2]_2$Cu} (**10**)	15,86±5,81	18,51±4,42	>50	39,60±4,58	4,47±1,88	>50
{Na[HC$(CO_2)(PyS)_2$]CuCl} (**11**)	8,26±0,94	5,25±0,61	---	---	---	---
{[HC$(CO_2H)(pz)_2]_3$Cu$(ClO_4)_2$} (**12**)	10,65±1,23	6,33±1,20	9,52±2,72	8,54±2,46	4,62±0,21	6,62±1,41
{[HC$(CO_2)(tz)_2$]Cu(ClO_4)} (**13**)	17,31±2,27	14,65±2,35	15,87±3,66	13,75±2,87	6,18±2,16	17,25±1,85
Cisplatin	1,65±0,51	7,34±1,17	15,25±2,21	8,78±1,38	7,46±1,21	2,22±1,03
Cells (3-8 × 10^4 mL−1) were treated for 72 h with increasing concentrations of tested compounds, Cytotoxicity was assessed by MTT test, IC50 values were calculated by a four parameter logistic model (P < 0,05), S.D.= standard deviation.						

Table 7. Cytotoxic activity of Cu(II) based complexes.

Compound	IC_{50} (μM) ± D.S.						
	A431	**BxPC3**	**HCT-15**	**MCF-7**	**A549**	**2008**	**Capan-1**
{[$(L^{MN})_2$Cu]Cl_2} (**14**)	12,65±1,93	8,67±2,12	6,12±2,09	10,58±3,13	15,55±4,08	13,18±3,76	13.31±2.54
{$(L^{MN1})_2CuCl_2$} (**15**)	11,28±2,10	10,54±4,11	9,11±2,54	10,85±2,86	8,28±2,41	11,25±3,19	---
{[(L^{MN})Cu$(PTA)_2$]}•(PF_6) (**19**)	1,35±0,91	3,67±1,86	7,04±2,48	7,25±1,43	6,49±1,25	8,23±1,36	---
{[(L^{MN1})Cu$(PTA)_2$]}(PF_6)•$2H_2O$ (**20**)	5,39±1,25	6,41±2,13	12,54±3,16	4,12±1,03	7,85±1,34	11,41±1,34	---
L^{MN} (**7**)	97.84±3.65	---	62.56±2.03	88.84±3.58	77.84±2.63	---	99.97±2.97
Cisplatin	1,65±0,51	7,34±1,17	15,25±2,21	8,78±1,38	7,46±1,21	2,22±1,03	7.65±1.05
Cells (3-8 × 10^4 mL−1) were treated for 72 h with increasing concentrations of tested compounds, Cytotoxicity was assessed by MTT test, IC_{50} values were calculated by a four parameter logistic model (P < 0,05), S.D.= standard deviation.							

Table 8. Cytotoxic activity of complexes based on functionalised species.

Compound	IC_{50} (μM) ± D.S.		
	LoVo	LoVo OXP	RF
{[HC(CO_2H)(pz^{Me2})$_2$]Cu[HC(CO_2)(pz^{Me2})$_2$]•ClO_4} (**9**)	6,25±0,85	7,75±0,57	1,2
{[HC(CO_2)(tz)$_2$]$_2$Cu} (**10**)	15,25±0,98	32,5±1,05	2,1
{[HC(CO_2H)(pz)$_2$]$_3$Cu(ClO_4)$_2$} (**12**)	3,37±0,45	4,12±0,55	1,2
{[HC(CO_2)(tz)$_2$]Cu(ClO_4)} (**13**)	5,50±0,22	7,51±0,50	1,4
{[HC(CO_2)(tz)$_2$]Cu} (**16**)	8,75±1,28	8,74±0,25	1
{[HC(CO_2H)(tz)$_2$]Cu(PF_6)}•H_2O (**17**)	12,85±0,15	25,00±1,05	1,9
{[HC(CO_2)(tz)$_2$][Cu(PBz_3)]$_4$}•(PF_6)$_3$ (**18**)	1,06±0,11	1,43±0,21	1,3
Oxaliplatin	15,25±2,24	1,36±0,73	17
Cells (3-8 × 10^4 mL^{-1}) were treated for 72 h with increasing concentrations of tested compounds. Cytotoxicity was assessed by MTT test. IC_{50} values were calculated by a four parameter logistic model ($P < 0.05$). S.D.= standard deviation. RF=IC_{50} (resistant subline)/IC_{50} (wild-type cells).			

Table 9. Oxaliplatin cross-resistance profiles.

Preliminary antimetastatic tests were carried out for the complex {[(L^{MN})$_2$Cu]Cl_2} (**14**) in comparison with the copper(I) complex Cu(PTA)PF_6.

Tumor cell invasion (**Fig. 3.30**) was carried out using a Transwell insert (8 μm, Corning, USA). LoVo cells were starved in a medium without fetal bovine serum overnight, and then 1×10^5 cells resuspended in 0.1 ml serum-free medium were added to the upper chamber and cultured for 24 h. The inserts were precoated with extracellular Matrigel (BD Biosciences, USA). Invaded cells were fixed and stained with 0.1% crystal violet. Five low-magnification areas (x100) were randomly selected and counted for the cell numbers. All experiments were performed in triplicate.

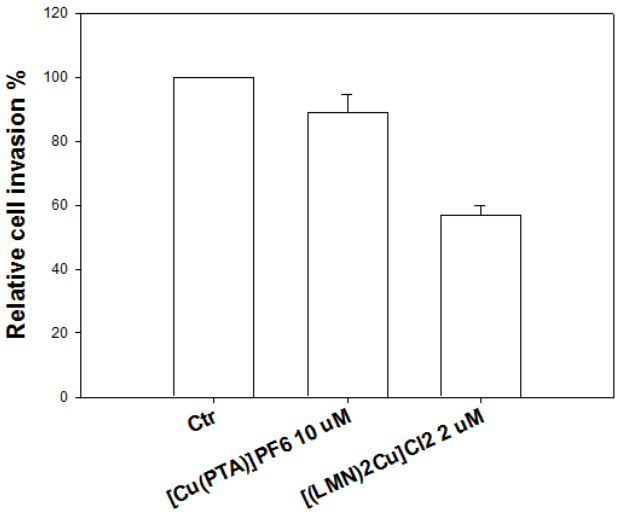

Figure 3.30. Model Tumor cell invasion data.

Inhibition assays (**Fig. 3.31** and **Fig. 3.32**) were performed at room temperature in buffer containing 50 mM Tris, pH 6.5, 100 mM NaCl, 1 mM EDTA, 0.1 mM dithiothreitol (DTT) and 0.01% Brij 35. Prior to the reaction, the enzyme was activated by incubation with 0.1 mM DTT for 30 min. Enzyme activity was measured in 96-well plates using 1.5 µM 6,8-difluoro-4-methylumbelliferryl phosphate (DiFMUP) as the substrate. Assays were conducted in triplicate measuring the fluorescence at 455 nm for 30 min and the results averaged and reported as relative fluorescence units.

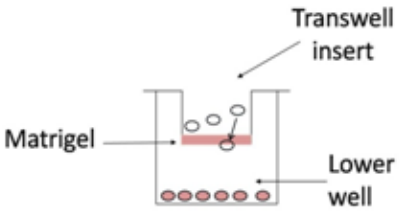

Figure 3.31. Experimental set-up.

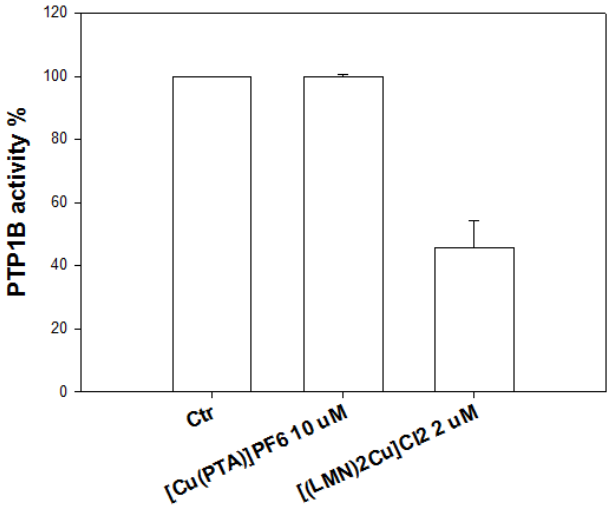

Figure 3.32. Inhibition assay data.

5. References

1 H. R. Bigmore, S. C. Lawrence, P. Mountford and C. S. Tredget, *Dalton Trans.* 2005, 635.
2 A. Otero, J. Fernandez-Baeza, A. Antinolo, J. Tejeda and A. Lara-Sanchez, *Dalton Trans.* 2004, 1499.
3 A. Otero, A. Lara-Sanchez, J. Fernandez-Baeza, E. Martinez-Caballero, I. Marquez-Segovia, C. Alonso-Moreno, L. F. Sanchez-Barba, A. M. Rodriguez and I. Lopez-Solera, *Dalton Trans.* 2010, 39, 930.
4 S. Trofimenko, *Scorpionates: The Coordination Chemistry of Poly(pyrazolyl)borate Ligands*, ImperialCollege Press, London, 1999.
5 C. Santini, M. Pellei, G. Gioia Lobbia and G. Papini, *Mini-Rev. Org. Chem.* 2010, 7, 84.
6 M. Pellei, G. Gioia Lobbia, G. Papini and C. Santini, *Mini-Rev. Org. Chem.* 2010, 7, 173.
7 H. Kopf, B. Holzberger, C. Pietraszuk, E. Huebner and N. Burzlaff, *Organometallics* 2008, 27, 5894.
8 A. Otero, J. Fernandez-Baeza, A. Antinolo, A. Lara-Sanchez, E. Martinez-Caballero, J. Tejeda, L. F. Sanchez-Barba, C. Alonso-Moreno and I. Lopez-Solera, *Organometallics.* 2008, 27, 976.
9 N. Burzlaff, I. Hegelmann and B.Weibert, *J. Organomet. Chem.* 2001, 626, 16.
10 A. Beck, B. Weibert and N. Burzlaff, *Eur. J. Inorg. Chem.* 2001, 521.
11 E. Huebner, T. Haas and N. Burzlaff, *Eur. J. Inorg. Chem.* 2006, 4989.
12 P. C. A. Bruijnincx, I. L. C. Buurmans, S. Gosiewska, M. A. H. Moelands, M. Lutz, A. L. Spek, G. van Koten and R. J. M. Klein Gebbink, *Chem.-Eur. J.* 2008, 14, 1228.
13 E. Galardon, M. Giorgi and I. Artaud, *Dalton Trans.* 2007, 1047.
14 T. C. Higgs and C. J. Carrano, *Inorg. Chem.* 1997, 36, 291.
15 T. C. Higgs and C. J. Carrano, *Inorg. Chem.* 1997, 36, 298.
16 C. Santini and M. Pellei, *Curr. Bioact. Compd.* 2009, 5, 243.
17 N. V. Fischer, G. Turkoglu and N. Burzlaff, *Curr. Bioact. Compd.* 2009, 5, 277.
18 B. S. Hammes and C. J. Carrano, *Chem. Commun.* 2000, 1635.
19 M. Pellei, G. Gioia Lobbia, C. Santini, R. Spagna, M. Camalli, D. Fedeli and G. Falcioni, *Dalton Trans.* 2004, 2822.
20 C. Marzano, M. Pellei, D. Colavito, S. Alidori, G. Gioia Lobbia, V. Gandin, F. Tisato and C. Santini, *J. Med. Chem.* 2006, 49, 7317.
21 F. Tisato, C. Marzano, M. Porchia, M. Pellei and C. Santini, *Med. Res. Rev.* 2010, 30, 708.
22 A. Otero, J. Fernandez-Baeza, A. Antinolo, F. Carrillo-Hermosilla, J. Tejeda, E. Diez-Barra, A. Lara-Sanchez, L. Sanchez-Barba, I. Lopez-Solera, M. R. Ribeiro and J. M. Campos, *Organometallics* 2001, 20, 2428.
23 S. C. Lawrence, B. D. Ward, S. R. Dubberley, C. M. Kozak and P. Mountford, *Chem. Commun.* 2003, 2880.
24 C. Cuomo, S. Milione and A. Grassi, *Macromol. Rapid Commun.* 2006, 27, 611.
25 S. Milione, V. Bertolasi, T. Cuenca and A. Grassi, *Organometallics* 2005, 24, 4915.
26 S. Milione, F. Grisi, R. Centore and A. Tuzi, *Organometallics* 2006, 25, 266.
27 S. Milione, C. Montefusco, T. Cuenca and A. Grassi, *Chem. Commun.* 2003, 1176.
28 C. Santini, M. Pellei, G. Gioia Lobbia, A. Cingolani, R. Spagna and M. Camalli, *Inorg. Chem. Commun.* 2002, 5, 430.
29 M. Pellei, C. Santini, G. Gioia Lobbia, F. Cantalamessa, C. Nasuti, M. Di Prinzio, R. Gabbianelli and G. Falcioni, *Appl. Organomet. Chem.* 2005, 19, 583.
30 M. Pellei, G. Gioia Lobbia, M. Ricciutelli and C. Santini, *J. Coord. Chem.* 2005, 58, 409.
31 F. Benetollo, G. Gioia Lobbia, M. Mancini, M. Pellei and C. Santini, *J. Organomet. Chem.* 2005, 690, 1994.
32 F. Marchetti, M. Pellei, C. Pettinari, R. Pettinari, E. Rivarola, C. Santini, B. W. Skelton and A. H. White, *J. Organomet. Chem.* 2005, 690, 1878.
33 M. Porchia, G. Papini, C. Santini, G. Gioia Lobbia, M. Pellei, F. Tisato, G. Bandoli and A. Dolmella, *Inorg. Chem.* 2005, 44, 4045.
34 M. Pellei, C. Santini, M. Mancini, S. Alidori, M. Camalli and R. Spagna, *Polyhedron* 2005, 24, 995.
35 M. Porchia, G. Papini, C. Santini, G. Gioia Lobbia, M. Pellei, F. Tisato, G. Bandoli and A. Dolmella, *Inorg. Chim. Acta* 2006, 359, 2501.
36 M. Pellei, S. Alidori, M. Camalli, G. Campi, G. Gioia Lobbia, M. Mancini, G. Papini, R. Spagna and C. Santini, *Inorg. Chim. Acta* 2008, 361, 1456.
37 S. Alidori, F. Cocchioni, G. Falcioni, D. Fedeli, G. E. Gioia Lobbia, M. Mancini, M. Pellei and C. Santini, *Appl. Organomet. Chem.* 2008, 22, 43.
38 M. Pellei, S. Alidori, F. Benetollo, G. Gioia Lobbia, M. Mancini, G. E. Gioia Lobbia and C. Santini, *J. Organomet. Chem.* 2008, 693, 996.
39 M. Giorgetti, L. Guadagnini, S. G. Fiddy, C. Santini and M. Pellei, *Polyhedron* 2009, 28, 3600.

40 C. Pettinari, A. Cingolani, G. Gioia Lobbia, F. Marchetti, D. Martini, M. Pellei, R. Pettinari and C. Santini, *Polyhedron* 2004, 23, 451.
41 G. Gioia Lobbia, M. Pellei, C. Pettinari, C. Santini, B.W. Skelton, N. Somers and A. H. White, *J. Chem. Soc., Dalton Trans.* 2002, 2333.
42 A. Otero, J. Fernandez-Baeza, A. Antinolo, F. Carrillo-Hermosilla, J. Tejeda, E.Diez-Barra, A. Lara-Sanchez, M. Fernandez Lopez, M. Lanfranchi, M. A. Pellinghelli, *J. Chem. Soc., Dalton Trans.* 1999, 3537.
43 A. Otero, J. Fernandez-Baeza, A. Antinolo, J. Tejeda, A. Lara-Sanchez, L. Sanchez-Barba, M. T. Exposito, A. M. Rodriguez, *J. Chem. Soc., Dalton Trans.* 2003, 1614.
44 I. Hegelmnann, N. Burzlaff, *Eur. J. Inorg. Chem.* 2003, 409.
45 B. S. Hammes, M. T. Kieber-Emmons, J. A. Letizia, Z. Shirin, C. J. Carrano, L. N. Zakharov, A. L. Rheigold, *Inorg. Chim. Acta* 2003, 346, 227.
46 A. Otero, J. Fernandez-Baeza, A. Antinolo, F. Carillo-Hermosilla, J. Tejeda, A. Lara-Sanchez, L. Sanchez-Barba, M. Fernandez-Lopez, A. M. Rodriguez, I. Lopez Solera, *Inorg. Chem.* 2002, 41, 5193.
47 A. Otero, J. Fernandez-Baeza, A. Antinolo, F. Carillo-Hermosilla, J. Tejeda, E. Diez-Barra, A. Lara-Sanchez, M. Fernandez-Lopez, *J. Chem. Soc., Dalton Trans.* 2000, 2367.
48 A. Otero, J. Fernandez-Baeza, A. Antinolo, J. Tejeda, A. Lara-Sanchez, L. Sanchez-Barba, A. M. Rodriguez, *Eur. J. Inorg. Chem.* 2004, 260.
49 D. L. Jameson, S. E. Hilgen, C. E. Hummel, S. L. Pichla, *Tetrahedron Lett.* 1989, 30, 1609.
50 B. S. Hammes, C. J. Carrano, *Inorg. Chem.* 1999, 38, 3562.
51 M. C. Carrion, A. Guerrero, F. Jalon, B. Manzano, A. Rodriguez, R. L. Paul, J. C. Jeffery, *J. Organomet. Chem.* 2002, 650, 210.
52 T. C. Higgs, D. Ji, R. S. Czernuszewicz, B. F. Matzanke, V. Schunemann, A. X. Trautwein, M. Helliwell, W. Ramirez, J. C. Carrano, *Inorg. Chem.* 1998, 37, 2383.
53 B. S. Hammes, C. J. Carrano, *J. Chem. Soc., Dalton Trans.* 2000, 19, 3304.
54 B. S. Hammes, C. J. Carrano, *Eur. J. Inorg. Chem.* 2002, 3632.
55 P. K. Byers, A. J. Canty, R. T. Honeyman, *J. Organomet. Chem.* 1990, 385, 417.
56 A. J. Canty, R. T. Honeyman, *J. Organomet. Chem.* 1990, 387, 247.
57 A. J. Canty, R. T. Honeyman, B. W. Skelton, *J. Organomet. Chem.*1990, 389, 277.
58 D. L. Reger, T. C. Grattan, K. J. Brown, C. A. Little, J. J. S. Lamba, A. L. Rheingold, R. D. Sommer, *J. Organomet. Chem.* 2000, 607, 120.
59 F. H. Herbstein, *Top. Curr. Chem.* 1987, 140, 107.
60 C. Janiak, *J. Chem. Soc., Chem. Commun.* 1994, 545.
61 F. T. Edelmann, *Angew. Chem., Int. Ed.* 2001, 40, 1656.
62 B. E. Hanson, *Coord. Chem. Rev.* 1999, 185, 795.
63 N. Navon, H. Cohen, P. Paoletti, B. Valtancoli, A. Bencini, D. Meyerstein, *Ind. Eng. Chem. Res.* 2000, 39, 3536.
64 K., V. Katti, H. Gali, C. J. Smith, D. E. Berning, *Acc. Chem. Res.* 1999, 32, 9.
65 S. Trofimenko, *J. Am. Chem. Soc.* 1966, 88, 1842.
66 C. Pettinari, C. Santini, *Polypyrazolylborate and Scorpionate Ligands*: Oxford, U.K., 2004, 1, 159.
67 S. Trofimenko, *J. Am. Chem. Soc*. 1970, 92, 5118.
68 E. Pullen, D. Rabinovich, C. Incarvito, T. E. Concolino, A. L. Rheingold, *Inorg. Chem.* 2000, 39, 1561.
69 E. Psillakis, J. C. Jeffery, J. A. McCleverty, M. D. Ward, *J. Chem. Soc., Dalton Trans* 1997, 1645.
70 T. N. Sorrell, W. E. Allen, P. S. White, *Inorg. Chem.* 1995, 34, 952.
71 M. Porchia, A. Dolmella, V. Gandin, C. Marzano, M. Pellei, V. Peruzzo, F. Refosco, C. Santini, F. Tisato, *J. Med. Chem.* 2013, 59, 218.
72 (a) C.J. Evans, in: P.J. Smith (Ed.), Chemistry of Tin, Blackie Academic and Professional, London, 1998, 442; (b) J. Otera, *Chem. Rev*. 1993, 93 1449; (c) S. Durand, K. Sakamoto, T. Fukuyama, A. Orita, J. Otera, A. Duthie, D. Dakternieks, M. Schulte, K. Jurkschat, *Organometallics* 2000, 19, 3220; (d) A. Orita, Y. Hamada, T. Nakano, S. Toyoshima, J. Otera, *Chem. Eur. J.* 2001, 7, 3321.
73 D. P. Miller, P. J. Craig, in: P. J. Smith (Ed.), *Chemistry of Tin*, Blackie Academic and Professional, London, 1998, 74, 541.
74 I. Omae, *Appl. Organometal. Chem*. 2003, 17, 81.
75 (a) M. Gielen, *Appl. Organometal. Chem.* 2002, 16, 481; (b) M. Gielen, *Coord. Chem. Rev*. 1996, 151, 41.
76 (a) R. R. Holmes, *Acc. Chem. Res.* 1989, 22, 190; (b) J. Beckmann, K. Jurkschat, *Coord. Chem. Rev*. 2001 215, 267; (c) V. K. Jain, *Coord. Chem. Rev*. 1994, 809, 135; (d) V. Chandrasekhar, S. Nagendran, V. Baskar, *Coord. Chem. Rev*. 2002, 235, 1.
77 (a) L. R. Hanton, K. Lee, *Inorg. Chem*. 1999, 38, 1634; (b) J. L. Chou, D. N. Horng, J. P. Chyn, K.M. Lee, F. L. Urbach, G.H. Lee, H. L. Tsai, *Inorg. Chem*. Comm. 1999, 2, 392.
78 (a) C. Y. Su, B. S. Kang, J. Sun, Y. X. Tong, Z. N. *Chen, J. Chem. Res. S*. 1997, 454; (b) J. L. Chou, J. P. Chyn, F. L. Urbach, D. F. Gervasio, *Polyhedron*, 2000, 19, 2215.
79 (a) M. V. Castano, A. Macıas, A. Castineiras, A. Sanchez- Gonzalez, E. Garcıa-Martınez, J. S. Casas, J. Sordo, W. Hiller, E. E. Castellano, *J. Chem. Soc., Dalton Trans*. 1990, 1001.

80 J. S. Casas, A. Castineiras, E. Garcıa-Martınez, A. Sanchez- Gonzalez, J. Sordo, E. M. Vazquez-Lopez, U. Russo, *Polyhedron* 1996, 15, 891.
81 J. S. Casas, A. Castineiras, E. Garcıa-Martınez, P. Rodrıguez- Rodrıguez, U. Russo, A. Sanchez, A. Sanchez-Gonzalez, J. Sordo, *Appl. Organomet. Chem*. 1999, 13, 69.
82 M. Gielen, E. R. T. Tiekink, in: M. Gielen, E. R. T. Tiekink (Eds.), *Metallotherapeutic Drugs & Metal-Based Diagnostic Agents. The Use of Metals in Medicine*, John Wiley & Sons Ltd., Chichester, England, 2005, 421.
83 Y. Hori, T. Hagiwara, *Int. J. Biol. Macromol.* 1999, 25, 237.
84 B. Jousseaume, M. Pereyre, in: P. Smith (Ed.), *The Chemistry of Tin*, 2nd ed., Blackie, London, 1998, 290.
85 A. Orita, A. Mitsutome, J. Otera, *J. Org. Chem*. 1998, 63, 2420.
86 A. Orita, K. Sakamoto, Y. Hamada, A. Mitsutome, J. Otera, *Tetrahedron* 1999, 55, 2899.
87 A. C. Draye, J. J. Tondeur, *J. Mol. Catal. A: Chem.* 1999, 140, 31.
88 S. H. L. Thoonen, B. J. Deelman, G. Van Koten, *J. Organomet. Chem*. 2004, 689, 2145.
89 F. M. Armbrech Jr., W. Tronich, D. Seyferth, *J. Am. Chem. Soc*. 1969, 3218.
90 M. Hoch. *Appl. Geochem.* 2001, 16, 719.
91 I. J. Boyer. *Toxicol.* 1989, 55, 253.
92 C. A Krone, J. E Stein. *Aquat. Toxicol.* 1999, 45, 209.
93 World Health Organization. *Tributyltin Compounds*. Report no.116. World Health Organization, United Nations Environment Programme: Geneva, 1990.
94 A. Otero, J. Fernandez-Baeza, A. Antinolo, J. Tejeda, A. Lara-Sanchez, L. Sanchez-Barba, M. Sanchez-Molina, S. Franco, I. Lopez-Solera and A. M. Rodriguez, *Eur. J. Inorg. Chem.* 2006, 707.
95 A. Otero, J. Fernandez-Baeza, A. Antinolo, J. Tejeda, A. Lara-Sanchez, L. Sanchez-Barba, M. Sanchez-Molina, S. Franco, I. Lopez-Solera and A. M. Rodriguez, *Dalton Trans.* 2006, 4359.
96 A. Otero, J. Fernandez-Baeza, A. Lara-Sanchez, C. Alonso-Moreno, I. Marquez-Segovia, L. F. Sanchez-Barba and A. M. Rodriguez, *Angew. Chem., Int. Ed*. 2009, 48, 2176.
97 A. Otero, J. Fernandez-Baeza, A. Lara-Sanchez, J. Tejeda and L. F. Sanchez-Barba, *Eur. J. Inorg. Chem.* 2008, 5309.
98 M. P. Hay, W. R. Wilson, J. W. Moselen, B. D. Palmer and W. A. Denny, *J. Med. Chem.* 1994, 37, 381.
99 A. Brecia, B. Cavalleri and G. E. Adams, *Nitroimidazoles, Chemistry, Pharmacology and Clinical Application*, Plenum, New York, 1982.
100 W. J. Koh, K. S. Bergman, J. S. Rasey, L. M. Peterson, M. L. Evans, M. M. Graham, J. R. Grierson, K. L. Lindsley, T. K. Lewellen and K. A. Krohn, *Int. J. Radiat. Oncol., Biol., Phys.* 1995, 33, 391.
101 G. V. Martin, J. H. Caldwell, M. M. Graham, J. R. Grierson, K. Kroll, M. J. Cowan, T. K. Lewellen, J. S. Rasey, J. J. Casciari and K. A. Krohn, *J. Nucl. Med.* 1992, 33, 2202.
102 A. Nunn, K. Linder and H. W. Strauss, *Eur. J. Nucl. Med. Mol. Imaging* 1995, 22, 265.
103 S. J. Read, T. Hirano, D. F. Abbott, J. I. Sachinidis, H. J. Tochon-Danguy, J. G. Chan, G. F. Egan, A. M. Scott, C. F. Bladin, W. J. McKay and G. A. Donnan, *Neurology* 1998, 51, 1617.
104 E. L. Engelhardt, R. F. Schneider, S. H. Seeholzer, C. C. Stobbe and J. D. Chapman, *J. Nucl. Med.* 2002, 43, 837.
105 Z. Li, T. Chu, X. Liu and X. Wang, *Nucl. Med. Biol.* 2005, 32, 225.
106 P. D. Bonnitcha, S. R. Bayly, M. B. M. Theobald, H. M. Betts, J. S. Lewis and J. R. Dilworth, *J. Inorg. Biochem.* 2010, 104, 126.
107 M. Pellei, G. Papini, A. Trasatti, M. Giorgietti, D. Tonelli, M. Minicucci, C. Marzano, V. Gandin, G. Aquilanti, A. Dolmella and C. Santini, *Dalton Trans*. 2011, 40, 9877.
108 W. Levason and C. A. McAuliffe, *Adv. in Inorg. Chem. and Radiochem*. 1972, 14, 173.
109 R. J. Cross, *Int. Rev. Science, Transition Metals* 1974, 5, 147.
110 M. M. Rahman, H. Y. Liu, A. Prock and W. P. Giering, *Organometallics* 1987, 6, 650.
111 C. A. Tolman, *Chem. Rev*. 1977, 77, 313.
112 F. A. Cotton and G. Wilkinson, *Advanced Inorganic Chemistry,* Wiley, 1988, 65.
113 M. J. S. Dewar, Bu U. *Chim. Soc. Fran*. 1951, 18, C71.
114 J. Chatt and L. A. Duncanson, *J. Chem. Soc*. 1953, 2939.
115 J. P. Collman and L. S. Hegedus, *Principles and Applications of Organotransition Metal*, University of Science, 1980, 19.
116 J. D. Lee, *Concise Inorganic Chemistry,* Van Nostrand, 1986, 427.
117 P. Comba, *Coord. Chem. Rev*. 1993, 122, 1.
118 G. Wilkinson (Ed.), *Comp. Coord. Chem*. 1987, 2, 1013.
119 D. R. Tyler, *Acc. Chem. Res*. 1991, 24, 325.
120 R. G. Parr and Z. Zhou, *Acc. Chem. Res*. 1993, 26, 256.
121 J. Mathew, T. Thomas and Suresh, C. H. *Inorg. Chem.* 2007, 46, 10800.
122 E. R. Jamieson, S. J. Lippard, *Chem. Rev.* 1999, 99, 2467.
123 K. B. Lee, D. Wang, S. J. Lippard, *Proc. Natl. Acad. Sci*. 2002, 99, 4239.
124 A. J. Louie, T. J. Meade, *Chem. Rev*. 1999, 99, 2711.
125 W. A. Volkter, T. J. Hoffman, *Chem. Rev*. 1999, 99, 2269.

126 S. M. Cohen, S. J. Lippard, *Mol. Biol*. 2001, 67, 93.
127 Q. He, C. H. Liang, S. J. Lippard, *Proc. Natl. Acad. Sci*. 2000, 97, 5768.
128 B. Wong, J. E. Masse, Y. M. Yen, P. Giannikoupolous, J. Feigon, R. C. Johnson, *Biochem*. 2002, 41, 5404.
129 N. J. Farrer, J. A. Woods, L. Salassa, Y. Zhao, K. S. Robinson, G. Clarkson, F. S. Mackay, P. J. Sadler, *Angew. Chem. Int. Ed*. 2010, 49, 8905.
130 S. J. Berners-Price, *Angew. Chem. Int. Ed*. 2011, 50, 804.
131 N. J. Farrer, J. A. Woods, L. Salassa, Y. Zhao, K. S. Robinson, G. Clarkson, F. S. Mackay, P. J. Sadler, *Angew. Chem*. 2010, 122, 9089.
132 F. S. Mackay, J. A. Woods, H. Moseley, J. Ferguson, A. Dawson, S. Parsons, P. J. Sadler, *Chem. Eur. J.* 2006, 12, 3155.
133 F. S. Mackay, J. A. Woods, P. Heringova, J. Kasparkova, A. M. Pizarro, S. A. Moggach, S. Parsons, V. Brabec, P. J. Sadler, *Proc. Natl. Acad. Sci*. 2007, 104, 20743.
134 M. Skander, P. Retailleau, B. Bourrie, L. Schio, P. Mailliet, A. Marinetti, *J. Med. Chem.* 2010, 53, 2146.
135 D. Chen, V. Milacic, M. Frezza, Q. P. Dou, Curr. *Pharm. Des*. 2009, 15, 777.
136 L. Au, D. Zheng, F. Zhou, Z. Y. Li, Y. Xia, *Am. Chem. Soc. Nano* 2008, 2, 1645.
137 G. Marcon, S. Carotti, M. Coronnello, L. Messori, E. Mini, P. Orioli, T. Mazzie,M. A. Cinellu, G. Minghetti, *J. Med. Chem*. 2002, 45, 1672.
138 L. Messori, F. Abbate, G. Marcon, P. Orioli, M. Fontani, E. Mini, S. Carroti, *J. Med. Chem*. 2000, 43, 3541.
139 Y. Zheng, L. Sanche, *Radiat. Res*. 2009, 172, 114.
140 S. Kapoor, *J. Cell Biochem*. 2009, 106, 193.
141 K. Ansari, J. Grant, S. Kasiri, G. Woldemariam, B. Shrestha, S. Mandal, *J. Inorg. Biochem*. 2009, 103, 818.
142 M. J. Clarke, *Coord. Chem.* 2003, 236, 299.
143 M. Galanski, V. B. Arion, M. A. Jakupec, B. K. Keppler, *Curr. Pharm*. 2003, 9, 2078.
144 C. S. Allardyce, P. J Dyson, D. J. Ellis, S. L. Health, *Chem. Commun*. 2001, 1396.
145 V. Anne, H. Micheal, A. Elizebeth Hillard, S. Emmanuel, *J. Med. Chem*. 2005, 48, 2814.
146 T. S Lange, K. K. Kim, R. K. Singh, R. M. Strongin, C. K. McCourt, L. Brard, *PLoS One* 2008, 3, e2303.
147 S. Ray, R. Mohan, J. K. Singh, M. K. Samantaray, M. M. Shaikh, D. Panda, P. Ghosh, *J. Am. Chem. Soc*. 2007, 129, 15042.
148 R. W. Sun, D. L. Ma, E. L. Wong, C. M. Che, *Dalton Trans*. 2007, 43, 4884.
149 M. C. Linder, *Biochemistry of Copper* 1991.
150 M. C. Linder, M. Hazegh-Azam, *Am. J. Clin. Nutr. Suppl*. 1996, 63, 797S.
151 M. C. Linder, *Mutat. Res.* 2001, 475, 141.
152 C. Santini, M. Pellei, G. Gioia Lobbia, D. Fedeli, G. Falcioni, *J. Inorg. Biochem.* 2003, 94, 348.
153 C. Santini, M. Pellei, G Gioia Lobbia, S Alidori, M. Berrettini, D. Fedeli, *Chim. Acta* 2004, 357, 3549.
154 M. Pellei, G. Gioia Lobbia, C. Santini, R. Spagna, M. Camalli, D. Fedeli, G. Falcioni, *Dalton Trans.* 2004, 2822.
155 C. X. Zhang, S. J. Lippard, *Current Opinion in Chemical Biology* 2003, 7, 481.
156 S. Puig, D. J. Thiele, *Current Opinion in Chemical Biology* 2002, 6, 171.
157 S. Puig, J. Lee, M. Lau, D.J. Thiele, *J. Biol. Chem.* 2002, 277, 26021.
158 S. H. van Rijt, H. Kostrhunova, V. Brabec, P. J. Sadler, *Bioconjugate Chemistry* 2011, 22, 218.
159 M. E. Bravo-Gomez, J. C. Garcia-Ramos, I. Gracia-Mora, L. Ruiz-Azuara, *J. Inorg. Biochem*. 2009, *103*, 299.
160 L. D. D'Andrea, A. Romanelli, R. Di Stasi, *Dalton Trans.* 2010, 39, 7625.
161 G. Crisponi, V. M. Nurchi, D. Fanni, C. Gerosa, S. Nemolato, G. Faa, *Coord. Chem. Rev*. 2010, 254, 876.
162 A. Gaeta, R. C. Hider, *British Journal of Pharmacology* 2005, 146, 1041.
163 C. Marzano, M. Pellei, F. Tisato, C. Santini, *Anti-cancer Agents in Medicinal Chemistry* 2009, 9, 185.
164 A. Gupte, R. J. Mumper, *Cancer Treat. Review* 2009, 35, 32.
165 F. R. Kona, D. Buac, A. M. Burger, *Current Cancer Drug Targets* 2011, 11, 338.
166 S. S. Bhat, A. A. Kumbhar, H. Heptullah, A. A. Khan, V. V. Gobre, S. P. Gejji, V. G. Puranik, *Inorg. Chem.* 2011, *50*, 545.
167 N. J. Sanghamitra, P. Phatak, S. Das, A. Samuelson, K. Somasundaram, *J. Med. Chem*. 2005, 48, 977.
168 C. Marzano, M. Pellei, S. Alidori, A. Brossa, G. Gioia Lobbia, F. Tisato, C. Santini, *J. Inorg. Biochem*. 2006, 100, 299.
169 C. Marzano, V. Gandin, M. Pellei, D. Colavito, G. Papini, G. Gioia Lobbia, E. Del Giudice, M. Porchia, F. Tisato, C. Santini, *J. Med. Chem*. 2008, 51, 798.
170 C. Santini, M. Pellei, G. Papini, B. Morresi, R. Galassi, S. Ricci, F. Tisato, M. Porchia, M. P. Rigobello, V. Gandin, C. Marzano, *J. Inorg. Biochem*. 2011, *105*, 232.
171 F. Dallavalle, F. Gaccioli, R. Franchi-Gazzola, M. Lanfranchi, L. Marchiò, M. A. Pellinghelli, M. Tegoni, *J. Inorg. Biochem*. 2002, 92, 95.
172 S. Tardito, O. Bussolati, F. Gaccioli, R. Gatti, S. Guizzardi, J. Uggeri, L. Marchiò, M. Lanfranchi, R. Franchi-Gazzola, *Histochem. Cell Biol*. 2006, 126, 473.
173. S. Tardito, O. Bussolati, M. Maffini, M. Tegoni, M. Giannetto, V. Dall'Asta, R. Franchi-Gazzola, M. Lanfranchi, M. A. Pellinghelli, C. Mucchino, G. Mori, L. Marchiò, *J. Med. Chem.* 2007, 50, 1916.

174 D. Chen, Q. Cui, H. Yang,Q. P. Dou, *Cancer Res*. 2006, 66, 10425.
175 B. Shwenzer, J. Schleu, N. Burzlaff, C. Karl, H. Fischer, *J. Organomet. Chem*. 2002, 641, 134.
176 I. Hegelmann, A. Beck, C. Eichhorn, B. Weibert, N. Burzlaff, *Eur. J. Inorg. Chem.* 2003, 339.
177 L. Peters, N. Burzlaff, *Polyhedron* 2004, 23, 245.
178 G. McDonnell and A. D. Russell, *Clin. Microbiol. Rev*. 1999, 12, 147.
179 W. K. Jung, H. C. Koo, K. W. Kim, S. Shin, S. H. Kim and Y. H. Park, *Appl. Environ. Microbiol*. 2008, 74, 2171.
180 B. S. Atiyeh, M. Costagliola, S. N. Hayek and S. A. Dibo, *Burns*, 2007, 33, 139.
181 M.-L. Teyssot, A.-S. Jarrousse, M. Manin, A. Chevry, S. Roche, F. Norre, C. Beaudoin, L. Morel, D. Boyer, R. Mahiou, A. Gautier, *Dalton Trans.* 2009, 35, 6894.
182 S Hadjikakou, N. Hadjiliadis, N. Kourkoumelis, L. Kyros, M Kubicki, M Baril, I. S. Butler, S. Karkabounas, J. Balzarini, *Inorg. Chim. Acta* 2009, 362, 1003.
183 A. Gautier, F. Cisnetti, *Metallomics* 2012, 4, 23.
184 C. N. Banti, A. D. Giannoulis, N. Kourkoumelis, A. M. Owczarzak, M. Poyraz, M. Kubicki, K. Charalabopoulos, S. K. Hadjikakou, *Metallomics* 2012, 4, 545.
185 M. Poyraz, C. N. Banti, N. Kourkoumelis, V. Dokorou, M. J. Manos, M. Simcic, S. Golic-Grdadolnik, T. Mavromoustakos, A. D. Giannoulis, I. I. Verginadis, K. Charalabopoulos, S. K. Hadjikakou, *Inorg. Chim. Acta* 2011, 375, 114.
186 P. C. Zachariadis, S. K. Hadjikakou, N. Hadjiliadis, S. Skoulika, A. Michaelides, J. Balzarini, E. De Clercq, *Eur. J. Inorg. Chem*. 2004, 7, 1420.
187 S. K. Hadjikakou, I. I. Ozturk, M. N. Xanthopoulou, P. C. Zachariadis, S. Zartilas, S. Karkabounas, N. Hadjiliadis, *J. Inorg. Biochem*. 2008, 102, 1007.
188 (a) L. Kyros, N. Kourkoumelis, M. Kubicki, L. Male, M. B. Hursthouse, I. I. Verginadis, E. Gouma, S. Karkabounas, K. Charalabopoulos and S. K. Hadjikakou, *Bioinorg. Chem. Appl*. 2010, 386860; (b) C. L. Fox Jr. and S. M. Modak, *Antimicrob. Agents Chemother*. 1974, 5, 582.
189 C. N. Banti, A. D. Giannoulis, N. Kourkoumelis, A. M. Owczarzak, M. Poyraz, M. Kubicki, K. Charalabopoulos and S. K. Hadjikakou, *Metallomics* 2012, 4, 545.
190 M. Poyraz, C. N. Banti, N. Kourkoumelis, V. Dokorou, M. J. Manos, M. Simcic, S. Golic-Grdadolnik, T. Mavromoustakos, A. D. Giannoulis, I. I. Verginadis, K. Charalabopoulos and S. K. Hadjikakou, *Inorg. Chim. Acta* 2011, 375, 114.
191 (a) B. Biersack, A. Ahmad, F. H. Sarkar and R. Schobert, *Curr. Med. Chem*. 2012, 19, 3949; (b) S. J. Tan, Y. K. Yan, P. P. F. Lee and K. H. Lim, *Future Med. Chem*. 2010, 2, 1591.
192 (a) M. L. Teyssot, A. S. Jarrousse, M. Manin, A. Chevry, S. Roche, F. Norre, C. Beaudoin, L. Morel, D. Boyer, R. Mahiou and A. Gautier, *Dalton Trans*. 2009, 6894; (b) A. Gautier and F. Cisnetti, *Metallomics*, 2012, 4, 23; (c) W. Liu and R. Gust, *Chem. Soc. Rev*. 2013, 42, 755.
193 B. Coyle, M. McCann, K. Kavanagh, M. Devereux, V. McKee, N. Kayal, D. Egan, C. Deegan and G. J. Finn, *J. Inorg. Biochem*. 2004, 98, 1361.
194 C. Abbehausen, T. A. Heinrich, E. P. Abrao, C. M. Costa-Neto, W. R. Lustri, A. L. B. Formiga and P. P. Corbi, *Polyhedron* 2011, 30, 579.
195 H. L. Zhua, X. M. Zhang, G. F. Liua and D. Q. Wang, *Anorg. Allg. Chem*. 2003, 629, 1059.
196 S. I. Mostafa and F. A. Badria, *Met.-Based Drugs* 2008, 723634.
197 M. L. Teyssot, A. S. Jarrousse, M. Manin, A. Chevry, S. Roche, F. Norre, C. Beaudoin, L. Morel, D. Boyer, R. Mahiou, A. Gautier, *Dalton Trans.* 2009, 35, 6894.
198 W. Liu, R. Gust, *Chem. Soc. Rev.* 2013, 42, 755.
199 D. A. Medvetz, K. M. Hindi, M. J. Panzner, A. J. Ditto, Y. H. Yun, W. J. Youngs, *Met. Based Drugs* 2008, 384010
200 T. J. Siciliano, M. C. Deblock, K. M. Hindi, S. Durmus, M. J. Panzner, C. A. Tessier, W. J. Youngs, *J. Organomet. Chem*. 2011, 696, 1066.
201 D. C. F. Monteiro, R. M. Phillips, B. D. Crossley, J. Fielden, C. E. Willans, *Dalton Trans*. 2012, 41, 3720.
202 (a) L. Carlucci, G. Ciani, D. M. Proserpio, *Coord. Chem. Rev*. 2003, 246, 247; (b) V. A. Blatov, L. Carlucci, G. Ciani, D. M. Proserpio, *CrystEngComm* 2004, 6, 378.
203 (a) D. Bradshaw, J. B. Claridge, E. J. Cussen, T. J. Prior, M. J. Rosseinsky, *Acc. Chem. Res*. 2005, 38, 273; (b) E. Coronado, D. Gatteschi, *J. Mater. Chem*. 2006, 16, 2513.
204 (a) R. Robson, *J. Chem. Soc. Dalton Trans*. 2000, 3735; (b) R. J. Hill, D.-L. Long, N. R. Champness, P. Hubberstey, M. Schrçder, *Acc. Chem. Res*. 2005, 38, 337.
205 N. W. Ockwig, O. Delgado-Friedrichs, M. OUKeeffe, O. M. Yaghi, *Acc. Chem. Res*. 2005, 38, 176.
206 (a) X. M. Zhang, R. Q. Fang, H. S. Wu, *J. Am. Chem. Soc.* 2005, 127, 7670; (b) X. L. Wang, C. Qin, E. B. Wang, Z. M. Su, *Chem. Eur. J*. 2006, 12, 2680.
207 D. Miao, Z. Zhi-Hui, T. Liang-Fu, W. Xiu.Guang, Z. Xiao-Jun, R. B. Stuart, *Chem. Eur. J*. 2007, 13, 2578.
208 S. Alidori, G. Gioia Lobbia, G. Papini, M. Pellei, M. Porchia, F. Refosco, F. Tisato, S. Lewis Jason, C. Santini, *J. Biol. Inorg. Chem.* 2008, 13, 307.
209 V. Gandin, M. Pellei, F. Tisato, M. Porchia, C. Santini, C. Marzano, *J. Cell. Mol. Med.* 2012, 16, 142.

210 C. Marzano, V. Gandin, A. Folda, G. Scutari, A. Bindoli, M. P. Rigobello, *Free Radical Biol. Med.* 2007, 42, 872.
211 G. Marverti, P. A. Andrews, G. Piccinini, S. Ghiaroni, D. Barbieri, M. S. Moruzzi, *Eur. J. Cancer* 1997, 33, 669.